



International Baltic Earth Secretariat Publication No. 5, August 2015

A Doctoral Students Conference

**Challenges for Earth system science in the Baltic Sea region:
From measurements to models**

University of Tartu and Vilsandi Island, Estonia, 10 - 14 August 2015

Programme, Abstracts, Participants



Impressum

International Baltic Earth Secretariat Publications

ISSN 2198-4247

International Baltic Earth Secretariat
Helmholtz-Zentrum Geesthacht GmbH
Max-Planck-Str. 1
D-21502 Geesthacht, Germany

www.baltic-earth.eu

balticearth@hzg.de

Photo credits

Front page: Ivo Kruusamägi (Vilsandi lighthouse), Ivar Leidus (University of Tartu Main Building)

Inside: University of Tartu

A Doctoral Students Conference

Challenges for Earth system science in the Baltic Sea region: From measurements to models

University of Tartu and Vilsandi Island, Estonia, 10 - 14 August 2015

Co-Organized by



Supported by



TARTU OBSERVATOORIUM
eesti kosmosekeskus



European Union
Structural Assistance



Investing in your future



Helmholtz-Zentrum
Geesthacht

Centre for Materials and Coastal Research

The conference is also supported by the Doctoral School of Earth Sciences and Ecology (2009-2015).

Scientific Committee

Jaak Jaagus, University of Tartu, Estonia

Andreas Lehmann, Geomar, Kiel, Germany

Kai Myrberg, Finnish Environment Institute, Helsinki, Finland

Anders Omstedt, University of Gothenburg, Sweden

Piia Post, University of Tartu, Estonia

Marcus Reckermann, International Baltic Earth Secretariat, Helmholtz-Zentrum Geesthacht,
Germany

Anna Rutgersson, Uppsala University, Sweden

Organizing Committee

Piia Post, University of Tartu, Estonia

Jaak Jaagus, University of Tartu, Estonia

Marcus Reckermann, International Baltic Earth Secretariat, Helmholtz-Zentrum Geesthacht,
Germany

Silke Köppen, International Baltic Earth Secretariat, Helmholtz-Zentrum Geesthacht,
Germany

Regina Alber, University of Tartu, Estonia

Tanel Voormansik, University of Tartu, Estonia

Velle Toll, University of Tartu, Estonia

Naima Kabral, University of Tartu, Estonia

Find up-to date information on the Baltic Earth website: www.baltic-earth.eu/tartu2015

Idea

Tartu Ülikooli Ilmade Observatoorium 150



On the 2nd of December 1865, [Arthur Joachim von Oettingen](#) started meteorological observations in Tartu (then: Dorpat) in his own house. With this he began up to date continuous series of meteorological measurements in Estonia. He was a professor of physics and founder of the Meteorological Observatory of Tartu University, precursor of the Estonian Weather Service and organizer of the first hydrological and meteorological

network in the Baltic countries. To celebrate the 150th anniversary of the Meteorological Observatory of the University of Tartu, the Faculty of Science and Technology will host the Baltic Earth Doctoral Students Conference from 10 to 14 August in Tartu (2 days) and on Vilsandi Island (2 days), Estonia.

The main goals of the Students Conference are:

- To bring together young researchers in the field of Earth system sciences from different countries surrounding the Baltic Sea
- To offer early stage scientists an opportunity for an oral talk and discussion in a relaxed informal atmosphere
- To provide young scientists with new perspectives and inspirations for their own projects
- To have renowned keynote speakers give insights into current hot topics in the area

The Students Conference will be composed of several segments:

1. Oral presentations of doctoral students/early career researchers
2. Keynote presentations by invited speakers
3. Special Lectures
4. Tours, site visits and other activities

Key Speakers:

Prof. Sergey Gulev , P.P. Shirshov Institute of Oceanology, Moscow, Russia

Prof Jaak Jaagus, University of Tartu, Estonia

Dr Andreas Lehmann, Geomar, Kiel, Germany

Dr Kai Myrberg, Finnish Environment Institute, Helsinki, Finland

Prof. Hanno Ohvri, University of Tartu, Estonia

Prof Anders Omstedt, University of Gothenburg, Sweden

Prof Urmas Raudsepp, Tallinn University of Technology, Estonia

Prof Anna Rutgersson, Uppsala University, Sweden

Dr. Erki Tammiksaar, University of Tartu, Estonia

Dr. Hannes Tõnisson, Tallinn University, Estonia

Schedule (as of 5 August)

Baltic Earth Doctoral Students Conference 10-14 August 2015 in Tartu and Vilsandi, Estonia

Time	10. August: University of Tartu Museum (Lossi 25)
13-14	Registration
14-14.30	Opening
14.30-15	Erki Tammiksaar: <i>Meteorological Observatory of Tartu University - 150</i>
15-16	Dörthe Röhrbein: <i>About the Quality of Historical Observation Data from Signal Stations along the Southern Baltic Sea Coast</i> Ülle Napa: <i>Current and historical patterns of heavy metals pollution in Estonia as reflected in natural media of different ages: ICP Vegetation, ICP Forests and ICP Integrated Monitoring data</i> Kaupo Komsaare: <i>Air ion formation events at Tahkuse Observatory, Estonia</i>
16-16.30	Coffee break, taking group photo
16.30-17	Sergei Gulev: <i>Atmospheric transports and the vision of the propagation of Atlantic signals to Europe</i>
17-18.20	Liisi Jakobson: <i>Arctic teleconnections to Baltic Sea region</i> Velle Toll: <i>Influence of the direct radiative effect of aerosols on atmospheric dynamics over Europe</i> Maris Palo: <i>Electric wind in a Differential Mobility Analyzer</i> Aigars Lavrinovics: <i>Filling the gaps: Applying the WRTDS model on interpolation of the major Latvian river loads to the Gulf of Riga</i>
18.20 -...	Little excursion in the museum Ice breaker

Time	11. August: Tartu, Physicum (Ravila 14c)
9.30-10	Anders Omstedt: <i>Understanding the water and energy exchanges in the coupled atmosphere-land-ocean system</i>
10-11	Sven-Erik Enno: <i>Estimating ATDnet detection efficiency on the basis of Lightning Mapping Array</i> Yu Yang: <i>Investigation of the climate impact on the snow and ice thickness in Lake Vanajavesi, Finland</i> Regina Alber: <i>Diurnal cycle of precipitation in Estonia</i>
11-11.30	Coffee
11.30-12	Kai Myrberg: <i>The basics of Baltic Sea physics</i>

12-13	<p>Victor Alari: <i>Response of water temperature to surface wave effects: experiments with the coupled NEMO-WAM</i></p> <p>Naglaa F. Soliman: <i>Potential Ecological Risk of Heavy Metals in Sediments from the Mediterranean Coast, Egypt</i></p> <p>Pille Meinson: <i>Continuous and high-frequency measurements in limnology: History applications and future challenges</i></p>
13-14	Lunch
14-14.30	Anna Rutgersson: <i>Natural hazards and extreme events in the Baltic Sea region</i>
14.30-15.30	<p>Jüri Kamenik: <i>Recurrence interval of Estonian precipitation extremes</i></p> <p>Tanel Voormansik: <i>Analysis of convective storms in Estonia based on the data from polarimetric weather radars and lightning detectors</i></p> <p>Eva Rocha: <i>Tree-rings as an indicator of climatic and anthropogenic influences in urban environments – The case study of Stockholm</i></p>
15.30-16	Coffee
16-16.30	Hanno Ohvril: <i>Atmospheric column transparency in Europe, 1906 -2014</i>
16.30-17.30	<p>Margit Aun: <i>Reconstruction of UVB and UVA radiation at Tõravere, Estonia, for years 1955-2003</i></p> <p>Kairi Raabe: <i>On the retrieval of the clumping index from multi-angular SWIR satellite imagery</i></p> <p>Evelin Kangro: <i>Validation of MERIS standard and processed data. Development of the relationship between phytoplankton absorption coefficient and chlorophyll-a concentration for remote sensing applications for large Estonian lakes</i></p>

12. August: Travel to Vilsandi Island

8.30 Departure by bus from Tartu to Saaremaa island.
11.00 Pärnu
13.20 Kuivastu
14.40 Lunch in Kaali
16.30 Papisaare
Boat trip from Papisaare port to Vilsandi island (Vikati port).
Accommodating
19 Dinner in tourist farms
20/21 Sauna in tourist farms

Time	13. August: Vilsandi Paadikuur
9.30-10	Jaak Jaagus: <i>150 years of meteorological observations at the Vilsandi maritime meteorological station: climate variability and climate changes</i>
10-11	Kaie Kriiska: <i>Forest belowground carbon cycle in Estonia – Vilsandi case- study</i> Naima Kabral: <i>Heavy metal accumulation in different parts of coniferous forest at Estonian ICP IM Vilsandi area</i> Katrin Saar: <i>The effect of climate change and eutrophication on sediment phosphorus fractions: results of a long-term enclosure experiment</i>
11-11.30	Coffee
11.30-12	Urmas Raudsepp: <i>Water circulation and nutrient dynamics in the Baltic Sea</i>
12-13	Ilja Maljutenko: <i>Circulation scheme of the Baltic Sea – based on the 40-year simulation with GETM</i> Toma Mingelaite: <i>Coastal upwelling in the SE Baltic Sea: basic statistics</i> Palina Lapo: <i>Verification of WRF-ARW model in Belarus</i>
13-14	Lunch
14-14.30	Andreas Lehmann: <i>Atmospheric conditions forcing large volume changes (LVCs) and major inflows (MBIs) to the Baltic Sea</i>
14.30-15.30	Julian Alberto Gallego Urrea: <i>Modelling the effects of NO_x, SO_x and NH_x deposition on the Baltic Sea carbon system</i> Mariliis Kõuts: <i>Long-term model study of nutrient and detritus dynamics in the Baltic Sea</i> Ivar Zekker: <i>Smooth temperature decreasing FOR nitrogen removal in cold (9-15° C) ANAMMOX biofilm reactor tests</i>
15.30-16	Coffee
16-16.30	Hannes Tõnisson: <i>Observations and analysis of coastal changes in West Estonian Archipelago to study the impacts of climatic and sea-level fluctuations and wave parameters on shore processes</i>
16.30 ...	Guided walk on the island
20	Camp fire evening (lõkkeõhtu) at Tolli Closing the conference Sauna

14. August: Travel back to Tartu	
7.30-8.30	Breakfast Free time for individual sightseeing in Vilsandi.
10.30	Boats from Vikati to Papisaare (first with the people to Tallinn)
11-16	Papisaare-Kuivastu-Virtsu-Tallinn airport (minibus)
11.30 - 19	Papisaare. Kuivastu- Virstu-Pärnu- Tartu (bus) (in Pärnu at 15:20)

Response of water temperature to surface wave effects: experiments with the coupled NEMO-WAM

Victor Alari, Joanna Staneva

Helmholtz-Zentrum Geesthacht, Germany (victor.alari@hzg.de)

1. Introduction

Traditionally ocean models and wind wave models have been applied separately for real geophysical problems. The reason for this is the different time scales of the processes investigated. While typical wind wave periods lay between 2-20 s, the typical time scales of water movement range from hours to years. Separating wave and ocean models is a pragmatic way, but unfortunately leads to violation of energy and momentum conservation.

The aim of this work is to study the influence of wind waves to Baltic Sea and North Sea dynamics and especially to water temperature. We use the hydrodynamic model NEMO coupled to wave model WAM. The coupled system was developed by ECMWF (Breivik et al. 2015). The examples provided in this study are considered as a step towards further developing new coupled ocean forecasting systems for the Baltic Sea area. The coupled system also paws the road to more realistic simulation of long-term variability of the Baltic Sea.

2. Wave effects

The NEMO ocean model has been modified to take into account the following three wave effects: (1) The Stokes-Coriolis forcing (Hasselmann 1971). The interaction of vertically shearing Stokes drift with the planetary vorticity introduces this additional term into the momentum equations. (2) Wave dependent ocean side stress (Janssen 1989; Janssen 2012). When wind starts blowing, it first has to transfer momentum to waves. This means than in young sea states the ocean receives less momentum compared to case where waves and not accounted for. In later stage of wave growth, white capping releases more momentum back to ocean than wind transfers to waves, and therefore the ocean side stress is locally enchanted. (3) Additional mixing due to breaking waves (Craig and Banner 1994). Breaking waves enhance the mixing by transferring energy to ocean. This is taken into account in *k-eps* parametrization, where the mixing is dependent of wave age and wave height (roughness length). The parametrization of waves into *k-eps* model has been performed by us.

3. Model setup

Both models have a horizontal resolution of 2 nautical miles and NEMO has 21 s-layers in vertical. The hourly atmospheric forcing is taken from German Weather Service (DWD). The open boundaries of the BS-NS model system are situated in west of English Channel and near the continental shelf break of the North Sea. At the open boundaries tidal amplitudes and velocities are prescribed as well as climatological temperature and salinity. The wave

model starts from rest, while ocean model uses climatology. The modelling period covers 01.10.2012-31.12.2013. The first seven months are used as a spinup and during that period LIM2 ice model is also activated. Here we analyze the effects of waves by computing differences between runs with wave processes accounted for and the control run without waves.

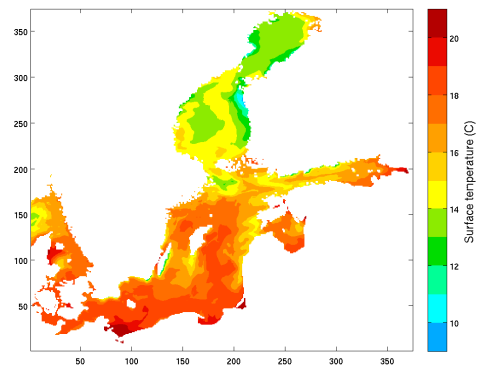


Figure 1. Snapshot of modelled SST on 10th August 2013. Colorbar from 9 degree to 21 degree.

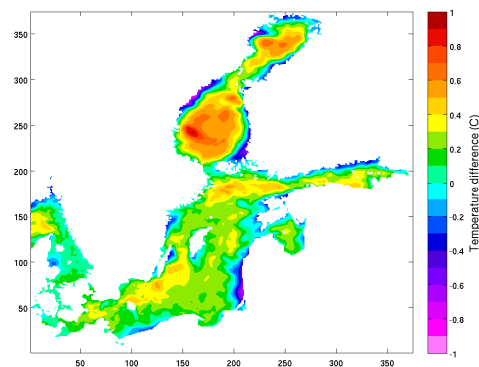


Figure 2. Difference of SST between run with all wave effects included and the control run, without waves. Seasonal average for June, July, August. Red tones means warming. Colorbar from -1 degree to 1 degree.

4. Results

The default NEMO model without waves is capable of simulating important SST patterns in the Baltic Sea (Figure 1). Therefore it is reasonable to switch on waves.

In the experiment where all wave effects were accounted for, the absolute warming or cooling due to

waves on a seasonal basis (JJA-summer, SON-autumn) is up to 1⁰C (Figure 2). Instantaneous differences at certain time moments lie between -5⁰ to 5⁰ C. The most prominent seasonal warming is located in the Northern parts of Baltic Sea in surface layer. In the bottom layers usually cooling dominates. Most of the cooling is found in coastal areas and warming in offshore regions. Autumn season displays larger values compared to summer. This is expected since the wave activity is also higher in autumn.

The near-coastal cooling is almost always related to Stokes-Coriolis forcing. This is especially true for deep layers. Compared to other processes, the vertical extent of influence of Stokes-Coriolis forcing is highest. It has the effect to intensify and induce upwellings near all coasts.

The effect of wave breaking is to warm the surface layer, which in turn reduces the cold bias when comparing model and measured data. The effect of ocean side stress is mostly to warm surface layer in summer and slightly cool intermediate and bottom layer in autumn.

5. Conclusion

The studies of wave effects to water dynamics in the Baltic Sea and North Sea are just starting to get more attention. With this work we take the first step of implementing NEMO-WAM model on seasonal time-scales. We have already described some first results, which demonstrate the importance of having a coupled system. We progress with our work to study more deeply the wave effects to temperature, salinity, currents and mixing.

Acknowledgements

We are grateful to ECMWF and especially to O.Breivik, K. Mogensen and J.R.Bidlot for sharing with us the coupled NEMO-WAM code.

References

- Breivik, O., Mogensen, K., Bidlot, J.-R., Balmaseda, M.A., Janssen, P.A.E.M (2015) Surface wave effects in the NEMO ocean model: Forced and coupled experiments. *Journal of Geophysical Research C: Oceans*, 120 (4), pp. 2973-2999.
- Craig, P.D., Banner, M.L. Modeling wave-enhanced turbulence in the ocean surface layer (1994) *Journal of Physical Oceanography*, 24 (12), pp. 2546-2559.
- Hasselmann, K (1971) On the mass and momentum transfer between short gravity waves and large-scale motions. *Journal of Fluid Mechanics*, 50 (1), pp. 189-205.
- Janssen, P.A.E.M (2012) Ocean wave effects on the daily cycle in SST. *Journal of Geophysical Research: Oceans*, 117 (9), art. no. C00J32
- Janssen, P.A.E.M (1989) Wave-induced stress and the drag of air flow over sea waves. *Journal of Physical Oceanography*, 19, pp. 745-754.

Diurnal cycle of precipitation in Estonia

Regina Alber

Institute of Ecology and Earth Sciences, University of Tartu, Tartu, Estonia (regina.alber@ut.ee)

1. Introduction

Precipitation is a very important climatic variable, which has an influence on water management, agriculture, water transport and humans' everyday life. Precipitation extremes can cause very severe nature damages in Estonia.

Precipitation has a very high spatial and temporal variability. The diurnal cycle of precipitation has relations with different other climatic cycles (e.g. surface temperature, air pressure).

Globally, the most pronounced diurnal precipitation amplitudes are characteristic to summer (Dai 2001). In some places occur bimodal distributions of precipitation maxima. The morning and afternoon maxima of precipitation were found in Shandong province in China (Zhuo et al. 2014), Eskdalemuir parish in Scotland (Svensson & Jakob 2002) and in Krakow in Poland (Twardosz 2007).

In Europe, over the land areas, the precipitation maxima in warm season are usually found in the afternoon and evening e.g. in Switzerland (Wüest et al. 2010), Austria (Yaqub et al. 2011) and Sweden (Jeong et al. 2011, Walther et al. 2013). The only country, which locates at the same latitude as Estonia, where the analogous study about the diurnal cycle of precipitation has done, is Sweden (Jeong et al. 2011).

The aim of this study is to analyse the diurnal cycle of precipitation in continental and coastal areas of Estonia. The analysis is done by means of hourly precipitation.

2. Data and methods

The precipitation data was obtained from the Estonian Weather Service. The analysis was based on two kind of data: hourly precipitation data from 13 automated weather stations during the warm period from April to October in 2003-2013 and pluviographic records' data from 10 stations from May to October in 1991-2003. The diurnal cycle of precipitation was described with mean annual amounts of hourly precipitation and with mean diurnal amplitudes of hourly precipitation. Coastal and continental stations were studied separately by describing monthly and seasonally the diurnal distribution of precipitation. The local East European Time (EET, which is equal to UTC+2 hours) was used.

3. Results

The continental stations had much clearer diurnal cycles and amplitudes of precipitation compared to the coastal stations in spring and summer (Fig. 1).

The maximum period of the precipitation amounts at the continental stations in spring was at 14-19 EET and in summer at 12-19 EET with the peaks correspondingly at 14-16 EET and 13-16 EET.

The distribution of the diurnal cycle of precipitation at the coastal stations was quite flat. In summer, the automated stations' recordings showed maxima at 13-21

EET. Albeit, in autumn existed two maxima: at 2-7 EET and at 18-22 EET.

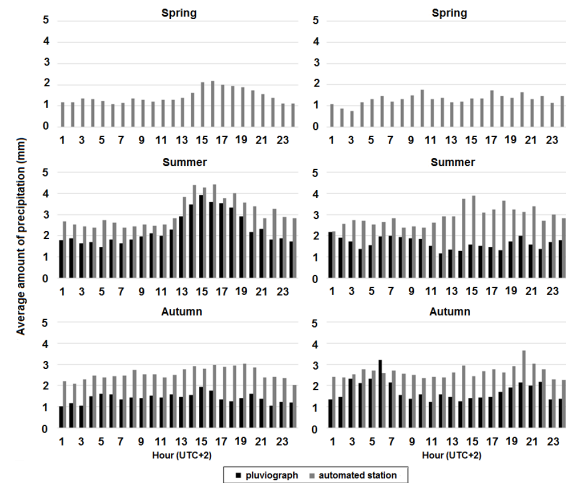


Figure 1. Mean diurnal distribution of hourly precipitation amounts (mm) in Estonia by seasons at the continental (left column) and at the coastal stations (right column) calculated from the pluviographic records and from the automated precipitation gauges.

Monthly, the diurnal cycle of precipitation had the most pronounced maximum periods from May to August (Fig. 2). In August, there were detected two maxima: in the afternoon and at night according to automated stations' data. In September existed weak maximum in the evening, while in April and October the distribution was quite even. The pluviographic and automated measurements showed a little different results in the times and amounts of the distribution of precipitation.

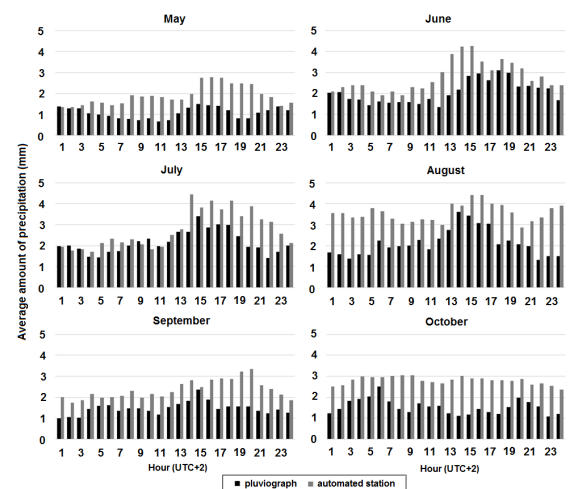


Figure 2. Mean diurnal distribution of hourly precipitation amounts (mm) in Estonia by months from May to October calculated from the pluviographic records and from the automated precipitation gauges.

4. Discussion

The differences of diurnal cycle of precipitation between coastal and continental stations were presumably caused by the influence of the Baltic Sea. As the sea surface is cooler than the land surface in spring and during the first half of the summer, the convection is then not so favorable over the sea. The afternoon and evening maxima of the diurnal cycle of precipitation at the continental stations were probably caused by more intense convective activity following the solar diurnal cycle. Besides, the afternoon peaks of the diurnal cycle of precipitation in Sweden were claimed to be caused by convective rainfalls (Jeong et al. 2011). Moreover, earlier and longer peak in summer compared to spring at the continental stations as well as bigger amplitudes in summer were apparently seen due to the higher position of the Sun, which causes warming of the surface and induces further convection. The early morning peak at the coastal stations in autumn was presumably caused by the warmer Baltic Sea induced higher convective activity over the sea. Formerly, Jaagus et al. (2010) stated that a large share of precipitation in the Baltic countries is caused by convective spells.

The differences between the results from automated gauges and pluviographs can be explained two ways. Firstly, pluviographs do not measure small amounts of precipitation. Secondly, the period, studied by pluviographs had less precipitation than the period studied by automated gauges.

5. Conclusion

The diurnal cycle of precipitation was different at the coastal and continental stations in Estonia. The clear cycle with precipitation maxima in the afternoon and evening and minimum from night to morning existed in continental stations, whereas at the coastal stations the distribution was more flat. The diurnal precipitation amplitudes were the highest in midsummer, especially at the continental stations. The maxima were probably related to warming of the surfaces and convective rainfall.

References

- Dai, A. 2001. Global precipitation and thunderstorm frequencies. Part II: diurnal variations. *Journal of Climate*, 14, 1092–1111.
- Jaagus, J., Briede, A., Rimkus, E., Remm, K. (2010). Precipitation pattern in the Baltic countries under the influence of large-scale atmospheric circulation and local landscape factors. *International Journal of Climatology*, 30, 705–720.
- Jeong, J.-H., Walther, A., Nikulin, G., Chen, D., Jones, C. (2011). Diurnal cycle of precipitation amount and frequency in Sweden: observation versus model simulation. *Tellus*, 63A, 664–674.
- Svensson, C., Jakob, D. (2002). Diurnal and seasonal characteristics of precipitation at an upland site in Scotland. *International Journal of Climatology*, 22, 587–598.
- Twardosz, R. (2007). Seasonal characteristics of diurnal precipitation variation in Krakow (South Poland). *International Journal of Climatology*, 27, 957–968.
- Walther, A., Jeong, J.-H., Nikulin, G., Chen, D., Jones, C. (2013). Evaluation of the warm season diurnal cycle of precipitation over Sweden simulated by the Rossby Centre regional climate model RCA3. *Atmospheric Research*, 119, 131–139.
- Wüest, M., Frei, C., Altenhoff, A., Hagen, M., Litschi, M., Schär, C. (2010). A gridded hourly precipitation dataset for Switzerland using rain-gauge analysis and radar-based disaggregation. *International Journal of Climatology*, 30, 1764–1775.
- Yaqub, A., Seibert, P., Formayer, H. (2011). Diurnal precipitation cycle in Austria. *Theoretical and Applied Climatology*, 103, 109–118.
- Zhuo, H., Zhao, P., Zhou, T. (2014). Diurnal cycle of summer rainfall in Shandong of eastern China. *International Journal of Climatology*, 34, 742–750.

Reconstruction of UVB and UVA radiation at Tõravere, Estonia, for years 1955-2003

Margit Aun, Kalju Eerme, Martin Aun, Ilmar Ansko

Institute of Physics, University of Tartu, Estonia (margit.aun@ut.ee)

1. Ultraviolet radiation measurements

Ultraviolet (UV) radiation, 280 – 400 nm, is known to cause negative effects on living organisms and materials. For estimating the influence data on changes in UV doses and spectral composition is needed. Measurements of UV radiation have been carried out only in the last decades. This raises the necessity for modeling and reconstruction of UV radiation. Another benefit of models is covering data caps that have occurred due to technical issues with instruments.

In Tõravere, Estonia, (58°16'N, 26°28'E, 70 m a.s.l.) UV spectral measurements started in summer 2004 with minispectrometer AvaSpec-256, described by Ansko et al. (2008). In summer 2009 AvaSpec was replaced by Bentham DMc150F-U.

2. Aim and construction of the models

The aim of the present study was to find and adapt a simple and accessible method for reconstructing UV doses in two wavelength ranges: UVB (280-315 nm) and UVA (315-400 nm). Two independent models were built for reconstructing daily doses for years 1955-2003. For constructing the models freely available software ARESLab (Jekabsons, 2011), based on Multivariate Adaptive Regression Splines method, was selected. As the input data measured daily column ozone, daily dose of global solar radiation, noon solar zenith angle and cloudless UV daily doses calculated with LibRadtran software packet (Mayer and Kylling, 2005) were used. The construction of the models was based on the UV spectral irradiance data measured at Tõravere from 2004 to 2006.

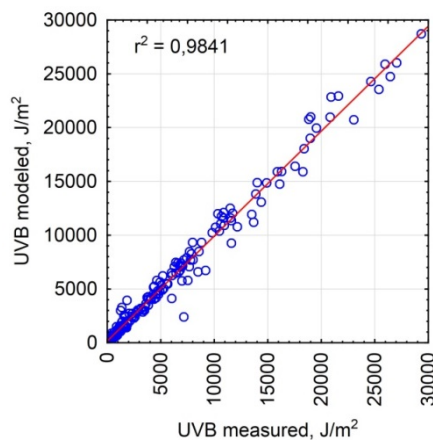


Figure 1. Correlation between the measured and modeled UVB daily doses in the year 2007.

Testing of the models was carried out on data from 2007. Both models had linear correlation coefficients of measured and calculated daily doses above 0.98.

Scatterplot of measured and modeled UVB daily doses are presented on Figure 1. Testing of the models was also carried out on data from Bentham DMc150F-U. The correlation between measured and modeled data was almost as strong.

3. Results

Daily doses from 1955 to 2003 were calculated. Changes in yearly doses in time are on Figure 2.

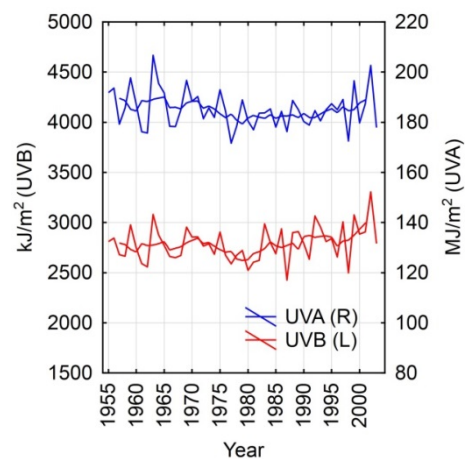


Figure 2. Reconstructed yearly doses of UVB and UVA radiation from 1955 to 2003 with 5-year moving average.

UV radiation level started to decline from the beginning of the 1970s, reaching its minimum in 1979. In the 1980s UVB started to increase while UVA stayed low until 1990s and started to rise after that.

The changes in UVB and UVA doses are supported by the fluctuations in measured column ozone and global solar radiation.

Besides giving an overview to changes in UV radiation the models built give an opportunity to fill data caps of recent measurements.

References

- Ansko, I., Eerme, K., Lätt, S., Noorma, M., Veismann, U. (2008) Study of suitability of AvaSpec array spectrometer for solar UV field measurements, *Atmospheric Chem. Phys.* **8**, pp. 3247–3253.
- Jekabsons, G. (2011) ARESLab, Adaptive Regression Splines toolbox for Matlab/Octave. <http://www.cs.rtu.lv/jekabsons/regression.html>
- Mayer, B., Kylling, A. (2005) Technical note: The libRadtran software package for radiative transfer calculations - description and examples of use, *Atmospheric Chem. Phys.* **5**, pp. 1855–1877.

Impacts of climate change on rivers water regime over Southern and Eastern part of the Republic of Belarus

Volha Baiduk

Russian State Hydrometeorological University (olya4ok@list.ru)

In relation to climate change, increasing anthropogenic influence on the rivers and their watersheds becomes serious problem of studying the surface waters of Belarus in modern conditions.

For the analysis of climate change and its impact on the hydrological regime of rivers of Belarus we used following characteristics: maximum flow rate of the spring flood ; layers of the spring flood; maximum discharges during rain floods; discharges during low-water period in winter and summer; the mean annual and seasonal air temperature; annual sums of precipitation; the maximum snow-water equivalent.

For the present study the data of hydrological observations on rivers of 22 stations and meteorological data from 12 stations have been used. Time-series of hydrological and meteorological data were represented for more than 50 years and included observations for the period up to 2011.

All the rivers were assigned to three hydrological regions (Verhnedneprovsky, Central Berezina and Pripyt` river regions). This distribution relayed on hydrological zoning of Belarus. All meteorological parameters have been tested for homogeneity with Student` and Fisher` criteria and trends were analyzed with the least-squares method.

In the regime of maximum discharge of spring flood there is a significant negative trend. In the opposite, the minimum discharge of low-water period in winter showed the presence of positive trend.

Analysis of meteorological parameters showed that annual precipitation changes significant for northern part of Belarus (Partasenok et al. 2014) but for the rest of the territory there are no significant changes. The mean annual air temperature according to all stations increased significantly. Changes in the mean annual temperature was mainly due to a significant increase in winter temperatures. In this regard, we reviewed the ranks of average temperatures for the winter period (December-February), which led to heterogeneity in the ranks. Increased winter temperatures led to increased thaw and as a consequence, to raise the minimum winter flow and reduce costs and maximize layers of spring floods.

Estimation of time-series of maximum snow-water equivalent with the t-test and Fisher test showed that data is homogeneous. The hypothesis of a significant trend has been disproved. The analysis showed that the least impact climate change has had on the average annual streamflow and maximum discharges during rain floods.

The main reason for raising the minimum summer-autumn streamflow is to the increase of the groundwater supply in the basins of the study region. Based on the above mentioned, it is possible to make a conclusion that the main factor of the change in the water regime of the rivers in Belarus is to increase the average air temperature in winter. The increase in temperature was not reflected in

the change of annual streamflow, but its influence on the intra-annual distribution: the streamflow during low-flow periods has increased and maximum streamflow during spring floods has decreased.

References

Partasenok I. S., Lopuch P.S. Influence of the atmosphere circulation of river water regime of the Republic of Belarus. – Minsk, BSU, 2014. – 216 p

Modelling the effects of NO_x, SO_x and NH_x deposition on the Baltic Sea carbon system

Julián Gallego-Urrea¹, Moa Edman², David Turner¹, Anders Omstedt¹, Björn Claremar³, Anna Rutgersson³

¹. Department of Marine Sciences, University of Gothenburg, Sweden, (julian_gallego@hotmail.com)

². Swedish Meteorological and Hydrological Institute, SMHI, Gothenburg, Sweden

³. Department of Earth Sciences, Uppsala University, Uppsala, Sweden

1. Abstract

The recognition that the ocean's uptake of fossil fuel CO₂ can be modified by acidic anthropogenic deposition has stimulated several simplified approaches to assess the consequences at global and regional scales. We present here the first detailed biogeochemical model addressing this question, focusing on the Baltic Sea.

In order to evaluate the effects of historical atmospheric depositions from land and shipping of sulfate, nitrate and ammonium on the CO₂ balance in the Baltic Sea, a numerical model including major physical, chemical and biological processes was used. The modelling encompasses the period 1750 to 2014, a period when land and ships emissions have undergone large changes with increasing carbon dioxide concentrations, increasing emissions of SO_x, NO_x, NH_x and increasing loads of nutrients.

The amount of CO₂ absorbed and exported was strongly influenced by the variations from land inflows. Less atmospheric CO₂ was absorbed when acidic deposition was included.

2. The probe-Baltic model

The PROBE-Baltic model the CO₂ cycle in the Baltic sea including the interaction between physical (stratification, temperature, salinity, penetration of solar radiation, and ice), chemical (alkalinity, pH, dissolved inorganic carbon, oxygen, and nutrients), and biological processes (plankton and dissolved organic carbon) (Omstedt et al. 2009). The model also includes a novel reconstruction of forcing fields and deposition and ship emissions, an additional alkalinity source derived from DOC inflows (Kuliński et al. 2014) and the possibility to include the alkalinity reduction due to acidic depositions (Omstedt et al. 2015). Three scenarios were run: a control run without any effect of the acidic deposition in alkalinity, a full model including alkalinity titration due to all inputs of acidic deposits and a model including only alkalinity reduction due to shipping activities. All models consider the input of NO_x as nutrients for the biological module.

3. The carbon system in the Baltic Sea

The results from the model showed an overall increase in the uptake of carbon from the atmosphere in all three scenarios with a peak in the decade between 1980 and 1990, mostly related to land emissions and the resulting regulation. The effect of the acidic depositions on the uptake of CO₂ presents also a maximum in this period with a reduction in CO₂ inflow for the entire Baltic Sea, of approximately 10-15% with respect to the control case (Figure 1).

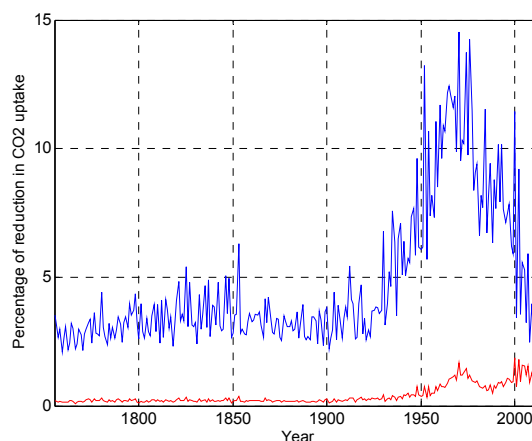


Figure 1. Percentage of reduction in the atmospheric CO₂ inflow to the Baltic Sea owing to acidic contribution of NO_x and SO_x with respect to the control scenario. The blue line corresponds to the case where all emissions contribute to consume alkalinity and the red line when only ship emissions are considered.

4. Conclusions

The influence of atmospheric acidic depositions on the CO₂ system for the Baltic Sea was modelled and analyzed. The results indicate that, in addition to the effects of land inputs, there is a considerable impact of the acidic depositions on the CO₂ uptake from atmosphere.

References

- Kulinski, K., B. Schneider, K. Hammer, U. Machulik and D. Schulz-Bull (2014). The influence of dissolved organic matter on the acid-base system of the Baltic Sea. *J Mar Syst* 132:106-115
- Omstedt, A., M. Edman, B. Claremar and A. Rutgersson (2015) Modelling the contributions to marine acidification from deposited SO_x, NO_x, and NH_x in the Baltic Sea: Past and present situations. *Cont Shelf Res*, in review
- Omstedt, A., E. Gustafsson and K. Wesslander (2009) Modelling the uptake and release of carbon dioxide in the Baltic Sea surface water. *Cont Shelf Res* 29(7):870-995

Atmospheric transports and the vision of the propagation of Atlantic signals to Europe

Sergey Gulev

IORAS Moscow, Russia, gul@sail.msk.ru

We concentrate on the mechanisms of the Atlantic Ocean impacts on European weather and climate. In a traditional paradigm, Gulf Stream and NAC in the Atlantic Ocean provide diabatic heating of the surface layer, affecting, thus, low level baroclinicity of the atmosphere. Anomalies in the intensity of air-sea exchanges result in intensification/de-intensification of the North Atlantic storm track and, as a consequence, in the higher/weaker energy and moisture transport to Europe. However, this conventional view is valid only for the first glance. First, the character of the impact of the North Atlantic onto atmospheric conditions through sea-air interaction processes depends on the time scales considered with the ocean being the active player on multidecadal scales and the atmosphere playing the active role on interannual to decadal scales (Bjerknes conjecture). Secondly, the strongest air-sea fluxes (and associated anomalous energy inputs to the atmosphere) are frequently associated with the cyclones which do not propagate to Europe and recycle the water vapor over the Atlantic. In this context cyclone activity in the Eastern Atlantic is even more important for forming atmospheric moisture and energy transports to Europe. These processes are responsible for forming both the pass ways for the tropical moisture transport to Europe and for forming atmospheric rivers, injecting anomalous moisture to European continent. These mechanisms will be considered using Eulerian and Lagrangian frameworks based upon computation of atmospheric moisture/heat transports and analysis of cyclone trajectories. Consequences of anomalous moisture transports associated with extreme precipitation, will be analysed using station and reanalysis data on both continental and regional scales.

150 years of meteorological observations at the Vilsandi maritime meteorological station: climate variability and climate changes

Jaak Jaagus

Department of Geography, Institute of Ecology and Earth Sciences, University of Tartu, Estonia (jaak.jaagus@ut.ee)

1. Introduction

Vilsandi is the westernmost inhabited island in Estonia west from the Saaremaa Island lying under the direct influence of the Baltic Proper (Figure 1). It represents the most maritime climatic conditions in Estonia.

Meteorological observations at the Vilsandi lighthouse have been made during 150 already, since September 1865. Although the measuring site has not been changed there have been several breaks, mostly in the 19th century and the longest one in 1913-1919. There have been also many instrument changes that make the longest time series inhomogeneous. Nevertheless, meteorological data from the Vilsandi station have been used in studies of climate variability and climate change (Orviku et al. 2003, Jaagus 2006, Jaagus et al. 2008, Jaagus and Kull 2011).



Figure 1. Location map of the Vilsandi station.

The main aim of this presentation is to point out the most important climatic peculiarities on the coast of the open sea and to analyse climate variability and changes on the eastern coast of the Baltic proper.

2. Data and methods

Monthly mean meteorological data from Vilsandi during 65 years (1950–2014) are used in this study. They have been compared with similar data from the Tartu station located in eastern Estonia and well representing the climatic conditions in the whole continental region of Estonia. Mean, maximum and minimum temperatures, daily temperature range, precipitation, wind speed, storminess and snow cover duration have been analysed.

Trend analysis using Mann-Kendall test has performed. It does not require the normal distribution of the studied

parameters, which is often the case in climatology. Trends are considered statistically significant on $p < 0.05$ level. Trends values are calculated using Sen's method and presented in changes per decade.

3. Peculiarities of the maritime climate on the coast of the Baltic Sea

Baltic Sea is an inland sea having many features characteristic for "continental" seas. First of all, it means considerable seasonal temperature variations. In comparison with the coast of the ocean, annual temperature range is much higher. As a consequence, seasonal ice cover in winter is typical for the Baltic Sea.

The annual curves of air temperature and precipitation in Vilsandi are significantly different than in the continental part of Estonia (Figure 2). The main feature – thermal inertia – is clearly presented at the coast of the Baltic Sea. The warming effect of the sea causes that air temperature in Vilsandi is higher than in Tartu from August to March with the maximum difference in January – 4.4 degrees. The cooling influence on the sea is evident from April to July. The annual distribution of precipitation in Vilsandi is also specific. Precipitation maximum in Estonia is in August and minimum in February. But in the coastal regions the period of the highest precipitation is shifted towards autumn. It is also a consequence of the thermal inertia of the sea.

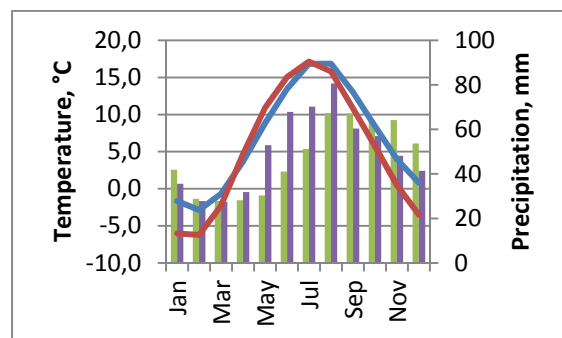


Figure 2. Monthly mean air temperatures and precipitation in Vilsandi and Tartu.

Due to the lack of wind obstacles on the sea coast, it is natural that mean wind speed in Vilsandi is much higher than in Tartu. It has the highest number of windstorms in Estonia. Hereby, a storm day is defined when the 10-minute mean wind speed 15 m/s or higher has been measured at least once a day. The mean number of storm days in Vilsandi is about 20. The storm season starts in September and lasts until March. The highest storminess has been observed in December, November and January (Jaagus et al. 2008).

Higher winter temperature induces less snow cover in Vilsandi. The mean number of days with snow cover in Vilsandi is about 73. At the same time, in the other regions of Estonia it varies between 100 and 120 days. The highest mean values above 130 days have been detected on the Haanja upland and in the north-eastern Estonia (Jaagus, 1997).

4. Long-term trends

Global climate change is present also in the Baltic Sea region (BACC II Author Team 2015). The increase in mean annual temperature in Vilsandi has been very significant (Figure 3). According to the linear trend it has increased by two degrees during 1950–2014 (Figure 3). The time series can be presented also using a large break since 1989 when the mean temperature level increased by 1.3 degrees.

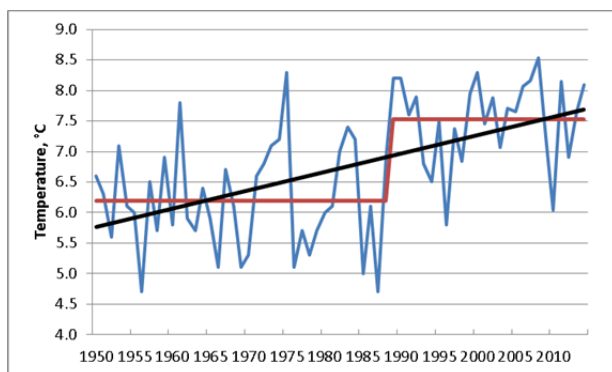


Figure 3. Time series of annual mean temperature in Vilsandi, its linear trend and broken line into two sub-periods.

Statistically significant warming has been detected in all seasons except winter. Trend values are high in winter – more than 0.3°C warming per decade – but they statistically insignificant due to a very high temporal variability of winter temperature. Statistically significant warming on the $p < 0.05$ level in Vilsandi was detected in March, April, May, July, August, September and November. The strongest increase by 0.4–0.5 degrees per decade detected for March and July.

Precipitation can be characterised by a very high temporal and spatial variability. Annual precipitation has increased significantly during 1950–2014 (Figure 4). The highest values (about 800 mm per year) were registered in 1990, 2007 and 2012. Statistically significant increase in precipitation was recorded in March and June while an insignificant decrease has been measured in September.

5. Conclusions

Valuable meteorological data have been observed in Vilsandi station during 150 years. It represents typical maritime climatic conditions on the eastern coast of the Baltic Sea. Thermal inertia plays an important role in formation of climatic difference between Vilsandi and the continental part of Estonia. The maritime climate in Vilsandi can be characterised by a cool and long spring, comparatively cool and late summer but hot autumn and winter. Annual mean temperature is clearly higher than in the continental Estonia. The maximum of precipitation has

shifted from summer to autumn. Storminess in Estonia is the highest at Vilsandi.

Increase in annual mean temperature by 2 degrees has been recorded during 1950–2014. The warming was more or less even in all seasons but statistically insignificant in winter. Significant increase in precipitation has been also recorded.

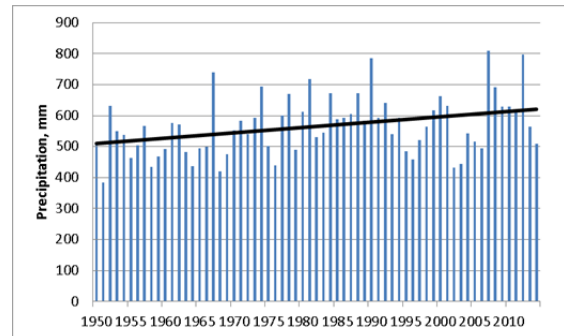


Figure 4. Time series of annual precipitation in Vilsandi and its linear trend.

References

- BACC II Author Team (2015) Second assessment of climate change for the Baltic Sea Basin. Springer, Heidelberg, 501 pp.
- Jaagus J. 2006. Climatic changes in Estonia during the second half of the 20th century in relationship with changes in large-scale atmospheric circulation. *Theoretical and Applied Climatology*, 83, 77-88.
- Jaagus J., Post P., Tomingas O. 2008. Changes in storminess on the western coast of Estonia in relation to large-scale atmospheric circulation. *Climate Research*, 36, 29-40.
- Jaagus J. and Kull A. 2011. Changes in surface wind directions in Estonia during 1966-2008 and their relationships with large-scale atmospheric circulation. *Estonian Journal of Earth Sciences*, 60, 220-231
- Orviku K., Jaagus J., Kont A., Ratas U., Rivas R. 2003. Increasing activity of coastal processes associated with climate change in Estonia. *Journal of Coastal Research*, 19, 364-375.

Arctic teleconnections to Baltic Sea region

Liisi Jakobson^{1,2}; Erko Jakobson^{1,2}, Piia Post¹

¹University of Tartu, Estonia; ²Tartu Observatory, Estonia; (Liisi.Jakobson@ut.ee)

1. Introduction

Over the past half century, the Arctic has warmed at about twice the global rate (IPCC 2014). Remarkable changes have been taking place, in particular, highly statistically significant decreases in sea-ice extent in all calendar months since 1979 (Simmonds 2015). The presence of the changes has naturally led to the question as to whether the impacts of these are confined to the Arctic region or if remote weather and climate is also influenced in a significant manner (Simmonds and Govekar 2014). A number of contrasting views on this subject have been expressed, several studies have demonstrated connections between warming and/or ice decline and midlatitude weather and climate extremes (Coumou et al., 2014; Tang et al., 2013, 2014; Petoukhov et al., 2013; Francis and Vavrus 2012;). Others have analyzed whether these associations are statistically and/or physically robust (Hassanzadeh et al., 2014; Screen et al 2014; Barnes et al 2014; Screen and Simmonds 2013, 2014; Barnes 2013), while some investigations suggest that the ostensible associations may have their origin, in part, in remote influences (Peings and Magnusdottir 2014; Screen et al., 2012). In light of this divergence of views on cause-and-effect, and of the importance of clarification, the investigation of Sato et al. (2014) makes a very valuable and illuminating contribution (Simmonds and Govekar 2014). They used the difference map of SLP (sea level pressure) and T950 (air temperature at 950 hPa) by subtracting the composites of cold Decembers from those of warm Decembers to show that apparent links between Barents sea-ice coverage and cold Eurasian winters are in fact associated with part of a teleconnection pattern, which originates from outside the Arctic, in the North Atlantic Gulf Stream region.

The question motivating the present writing is *'If and how the Arctic warming influences the air temperature in Baltic Sea region in winter'*? Correlations between air temperature in testing point in Estonia and different climate parameters in Arctic are analyzed. Different climate situations are considered to uncover the forcing mechanisms.

2. Data

We used NCEP-CFSR and ERA-INT reanalyses monthly mean values for 1979 – 2014 of temperature, specific humidity, precipitable water and wind speed vertical profiles up to 300 hPa and sea level pressure. There were only slight differences between NCEP-CFSR and ERA-Interim reanalyses results, without significant disagreements in trends or correlation patterns. NAO and AO monthly means from NOAA CPC database were also used.

To ensure that the correlations are not product of positive trends, correlations with detrended data were used, though detrending did not change the correlations

much. Differences between the areal averages of correlations were maximally 2% in both directions.

3. Testing point correlations

A testing point (TP) was selected in southern Estonia (58N, 26E) for teleconnection patterns. As expected, TP has high mutual correlations ($R > +0.5$) between temperature, specific humidity and precipitable water with surrounding areas covering the whole northern Europe in all seasons. There were also vast areas far from TP with significant correlations. For example, TP 1000 hPa temperature in winter had high negative correlation with 1000 hPa temperature over Greenland and Canadian Arctic (Figure 1). Similar patterns show also precipitable water (pw), specific humidity (q) and wind speed at 1000 hPa. Air pressure shows continuous negative correlation with the whole region from Baltic Sea region to Canadian Arctic.

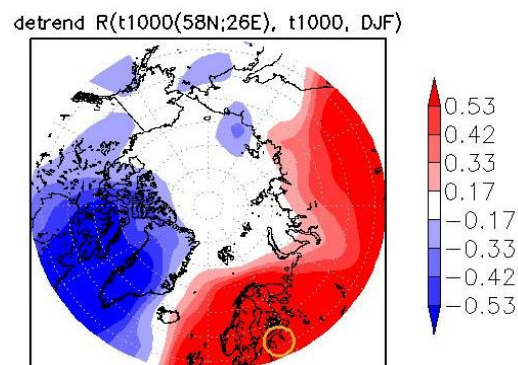


Figure 1. Winter 1000 hPa air temperature correlations between testing point and surrounding areas for period 1979 – 2014 (95% confidence level).

4. Different climatological patterns

To analyze the causality of teleconnection between Arctic and Baltic Sea region, warm and cold winters were selected (warmer and colder than 1 standard deviation accordingly) and subtracted from each other. The selection of winters has been done in two groups, according to 1) Estonian testing point 2) Arctic testing point from Baffin Bay (a center of the region of significant correlations). The results show that precipitable water (pw), specific humidity (q) (Figure 2) and wind speed at 1000 hPa are between two groups in opposite phase, while temperature and air pressure do not show any significant differences.

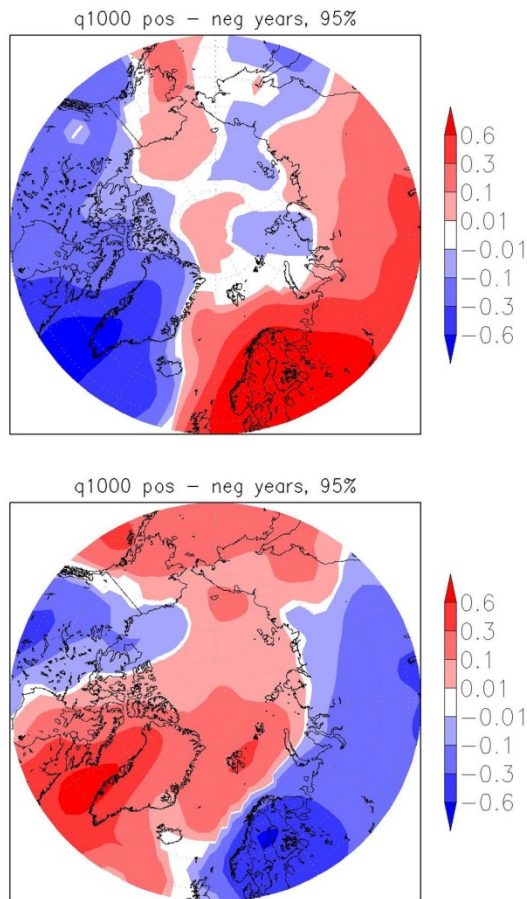


Figure 2. Difference maps in 1000 hPa specific humidity warm winters minus cold winter: (upper) winter selection based on Estonian testing point; (lower) winter selection based on Buffin Bay testing point (95% confidence level).

References

- Barnes, E. A. (2013) Revisiting the evidence linking Arctic amplification to extreme weather in mid-latitudes, *Geophys. Res. Lett.*, 40, 17, 4734–4739.
- Barnes, E. A. et al. (2014) Exploring recent trends in Northern hemisphere blocking, *Geophys. Res. Lett.*, 41, 638–644.
- Coumou, D. et al. (2014) Quasi-resonant circulation regimes and hemispheric synchronization of extreme weather in boreal summer, *Proc. Nat. Acad. Sci. USA*, 111, 12331–12336.
- Francis, J. A. and Vavrus, S. J. (2012) Evidence linking Arctic amplification to extreme weather in mid-latitudes, *Geophys. Res. Lett.*, 39, L06801, 6 pp.
- Hassanzadeh, P., Kuang, Z., and Farrell, B. F. (2014) Responses of midlatitude blocks and wave amplitude to changes in the meridional temperature gradient in an idealized dry GCM, *Geophys. Res. Lett.*, 41, 5223–5232.
- IPCC, Stocker, T. F. et al. (2013) *Climate Change*, Cambridge University Press, 1535 pp.
- IPCC, Pachauri, R. K. et al. (2014) *Climate Change*, Geneva, Switzerland, 151 pp.
- Peings, Y., and Magnusdottir, G. (2014) Forcing of the wintertime atmospheric circulation by the multidecadal fluctuations of the North Atlantic ocean, *Environ. Res. Lett.*, 9, 034018, 8pp.
- Petoukhov, V. et al. (2013) Quasiresonant amplification of planetary waves and recent Northern hemisphere weather extremes, *Proc. Nat. Acad. Sci.*, 110, 5336–5341.
- Sato, K., Inoue, J., Watanabe, M. (2014) Influence of the Gulf Stream on the Barents Sea ice retreat and Eurasian coldness during early winter, *Environ. Res. Lett.*, 9, 084009, 8pp.
- Screen, J. A., Deser, C., and Simmonds, I. (2012) Local and remote controls on observed Arctic warming, *Geophys. Res. Lett.*, 39, L10709.
- Screen, J. A., and Simmonds, I. (2013) Caution needed when linking weather extremes to amplified planetary waves, *Proc. Nat. Acad. Sci.*, 110, E2327.
- Screen, J. A., and Simmonds, I. (2014) Amplified mid-latitude planetary waves favour particular regional weather extremes, *Nature Clim. Change*, 4, 704–709.
- Screen, J. A. et al. (2014) Atmospheric impacts of Arctic sea-ice loss, 1979–2009: separating forced change from atmospheric internal variability, *Clim. Dyn.*, 43, 333–344.
- Serreze, M. C. et al. (2000) Observational evidence of recent change in the northern high-latitude environment. *Clim Change*, 46, 159–207.
- Simmonds, I. (2015) Comparing and contrasting the behaviour of Arctic and Antarctic sea ice over the 35-year period 1979–2013, *Ann. Glaciol.*, 56, 18–28.
- Simmonds, I., and Govekar, P. D. (2014) What are the physical links between Arctic sea ice loss and Eurasian winter climate? *Environ. Res. Lett.*, 9, 101003, 3 pp.
- Tang, Q. et al. (2013) Cold winter extremes in northern continents linked to Arctic sea ice loss, *Environ. Res. Lett.*, 8, 014036.
- Tang, Q., Zhang, X., and Francis, J. A. (2014) Extreme summer weather in northern mid-latitudes linked to a vanishing cryosphere, *Nature Clim. Change*, 4, 45–50.

Heavy metal accumulation in different parts of coniferous forest at Estonian ICP IM Vilsandi area

Naima Kabral

University of Tartu, Estonia, (naima.kabral@ut.ee)

International Cooperative Programme on Integrated Monitoring of Air Pollution Effects on Ecosystems in Estonia started 1994 at Vilsandi and Saarejärve area. Vilsandi area (0.78 ha) is located on Estonia's westernmost island (58°23' N, 21°50' E) and Saarejärve is located at the forested sub-catchment area (109.2 ha) of Lake Saare in eastern Estonia (58°39' N, 26°45' E). All samples were collected at one permanent plot in Vilsandi (105-year old Scots pine stand) and from two permanent plots at Saarejärve (125-years old Scots pine and 95-year old Norway spruce stands).

Heavy metal concentrations have been analysed in bulk deposition, throughfall, stemflow, soil water, needle fraction of litter, non-needle litter, bark, moss in open area, current year needles, soil organics, pine roots and moss under pine canopies.

Cd, Cr, Cu, Fe, Ni, Pb and Zn were analysed by Estonian Environmental Research Centre using acid digestion method in closed system pretreatment and atomic absorption spectrometry (AAS).

Heavy metal concentrations of Cu, Cd, Cr, Fe, Ni, Pb and Zn in current year needles during 1995-2014 show statistically significant increasing trend for Cu and decreasing trend for Pb. Pb concentrations are decreasing also in litter needles. In open area the bulk deposition of Cu, Pb and Zn show statistically significant decreasing trend. In stemflow samples Pb and Cd concentrations show significant decreasing trend.

Recurrence interval of Estonian precipitation extremes

Jüri Kamenik

Department of Geography, Institute of Ecology and Earth Sciences, University of Tartu, Tartu, Estonia
(kamenikmeister@gmail.com)

1. Introduction

Precipitation is the mostly variable climatic parameter in space and time but also one of the most important climatic variables having a direct effect on many kinds of human activity. Precipitation regime has an effect on water management, agriculture, water transport and other sides on the humans' everyday life (Alber, Jaagus, 2015).

Therefore, precipitation extremes – continuing periods with little or without any precipitation and extremely high daily precipitation amounts leading to droughts or floodings – are related to the severest damages to human activities in nearly all regions of the world. Because of this and the global climate warming are the reasons why the analysis of extreme precipitation and drought events and their long-term trends has become an important topic in climatological research. Also, an increase in the number of extreme precipitation events has been noticed and proposed to be generally related with possible climate warming in the future (Groisman et al. 2005; IPCC, 2013).

There have been done some climatological analysis related to precipitation extremes. For example, a climatological analysis demonstrated a significant increase in the frequency of precipitation extremes at 51 stations over the territory of Estonia during 1957–2009 (Tammets, Jaagus, 2013).

The purpose of this thesis is to study the regime of extreme precipitation in Estonia, and its task is to find various recurrence intervals and respective precipitation amounts for Estonian weather stations. In addition, this work will be evaluated for fitting of the fevd function.

2. Data and methods

The study is based on the Estonian Weather Service dataset from the period 1948–2013 comprising of 25 stations, but the exact length of the period is station-dependent. For statistical analysis, the R statistical programming language and its package extRemes (version ≥ 2.0) was used.

Specific statistical probability – recurrence interval, which gives an estimate of the likelihood of an event, such as an earthquake, flood or other to occur, was used in this study. To establish a recurrence interval for given daily precipitation amounts and vice versa, daily precipitation amounts corresponding to a given recurrence interval were fitted to a function, these intervals and corresponding precipitation amounts were calculated for each station by a specific distribution formula – GEV (generalized extreme value). Finally, the results were mapped using point kriging for spatial interpolation in Surfer (Golden Software, Inc.). Additionally, correctness of the fitting to GEV was evaluated.

3. Findings and discussion

Results show that corresponding daily precipitation amounts for 2-, 5-, 10-, 20- and 100-year recurrence interval varies over Estonia 26–36, 33–51, 40–62, 47–74 and 55–131 mm (figure 1), respectively. Recurrence interval for 20, 30, 40, 50, 60 mm daily precipitation amounts varies 1–1,2, 1,4–3,3, 2,6–10,5, 4,9–32,7 and 9,2–56,7 year, respectively. Mapping of these results confirm the respective field of values is very inhomogeneous. Results also revealed that the longer the period, the less frequent corresponding precipitation events are, and that these are more randomly distributed due to the growth of relative importance of randomness.

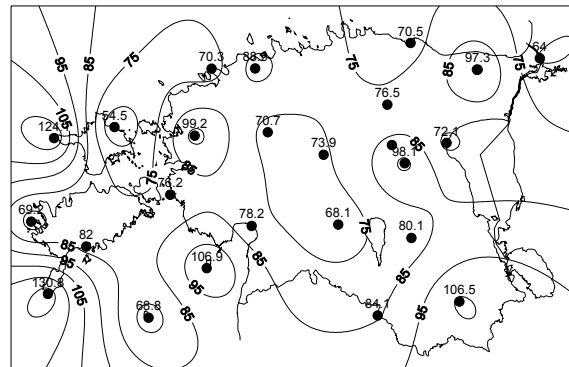


Figure 1. Corresponding daily precipitation amounts in mm for 100 years recurrence intervals

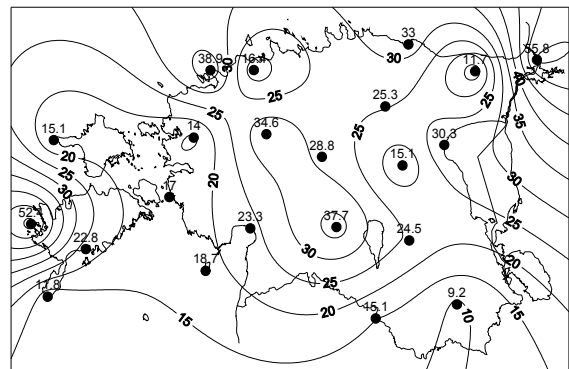


Figure 2. Recurrence interval for 60 mm daily precipitation amounts.

However, the corresponding daily precipitation amounts for 2 and 5 years recurrence intervals are longer in the mainland, but smaller in the islands and coastal regions. The primary reason for this is certainly a different type of surface: the land warms up faster and stronger. As a result there is a higher amount of convective precipitation which is characterized by higher accumulations and intensity. However, exceptions exist, such as in Jõhvi and Lääne-Nigula. These are caused by

specific events which fall inside the used time period and have an effect on the results. It has to be taken into consideration that there is a high share of randomness. This is caused by the convective nature of the majority of extreme precipitation events as well as more general large spatial and temporal variability of precipitation.

Recurrence intervals for smaller daily precipitation amounts between different stations are quite similar, being a year or a few months longer because the randomness is not so high – events with a daily precipitation amount between 20 and 30 mm occur at a higher frequency and the determining factor is probably the circulation.

The situation becomes considerably more complicated in the case of recurrence interval for 30 mm. Even greater territorial differences are observable at the recurrence intervals for 50 and 60 mm (figure 2): they differ between stations more than six times. The reason for these variabilities is possibly a less frequent occurrence of these events (daily precipitation amount of 50 mm and more) as well as the length of the time series – in the stations where the time series is longer, there is a greater probability of a rare precipitation event. Additionally, the location affects the recurrence interval – with the proximity to the sea where the convection is more inhibited, coastal stations have less (with a longer recurrence interval) events with large rainfall than those on the mainland.

50 to 70 years long empirical observation does not allow to find a 100-year event unless approximating the distribution of observations with some theoretical distribution for the dataset. Since the fitting to a function was used, an important issue exists: how well the selected function (GEV) is capable of fitting for these specific datasets used. Approximation graphs generated in R indicated that not all the stations fit well with GEV. Some stations, such as Sõrve, had a very good fit while stations like Võru did not. For stations that are not fitting well, alternatives should be sought to GEV.

Thus, these datasets were also tried to fit with other functions: usage `devd(type = c("GEV", "GP", "PP", "Gumbel", "Frechet", "Weibull", "Exponential", "Beta", "Pareto"))` – functions available in R are marked with quotation marks. Results show that usually only the GP and PP are at least same good as the GEV with feature that corresponding daily precipitation amounts for 50 and especially for 100 years recurrence interval does not fit very well with the observed extreme precipitation amounts. Some functions give mostly the same outcome as the GEV, e.g., Frechet, or do not work at all, e.g., Pareto, because the shape parameter < 0 or just does not fit, e.g., Exponential.

References

- Alber, R., Jaagus, J., 2015. Diurnal cycle of precipitation in Estonia. In the publishing
- Groisman, P. Y., Karl, R. T., Easterling, R. D., Knight, R. W., Jamason, F. P., Hennessy, J. K., Suppiah, R., Page, M. C., Wibig, J., Fortuniak, K., Razuvaev, N. V., Douglas, A., Førland, E. ja Zhai, P., 1999. Changes in the probability of heavy precipitation: Important indicators of climatic change. *Climatic Change* 42, 40.
- IPCC, 2013: Summary for Policymakers. In: *Climate Change 2013: The Physical Science Basis. Contribution of Working Group I to the Fifth Assessment Report of the Intergovernmental Panel on Climate Change* [Stocker, T.F., D. Qin, G.-K. Plattner, M. Tignor, S.K. Allen, J. Boschung, A. Nauels, Y. Xia, V. Bex ja P.M. Midgley (eds.)]. Cambridge University Press, Cambridge, United Kingdom ja New York, NY, USA. IPCC.
- Jaagus, J., Tammets, T., 2013. Climatology of precipitation extremes in Estonia using the method of moving precipitation totals. *Theoretical and Applied Climatology* 111, 623–639.

Development of the relationship between phytoplankton absorption coefficient and chlorophyll-*a* concentration for remote sensing applications for large Estonian lakes. Validation of MERIS standard and processed data

Evelin Kangro

Tartu Observatory, Tartu, Estonia (evelin.kangro@to.ee)

1. Abstract

The research focuses on the relationship between the phytoplankton absorption coefficient ($a_{ph}(442)$) and chlorophyll-*a* (Chl-*a*) concentration (C_{Chl-a}) in shallow and eutrophic Estonian lakes. Physical, chemical and biological parameters of lakes Peipsi and Võrtsjärv have been investigated regularly and thoroughly for decades. Cyanobacteria dominate in phytoplankton community in both lakes during summer and autumn but surface blooms are common in lake Peipsi (*Gloeotrichia echinulata*, *Aphanizomenon ssp.*, *Microcystis ssp.*). Phytoplankton is one of the most examined and monitored parameter that determines optical properties of the waterbody. It is also an indicator of ecological state of natural waters and as some species of cyanobacteria could be toxic to water organisms and humans it is important to provide a continuous monitoring of this parameter.

In addition to field measurements satellite products enable us to supplement and enrich our knowledge about the water quality seasonally and spatially. Nowadays implemented technology of satellite remote sensing has become a useful tool to monitor not only open sea areas but also optically complex inland waterbodies. During its ten year mission MERIS (MEdium Resolution Imaging Spectrometer) onboard of ENVISAT (ENVIRONMENTAL SATellite) has offered valuable information about water quality parameters of coastal waters and large lakes. MERIS products and algorithms have passed several improvements in order to minimize atmospheric scattering and therefore evaluate the water-leaving radiance reflectance more successfully (ESA, Evolution of the MERIS IPF, 2012).

Results of the study indicated that power law describes the positive relationship between $a_{ph}(442)$ and C_{Chl-a} most successfully (Figure 1). MERIS Case II water algorithm derives C_{Chl-a} values from absorption coefficients (442 nm) of phytoplankton ($a_{ph}(442)$) using empirical formulas (Doerffer & Schiller, 2007). The evolved algorithm based on data from 2010 to 2013 was also applied to MERIS satellite images (2010-2011) in order to investigate whether the reliability and accuracy of determining the concentration of Chl-*a* by lake-specific conversion factors will increase. MERIS 2nd and 3rd reprocessed water quality products were investigated, both corrected against adjacency effect caused by land pixels. Results showed that these products overestimated $a_{ph}(442)$ and therefore C_{Chl-a} values. Moreover, both reprocessed products failed with determining relative proportions of absorption of phytoplankton and other optically active substances in total absorption and therefore applied empirical algorithm did not improve C_{Chl-a} retrieval compared with MERIS standard algorithm. However, investigated products, especially

MERIS 2nd reprocessed products followed the seasonal and spatial variability of $a_{ph}(442)$ and C_{Chl-a} values rather well.

Validation results of products processed with MCI (Maximum Chlorophyll Index), FLH (Fluorescence Line Height) and MPH (Maximum Peak Height) processors were notably better (accordingly $R^2 = 0.63$, $R^2 = 0.69$, $R^2 = 0.71$) compared to MERIS standard products ($R^2 = 0.38$). These processors are specially designed for Chl-*a* retrieval from eutrophic waterbodies. Algorithms exploit spectral features in the red and near-infrared part of the reflectance spectrum and have also indicated suitability for inland and coastal waters (Alikas, Reinart, Kangro, 2008; Mathews, Bernard, Robertson, 2012).

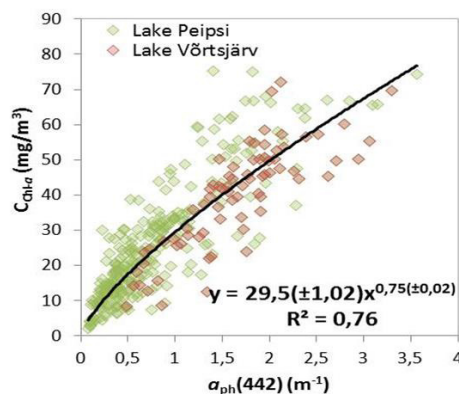


Figure 1. The empirical relationship between $a_{ph}(442)$ and C_{Chl-a} for large Estonian lakes based on *in situ* data.

References

- Alikas, K., Kangro, K., Reinart, A. (2010). Detecting cyanobacterial blooms in large North European lakes using Maximum Chlorophyll Index. *Oceanologia*, Vol 52, No 2, pp. 237-257.
- Doerffer, R., Schiller, H. (2007). The MERIS Case 2 algorithm. *International Journal of Remote Sensing*, Vol 28, No 3-4, pp. 517-535 pp. DOI: 10.1080/01431160600821127.
- ESA, Evolution of the MERIS IPF. (2012). http://earth.eo.esa.int/pcs/envisat/meris/documentation/MERIS_IPF_evolution.pdf
- Mathews, W., M., Bernard, S., Robertson, L. (2012). An algorithm for detecting trophic status (chlorophyll-*a*), cyanobacterial-dominance, surface scums and floating vegetation in inland and coastal waters. *Remote Sensing of Environment*, Vol 124, pp. 637-652.

Air ion formation events at Tahkuse Observatory, Estonia

Kaupo Komsaare, Urmas Hörrak, Hilja Iher

Institute of Physics, University of Tartu, Ülikooli 18, 50090 Tartu, Estonia (kaupo.komsaare@ut.ee)

1. Introduction

Air ions are known as carriers of electric current and space charge in the atmosphere, but they are involved also in the new particle formation called the aerosol nucleation. The importance of new particle formation and ionization on the Earth's climate has been discussed in many papers (Tinsley and Yu, 2004, Andreae and Rosenfeld, 2008). The nucleation events were frequently observed at many places in Europe (Manninen et al. 2010) and in the world (Kulmala et al. 2004). Intermediate air ions represent the charged fraction of the smallest stable aerosol particles in the diameter interval of 1.6–7.4 nm and can be used to study the new particle formation in the atmosphere (Hörrak et al. 2000). Cluster ions (below 1.6 nm) are almost always present in ground level measurements, they are produced by cosmic rays and natural radioactivity, eg. radon (Komsaare et al. 2004).

New particles of this size can grow above 60 nm and become condensation centers for water vapor and further cloud condensation nuclei (CCN), which affect the cloud dynamics and radiative balance of the Earth (Carslaw et al. 2010). The mechanism and species responsible for the nucleation are not well understood. One of the major contributor to new particle formation is sulphuric acid (Almeida et al. 2013) and, as recent studies show, also biogenic volatile organic compounds (Ehn et al. 2014). Although, the isoprene emissions from trees may suppress particle formation (Kiendler-Scharr et al. 2009).

2. Measurements

Tahkuse Observatory (58°31'N 24°56'E) is located in a sparsely populated rural region at eastern shore of Pärnu river. Nearest city is Pärnu, which is located about 25 km to south-west direction. Pärnu, with 50000 inhabitants, is located on the coast of the Gulf of Riga, at the east coast of the Baltic Sea (Figure 1).

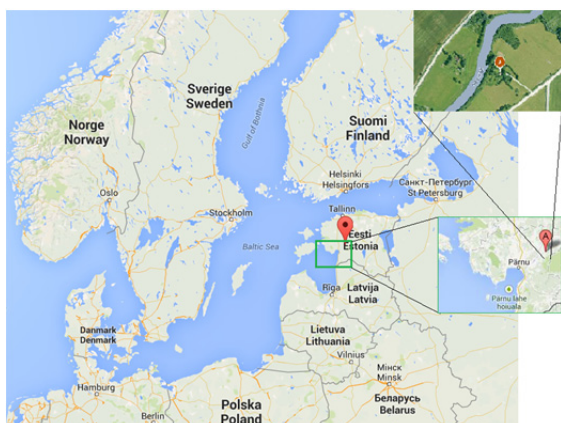


Figure 1. Location of Tahkuse Observatory

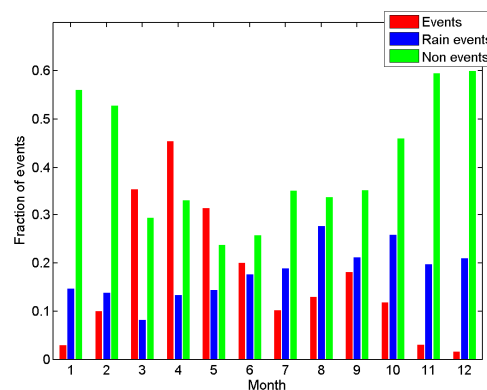


Figure 2. Annual variation of new particle formation events, rain events and non-events.

Air ion size distributions are measured by Air Ion Spectrometers (AIS), which covers size range 0.8–70 nm. (Hörrak et al. 2000, Mirme et al. 2007). Measurements took place during July 2003 to December 2014, measurement data are available for 3792 days, which is 90 % of total days.

3. Results and discussion

We have classified the intermediate air ion formation events at Tahkuse according to similar principles as (Hirsikko et al. 2007), but taking into account the specificity of new particle formation events at Tahkuse.

Four classes of intermediate air ion formation events are associated with photochemical nucleation mechanism in fair weather conditions, that we call as “events” and one class with ion generation during rain, we call those as “rain events”. In the case of “rain events”, the concentration of intermediate ions, depends on the rainfall duration and intensity. As the mechanism of ion formation during rain is totally different from nucleation mechanism, those events cannot be considered as nucleation events (Tamm et al. 2009). Commonly, during rainfall the concentration of negative intermediate ions was higher than that of positive ones, except some cases when snowfall with snowdrift occurred.

In the case of “events”, a growth of newly formed particles can be seen. According to the shape of particle growth followed by the evolution of particle size distribution, these events can be classified as follows:

Class Ia. The formation and subsequent growth of particles is well developed. The size distribution has no gap between the cluster (below 1.6 nm) and intermediate ions indicating that the cluster ions are involved in the nucleation.

Class Ib.1. Similarly to class Ia, the formation of particles starts from the cluster ion mode, but the growth of the particles is retarded before they reach the size of

5–10 nm, after that the event reverts. The reason of this type of event might be an insufficient concentration of nucleating vapors.

Class Ib.2. The particle formation does not start from the cluster ion mode and low concentration gap exists between cluster and intermediate ions at about 2 nm. The formation of particles can be seen starting from above 3 nm. The event might be due to the particle formation by the neutral nucleation with a subsequent diffusion-charging of particles by cluster ions. The contribution of ion-induced nucleation seems to be negligible.

Class II. The events are of unclear shape and/or with low concentration of intermediate ions. In the beginning, an event is similar to a Class Ia event, but the growth of new particles above the size of about 10 nm is difficult to estimate, due to the low concentration of new particles.

Non-event days. The air ion mobility distribution is reliably determined and there is a deep depression between the cluster ion mode and large ions with a nearly zero concentration of intermediate ions.

The examples of days associated with different event classes are presented in Figure 3 with the contour plots of the air ion size distribution variation.

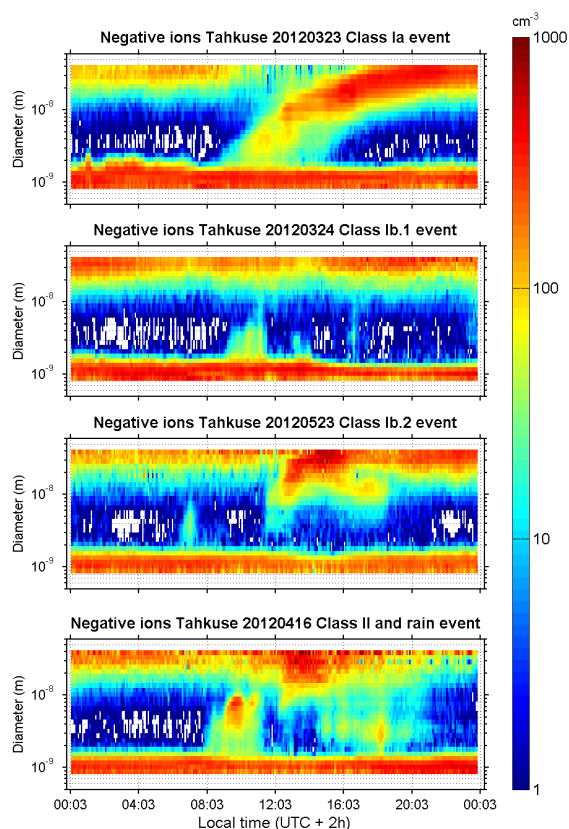


Figure 3. Classification of NPF events and the evolution of particle size distribution during different event days. Color code indicates particle concentrations in cubic centimeter of air.

4. Conclusions

During the study period, we found that the intermediate ion events and non-events had a clear seasonal variation with the maximum frequency during

spring and the second maximum during autumn (Figure 2). Days with nucleation events and rain-events form about 20% and 21% of total measurement days respectively, whereas 45% days was non-event days with no intermediate ion formation. Event distribution by classes was that class Ia form 15%, class Ib.1 23%, class Ib.2 9% and class II 43% of total events.

References

- Almeida, J. et al. (2013) Molecular understanding of sulphuric acid–amine particle nucleation in the atmosphere. *Nature* 502, 359–363, doi:10.1038/nature12663
- Andreae, M. O. and Rosenfeld, D. (2008) Aerosol-cloud-precipitation interactions. Part 1. The nature and sources of cloud-active particles, *Earth-Sci. Rev.*, 89, 13–41
- Carslaw, K. S., Boucher, O., Spracklen D. V., Mann G. W., Rae J. G. L., Woodward, S. and M. Kulmala, M. (2010) A review of natural aerosol interactions and feedbacks within the Earth system *Atmos. Chem. Phys.*, 10, 1701–1737
- Ehn, M. et al. (2014) A large source of low-volatility secondary organic aerosol. *Nature* 506, 476–479
- Carslaw, K. S. et al. (2010) A review of natural aerosol interactions and feedbacks within the Earth system. *Atmos. Chem. Phys.* 10, 1701–1737
- Hirsikko, A., Bergman, T., Laakso, L., Dal Maso, M., Riipinen, I., Hörrak, U and Kulmala, M. (2007) Identification and classification of the formation of intermediate ions measured in boreal forest, *Atmos. Chem. Phys.*, 7, 201–210
- Hörrak, U., Salm, J., and Tammet, H. (2000) Statistical characterization of air ion mobility spectra at Tahkuse Observatory: Classification of air ions, *J. Geophys. Res. Atmospheres*, 105, 9291–9302
- Kiendler-Scharr, A. et al. (2009) New particle formation in forests inhibited by isoprene emissions. *Nature Letters*. 461, 381–384, doi:10.1038/nature08292
- Komsaare, K., Mirme, A., Hörrak, U. (2004) Small air ion and radon measurements at Tahkuse Observatory. *J. Aerosol Sci.* 35, S1009–S1010
- Kulmala, M., Vehkamäki, H., Petäjä, T., Dal Maso, M., Lauri, A., Kerminen, V.-M., Birmili, W., McMurry, P.H. (2004) Formation and growth rates of ultrafine atmospheric particles: a review of observations, *Aerosol Science* 35, 143–176
- Manninen, H. E. et al. (2010) EUCAARI ion spectrometer measurements at 12 European sites – analysis of new particle formation events. *Atmos. Chem. Phys.*, 10, 7907–7927
- Mirme, A., Tamm, E., Mordas, G., Vana, M., Uin, J., Mirme, S., Bernotas T., Laakso, L., Hirsikko, A. and Kulmala, M. (2007) A wide-range multi-channel Air Ion Spectrometer. *Boreal Env. Res.* 12, 247–264
- Tammet, H., Hörrak, U and Kulmala, M. (2009) Negatively charged nanoparticles produced by splashing of water. *Atmos. Chem. Phys.*, 9, 357–367
- Tinsley, B.A. and Yu, F. (2004) Atmospheric Ionization and Clouds as Links between Solar Activity and Climate, in *Solar Variability and its Effect on Climate*, Geophys. Monograph Series, 141, 321–340

Long-term model study of nutrient and detritus dynamics in the Baltic Sea

Kõuts M.⁽¹⁾, Raudsepp U.⁽¹⁾, Maljutenko I.⁽¹⁾, Treimann M.L.⁽²⁾

⁽¹⁾ Marine Systems Institute at Tallinn University of Technology, Akadeemia tee 15a, Tallinn. (mariliis.kouts@msi.ttu.ee)

⁽²⁾ Institute of Physics at University of Tartu, Riia 142, Tartu

1. Introduction

Eutrophication resulting from direct and indirect input of nutrients is considered one of the major environmental problems in the sub-basins of the Baltic Sea. Stronger eutrophication is manifested through increased summer cyanobacteria blooms and expanding hypoxia. It has been recognized that cycling of organic matter is a considerable source of nutrients in the Baltic Sea. Nutrient pools in the sediments have increased over the last decades (Gustafsson et al. 2012). Our study aims at understanding the eutrophication of the Baltic Sea by looking at spatial patterns and temporal variation of biogeochemical parameters. We are focusing on spatial detritus dynamics during the period of 40 years in the Baltic Sea.

2. Materials and Methods

We used the regional 3-dimensional coupled ecosystem model ERGOM. The model holds 3 sources of nutrients: NO_3 , PO_4 , NH_4 ; 3 functional groups of phytoplankton – diatoms, dinoflagellates and cyanobacteria; and also factors such as oxygen, zooplankton, detritus and iron-phosphate (FePO_4).

We focused on the spatial variation, temporal scale and vertical distribution of the study variables in shallow and deep stations.

3. Results and discussion

We found that chlorophyll-a (sum of functional algal groups) mostly represents the distribution of diatoms and follows high surface concentration of nutrients in coastal areas and river estuaries (Fig 1a).

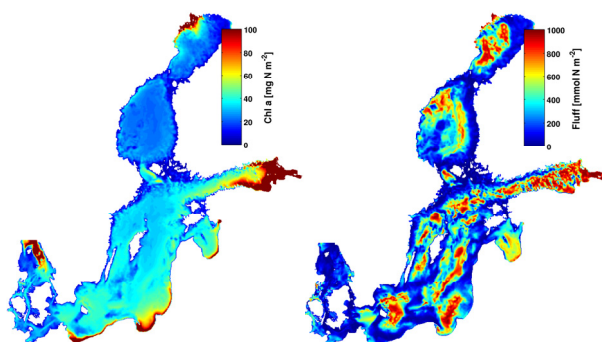


Figure 1. a) Integral Chlorophyll-a distribution and b) Detritus distribution on the bottom of the Baltic Sea.

Detritus distribution on the sea bottom is correlated with deep, low-oxygen areas and river estuaries (Fig 1b). High amounts of NO_3 , PO_4 and NH_4 concentrate in the bottom layer and sediments in detritus accumulation areas.

Analysis of time series indicates that seasonality is the dominant component of nutrient and primary production cycles in the Baltic Sea. Still, vicinity of rivers hinders seasonality. While shallow stations display a coupled seasonal pattern of bottom and surface variables, deep stations lack seasonal variability in the bottom. Seasonal amplitudes were similar for nutrients and oxygen with peak values in winter and low in summer. Detritus has less apparent amplitude with high values in summer and decrease in winter.

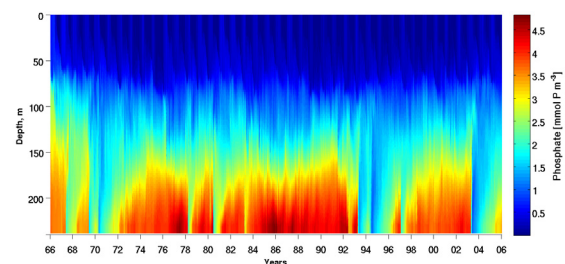


Figure 2. Vertical time series of phosphate in the Gotland Deep.

Analysis of vertical distribution revealed that the mixed surface layer extends down to 70m depth, followed by strong halocline and less stratified deep layer starting at about 100m depth. In shallow areas the water column is mostly ventilated throughout the year with nutrient coupling between surface and bottom. In deep areas, however, the stagnant water column below halocline is ventilated only during MBIs. Only a fraction of nitrates and phosphates (fig 2) is mixed up to the surface layer during winter and consumed by phytoplankton in spring. High amounts of PO_4 apparent on anoxic bottoms are probably swept to the upstream basin during MBIs. After the MBIs higher amounts of the generated NO_3 are mixed upward from the bottom and probably transported further to downstream basins. We speculate that NO_3 increases below the halocline due to transport from upstream basin to the intermediate layer during no inflow

4. Conclusions

Spatial distribution of phytoplankton and nutrients on the surface correspond to each other. Detritus and nutrients on the bottom tend to concentrate in deep, low-oxygen areas.

Seasonal cycle of the study variables is dominant in shallow areas (water depth less than 60 m approximately). Nutrients and organic matter are actively recycling there. Bottom seasonality is stronger than surface seasonality, except for river estuaries, where seasonality is hindered altogether.

Deep areas have strong surface seasonality and weak bottom seasonality. Deep areas are storage areas for organic matter (trapped and buried there), but become

source of nutrients during MBIs. Halocline is sort of a barrier for nutrients from leaking to the upper layer, but is not 100% effective as there still seems to be a slight nutrient exchange between bottom and surface layers throughout the year.

Horizontal transport of nutrients from upstream basins of the Baltic Sea is considerable source of nutrients for downstream basins. In particular it may explain peculiar behavior of the Gulf of Finland.

References

- Gustafsson, B.G., Schenk, F., Blenckner, T., Eilola, K., Meier, H.E.M., Müller-Karulis, B., Neumann, T., Ruoho-Airola, T., Savchuk, O.P., Zorita, E. (2012). Reconstructing the Development of Baltic Sea Eutrophication 1850–2006. *Ambio* 2012, pp. 41:534–548.

Forest belowground carbon cycle in Estonia – Vilsandi case-study

Kaie Kriiska, Jane Frey, Ülle Napa, Naima Kabral, Ivika Ostonen

Institute of Ecology and Earth Sciences, University of Tartu, Tartu, Estonia (kaie.kriiska@ut.ee)

1. Introduction

Carbon (C) stored in soils worldwide exceeds the amount of carbon stored in phytomass and the atmosphere (Scharlemann et al, 2014). Climate change, accompanied by increasing temperature and precipitation in the boreal region is likely to accelerate soil organic carbon sequestration and decomposition, increase CO₂ emissions from soil and alter soil fertility (EEA Report, 2012). Thus, better understanding of belowground biogeochemical carbon cycle is essential for predicting changes in terrestrial ecosystems as well as global carbon cycle, improving carbon management and climate change mitigation.

Carbon fixed in trees and understory is cycled through litter into soil where it is released back into the atmosphere by autotrophic (plant) and heterotrophic (soil microbial and animal) respiration (IPCC, 2013).

Current study is part of a PhD project, which aim is to determine main soil C input and output fluxes, and compile soil C budget for different coniferous forest types in Estonia.

2. Methods

Vilsandi ICP Integrated Monitoring site is one of the best studied forest stands in Estonia. Vilsandi forest is a *Fragaria* site type on Eutri-Calcaric Arenosol, Scots pine (*Pinus Sylvestris*) being the dominant tree species.

Below ground carbon cycle consists of several input and output components that were measured at the Vilsandi study site.

Field measurements included:

Soil carbon inputs

- Aboveground tree litter is collected 6-9 times per year with 10 litter traps, Ø 0.8 m. Litter is sorted into pine needles and other litter, dried at 70°C after which litter mass is measured and litter chemical composition is determined.
- Fine root biomass, net primary production (NPP) and turnover rates of understory and dominant tree species. Soil coring was used to estimate fine root (<2 mm) biomass and 15 soil cores (diameter 38 mm) were taken in September 2011. Soil cores were divided into five layers by depth: forest floor, 0–5 cm, 5–10 cm, 10–20 cm and 20–30 cm. Ingrowth net method (Lukac & Godbold, 2010) was used for estimating annual fine root NPP of pine and understory plants. In September 2011, 100 net sheets (1.2 mm mesh size, 7 cm width and 25 cm length) were inserted vertically into the soil with the help of a steel plate in three random lines in the stand. The root nets were collected in Sept 2012, 2013 and 2014. To extract the nets, the soil blocks with net inside it were excavated and transported to the lab, where fine roots penetrating the net were shortened to 1 cm on either side of the net to create a 'virtual' core 2 cm thick, 7 cm wide and 15-20 cm deep, then removed

from the net, washed free of soil particles, dried at 70°C and weighed. Root turnover rate (year⁻¹) was calculated as annual root production (g m⁻² year⁻¹) divided by mean fine root biomass (g m⁻²).

Soil carbon outputs

- Soil respiration measurements are carried out monthly during the vegetation period with infrared closed chamber gas analyser (EGM-4, PP Systems). In 2015, total and heterotrophic respiration is measured separately. The latter was done by trenching, where 200 mm Ø PVC tubes were installed in 50 cm depth in the soil.
- Litter decomposition studies. Needle and fineroot litterbags and α-cellulose was placed on the O and in A soil horizons and mass loss is measured during 3 years.
- In addition soil temperature and precipitation are measured daily.

3. Results

The most dynamic forest biomass component is litter, thus the major part of carbon flow into forest soil consists of continually renewed fine roots and aboveground litterfall. Aboveground litter input into soil is approximately 4.8 t ha⁻¹ yr⁻¹, of which pine needles constitute 55% (Kabral, 2015). Understory fine root NPP is 0.5 t ha⁻¹, constituting a quarter of total belowground litter NPP in Vilsandi stand.

In 2014, soil respiration varied between 48-121 mg C m⁻² h⁻¹, depending on soil temperature and moisture conditions (Figure 1).

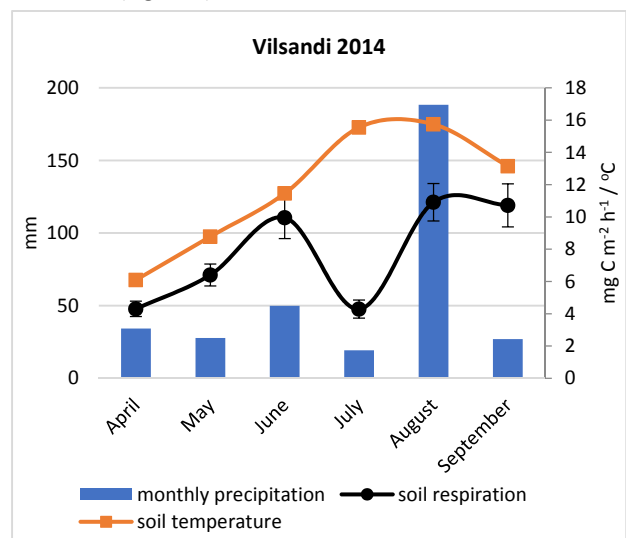


Figure 1. Soil temperature, precipitation and soil respiration during vegetation period in Vilsandi (2014).

A-cellulose decomposition was studied in order to estimate the impact of different environmental factors

(eg moisture, temperature) on the decay rate of organic matter, since all plant tissues contain cellulose. α -cellulose has the fastest decomposition rate because it is a homogeneous material and does not contain other complex organic compound, eg lignin. The rate of needle decomposition was twice as fast as fine root decay, depending on the chemical composition of the material and on the medium where it occurs (Figure 2).

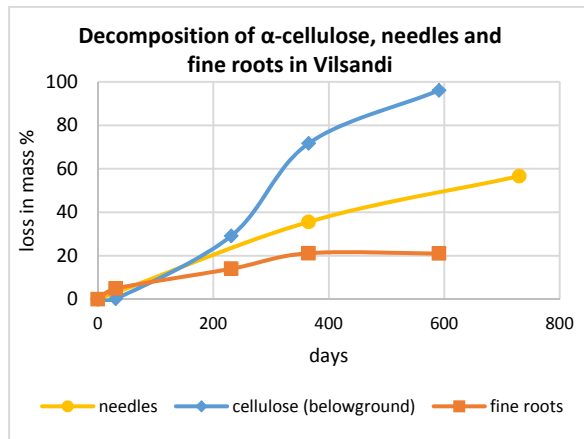


Figure 2. Decomposition of α -cellulose, needles and fine roots in Vilsandi.

Study results will be further discussed.

4. Conclusions and discussion

Above ground litterfall and fine root decomposition accompanied by soil respiration are major factors contributing to soil carbon cycle. Large scale forest soil carbon dynamics have not been studied before in Estonia. In the frame of current PhD project belowground carbon budget of 8 coniferous forest site types (including Vilsandi) across soil fertility and moisture gradients is studied. Based on collected empirical data, Yasso07 model will be applied to estimate soil organic carbon stock changes on the

national scale. Research results will be reported in the national greenhouse gas emissions inventory under the UNFCCC and the Kyoto Protocol.

Acknowledgements

This study was supported by grant No. 7452 of the Estonian Science Foundation, by Target projects No. SF0180025s12 and IUT2-16 of the Ministry of Education and Science of Estonia and by the EU through the European Regional Development Fund (Centre of Excellence ENVIRON). Soil respiration measurements and chemical analyses were supported by Environmental Investment Centre projects No. 3793 and 6250.

References

- EEA Report (2012). Climate change, impacts and vulnerability in Europe 2012. An indicator-based report. European Environment Agency. 304 pp
- IPCC (2013). Climate Change 2013: The Physical Science Basis. Contribution of Working Group I to the Fifth Assessment Report of the Intergovernmental Panel on Climate Change [Stocker, T.F., D. Qin, G.-K. Plattner, M. Tignor, S.K. Allen, J. Boschung, A. Nauels, Y. Xia, V. Bex and P.M. Midgley (eds.)]. Cambridge University Press, Cambridge, United Kingdom and New York, NY, USA, 1535 pp
- Kabral, N (2015). Vilsandi kompleksseire. Eesti Keskkonnauuringute Keskus, Tallinn, 39 pp
- Lukac, M., Godbold, DL. (2010). Fine root biomass and turnover in southern taiga estimated by root inclusion nets. Plant and soil, 331 (1-2), 505-513
- Scharlemann, J., Tanner, E., Hiederer, R., Kapos, V (2014). Global soil carbon: understanding and managing the largest terrestrial carbon pool. Carbon Management, 5(1), 81-91

Verification of WRF-ARW model in Belarus

Palina Lapo, Yaroslav Mitskevich

Center of Hydrometeorology And Control of Radioactive Contamination And Environmental Monitoring of the Republic of Belarus, Minsk, The Republic of Belarus (Polly_LO@tut.by), Faculty of Geography, Belarusian State University; National Ozone Monitoring Research and Education Center, Minsk, Belarus (yaroslav.mitskevich@gmail.com)

1. Introduction

Mesoscale modeling with the Weather Research & Forecasting (WRF) system makes it possible to predict different types of hazards and typical weather events. Since 2013 the Hydromet Center of Belarus has used the WRF-ARW model for operational forecasting for the territory of our country.

Presently computing power permits to realize operational modeling four times a day, with lead time of 48 hours and two types of resolution – 15 and 3 km. WRF is now widely used for synoptic weather research and prediction in Belarus.

In the present study, we try to analyze the features of the model for Belarusian territory. Also we test different model parameterizations and try to find the best configuration for different weather conditions.

2. Model verification

We have evaluated different parameterizations for the territory of our country for the period of over two years. The evaluation has been conducted for all seasons, including cold and warm frontal events as well as anticyclones. Verification of modelling results made it possible to define model parameterizations giving the smallest forecast error for the territory of Belarus.

For verification of modelling results we have used the MET (Model Evaluation Tools) package, utilizing the point-stat and grid-stat methods. We select the following parameters: geopotential height and temperature on 500, 700 and 850 hPa isobaric levels, surface pressure, temperature at 2 meters, and precipitation amount. Furthermore, we evaluate prognostic and actual variability.

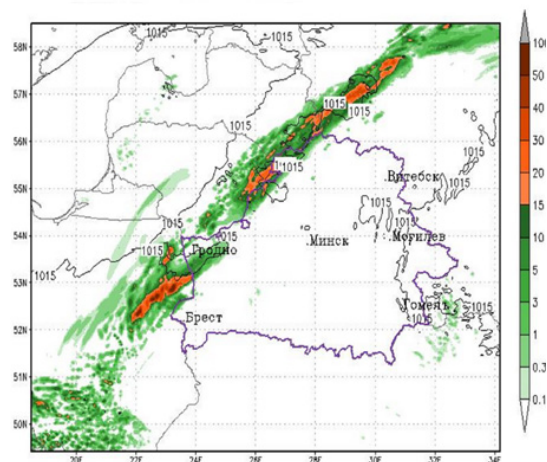


Figure 1. Surface pressure and precipitation 12 UTC 01-08-2014, 3 km resolution, Belarus

For forecasts evaluation, we have used such characteristics as absolute error, relative error, standard

deviation, mean-square error, correlation and other indexes.

The most difficult part for accurate forecasts was the prediction of summertime severe convection events, that is why it was really interesting to verify model precipitation forecasts in 3 km resolution, giving the opportunity to predict thunderstorms on cold atmospheric fronts and in stable air masses.

Model verification gives different results for different parts of Belarus, the biggest mean-square error being in the eastern part. The smallest error can be seen in central and western parts of Belarus.

Table 1. Verification results of surface temperature prediction for the territory of Belarus on 24 hour

Part of the country	ME	MAE	RMSE	EDEV	R
East	1.71	1.94	2.51	1.83	0.55
West	0.30	1.44	1.67	1.64	0.73
All territory	0.89	1.62	1.78	1.64	0.66

3. Present study

The accuracy of numerical weather prediction depends on many factors: physical processes, accuracy of the input data, the possibility of data assimilation in weather research and forecasting.

The problem of models verification and development is particularly important with a large amount of available information and with various numerical prediction models available. Verification of numerical mesoscale forecast to pass a variety of changes, adaptation of new data has a number of features due to the high spatial and temporal resolution of meteorological parameters fields.

In 2015 year we try to assimilate different types of data sources into the WRF Preprocessing System to improve its geographical data.

For example, at this moment the absolute terrain height has been assimilated. We assimilate topography data for the territory of Belarus and Europe with a resolution of 3 arc sec from the SRTM (Shuttle Radar Topography Mission), which is an international research project to generate the most complete high-resolution digital topographic database.

These data assimilation helped us to improve the representation of different local features in the WRF model, e.g. turbulence, local precipitation and

temperature differences, which deal with high resolution topography.

4. Conclusions

Verification results demonstrate good predictive skill of the WRF model for thunderstorms development and other severe events forecasting in different seasons.

The evaluation of the modeling results obtained with assimilated satellite data has helped to improve accuracy of the local forecasts for all parts of Belarus.

Now we try to verify the WRF modelling results obtained with other assimilated geographical data, e.g. albedo.

References

- Stensrud David J. (2007) Parametrization schemes: keys to understanding numerical weather prediction models, Cambridge University Press, pp. 460
- Bouttier F., Kelly G. (2001) Observing-system experiments in the ECMWF 4D-Var data assimilation system. Q J R Meteorol Soc., 127, pp.1469-1488

Filling the gaps: Applying the WRTDS model on interpolation of the major Latvian river loads to the Gulf of Riga

Aigars Lavrinovičs¹, Rita Poikāne¹, Bärbel Müller – Karulis^{1,2}

¹Latvian Institute of Aquatic Ecology, 8 Daugavgrivas str., LV-1007, Riga, Latvia (aigars.lavrinovics@lhei.lv, rita.poikane@lhei.lv)

²Baltic Nest Institute, Baltic Sea Centre, Stockholm University, SE-106 91, Stockholm, Sweden (barbel.muller.karulis@su.se)

1. Introduction

According to the EU's Marine Strategy Framework Directive, countries surrounding the Baltic Sea are required to achieve a good ecological status of the Baltic marine environment by the year 2020. In order to successfully accomplish this goal the Baltic Sea countries have agreed to fulfill the Baltic Sea Action Plan and to collaborate with HELCOM. The main prerequisite for obtaining the goal of a healthy Baltic Sea is an effective national program of environmental health that includes effective monitoring strategy of pollution loads from land to the sea.

The main sources of pollution from Latvia to the Gulf of Riga are the major Latvian rivers – Daugava, Gauja, Lielupe and Salaca. The archives of continuous measurements of the river runoff as well as concentrations of nutrients in these rivers date back to 1977 while data of periodic hazardous substance concentration measurements are available from early eighties. Due to the budget cuts in 2009 the frequency of water quality monitoring for the main Latvian rivers was reduced from monthly to 3 – 4 times per year which is insufficient to effectively track the variance of pollution loads.

2. Materials and methods

A common practice of obtaining the missing data of monitoring time-series is to use model estimations. Therefore, considering the recommendations of HELCOM LOAD expert group the missing water quality data was calculated using a linear interpolation method. Among many models of this kind the Weighted Regressions on Time, Discharge and Season (WRTDS; Hirsch, 2010) was found to be more suitable than others.

The accuracy and agreement between model data and observations were estimated by Pearson's R value.

To find more effective sampling strategy for the national monitoring program, a Monte Carlo test (Metropolis & Ulam, 1949) was applied for three different scenarios – the present scenario, sampling at three months with highest river runoff, and skipping the sampling at three months with the lowest river runoff. Each sampling scenario was simulated for the period from 1991 to 2008 and the bias and relative deviation were compared between the generated time-series where missing data are filled with WRTDS model results according to pre-defined sampling scenario and the original time-series without gaps.

3. Results and main conclusions

The best interpolation results were obtained for nitrates in all the rivers showing the Pearson's R in the range of 0.70 and 0.87, while BOD5 showed lower

Pearson's R values (between 0.53 and 0.64) than other water quality parameters.

The available time-series for concentrations of hazardous substances are too irregular to use it for reliable interpolation.

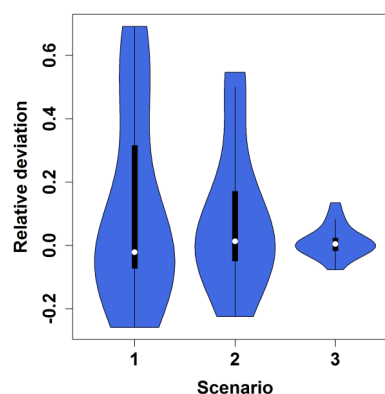


Figure 1. Relative deviation from the observations of interpolated NO_{2+3} loads of river Daugava according to the sampling strategy. 1 – present sampling scenario; 2 – sampling at high river runoff months; 3 – sampling scenario excluding months with low river runoff.

The Monte Carlo test results show that for all the water quality parameters in all the rivers included in this study, the smallest deviation from the median observed pollution load can be obtained, when using the sampling strategy, which excludes the months of low river runoff. For the time-series filled with interpolations, the maximal deviation above and below the median measured river loads would decrease by 56 and 18 % respectively if measurements of nitrate concentrations in River Daugava were taken from October to June (Figure 1, scenario 3). Therefore it is highly recommended that the national monitoring program of inland water quality is improved and the sampling strategy provides higher number of samples per year, or at least the high river runoff months are picked for sample collection.

References

- Hirsch, R. M., Moyer, D. L. and Archfield, S.A., 2010. Weighted Regressions on Time, Discharge, and Season (WRTDS), with an application to Chesapeake Bay river inputs. *Journal of the American Water Resources Association*. 46(5): 857-880.
- Metropolis, N., Ulam, S., 1949. The Monte Carlo method. *Journal of the American Statistical Association*. 44(247): 335-341.

Atmospheric conditions forcing large volume changes (LVCs) and major inflows (MBIs) to the Baltic Sea

Andreas Lehmann

GEOMAR Helmholtz Centre for Ocean Research Kiel, Germany

Abstract

The salt budget of the Baltic Sea is determined by a balance between saline inflow from the Kattegat and brackish water outflow from the Baltic through the Danish Straits. Generally, during dry periods with less river runoff the mean salinity of the Baltic Sea increases while during wet periods a decrease will happen. These long-term changes are overlaid by the atmospheric-driven water exchange between North Sea and Baltic Sea. The salinity and the stratification in the deep basins are linked to the occurrence of Major Baltic Inflows (MBIs) of higher saline water of North Sea origin, which occur sporadically and transport higher saline and oxygenated water to deeper layers. These major inflows are often followed by stagnation periods with no strong saline inflows, during which the permanent halocline weakens, even disappears in some basins, and extended areas of oxygen deficiency develop in those regions where the salinity stratification remains.

Since the mid-1970s, the frequency and intensity of MBIs have decreased. They were completely absent between February 1983 and January 1993. However, in spite of the decreasing frequency of MBIs, there was no obvious decrease of larger Baltic Sea volume changes (LVCs). A LVC is defined by the volume change of at least 60 km^3 . LVCs can be identified from the sea level change at Landsort which is known to represent the mean sea level of the Baltic Sea very well. Strong inflows leading to LVCs are associated with certain sequences of atmospheric flow patterns over the larger North Atlantic/North European region. Most effective inflows occur if about a month before the main inflow period eastern air flow with anticyclonic vorticity over the western Baltic prevails. These conditions reduce the mean sea level of the Baltic Sea and lead to an increased saline stratification in the Belt Sea area. An immediate period of strong to very strong westerly winds trigger the inflow and force LVCs/MBIs. Furthermore, most effective inflows occur if deep cyclones follow particular pathways in a certain frequency over the Baltic Sea area. There are three main routes, one is approaching from the west at about $58 - 62^\circ\text{N}$, passing the northern North Sea, Oslo, Norway and the Island of Gotland, while a second, less frequent one, is approaching from the west at about 65°N , crossing Scandinavia south-eastwards passing the Sea of Bothnia and entering Finland, and a third very frequent one entering the study area north of Scotland turning north-eastwards along the coast of Scandinavia.

In December 2014 a MBI comparable to the very strong events in December 1951 and in January 1993 happened. It occurred after a period of easterly winds in November leading to an extremely low mean water level (-0.4 m) of the Baltic Sea on 2nd December. On 24th December after the passage of a number of deep cyclones the water level increased to 0.5 m above mean water. The sea level difference was associated with a total water volume change of about 300 km^3 . This LVC/MBI will be discussed in detail.

Circulation scheme of the Baltic Sea – based on the 40-year simulation with GETM

Ilja Maljutenko

Marine Systems Institute at Tallinn University of Technology (ilja.maljutenko@msi.ttu.ee)

1. Introduction

The general circulation of the Baltic Sea has been characterized as cyclonic in all sub-basins based on numerous measurements and model simulations. From the long-term hydrodynamical simulation our model results have verified the general cyclonic circulation in the Baltic Proper and in the Gulf of Bothnia, but the Gulf of Finland and the Gulf of Riga have shown tendency to anticyclonic circulation.

2. Model implementation

We have applied the General Estuarine Transport Model (GETM) for the period of 1966 – 2006 with a 1 nautical mile horizontal resolution and density adaptive bottom following vertical coordinates to make it possible to simulate horizontal and vertical density gradients with better precision. The atmospheric forcing from dynamically downscaled ERA40-HIRLAM and parametrized lateral boundary conditions are applied.

3. Results

Model simulation show close agreement with measurements conducted in the main monitoring stations in the BS during the simulation period. The geostrophic adjustment of density driven currents along with the upward salinity flux due to entrainment could explain the anticyclonic circulation and strong coastal current. Mean vertical velocities show that upward and downward movements are forming closed vertical circulation loops along the bottom slope of the Baltic Proper and the Gulf of Bothnia. The model has also reproduced patchy vertical movement across the BS with some distinctive areas of upward advective fluxes in the GoF along the thalweg. The distinctive areas of deep water upwelling are also evident in the Gdansk Basin, western Gotland Basin, northern Gotland Basin and in the northern part of the Bothnia Sea.

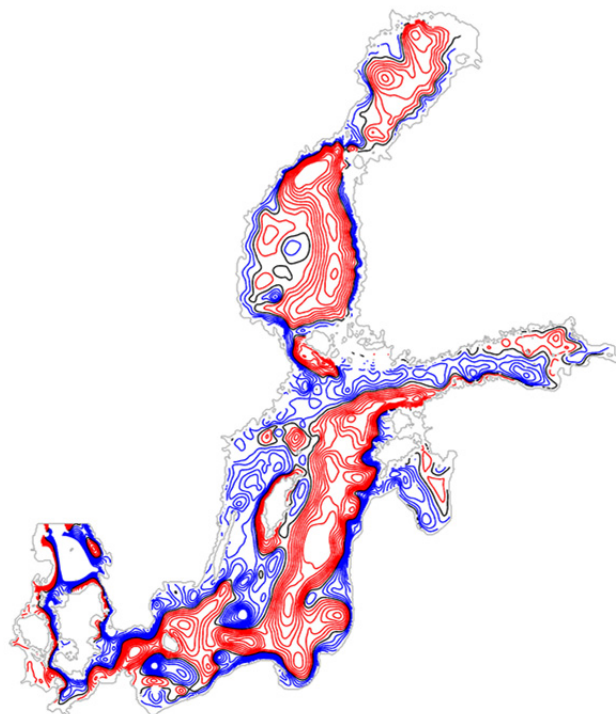


Figure 1. Stream function calculated from 40 year mean velocity field averaged over upper 10 m. Red contours denote cyclonic and blue contours denote anticyclonic shear.

Continuous and high-frequency measurements in limnology: History applications and future challenges

Pille Meinson, Agron Idrizaj, Peeter Nõges, Tiina Nõges, Alo Laas

Center for Limnology, Institute of Agricultural and Environmental Sciences, Estonian University of Life Sciences, Estonia
(pille.meinson@student.emu.ee)

1. Introduction

Over the past 15 years, an increasing number of studies in limnology has been using data from high-frequency measurements (HFM). This new technology offers scientist a chance to investigate lakes at time scales that was not possible earlier and places where regular sampling would be complicated or even dangerous. This has allowed capturing the effects of episodic events or extreme events, e.g. typhoons on lakes. Until recently, the majority of standard lakes monitoring programs were based on manual in situ measurements that can be time-consuming and costly and lack both the necessary spatial coverage as well as an appropriate sampling frequency Vos et al. (2003). Time and reliability issues can be efficiently addressed by replacing manual measurements with automatic high-frequency measurements. Even though the automatic recording is vulnerable to vandalism, biofouling, and occasional failures in the system, while maintenance causes gaps in time series Dur et al. (2007). In this presentation we review the various fields of limnology such as monitoring, studying highly dynamic processes, lake metabolism studies, and budget calculations where HFM has been applied, and the study purposes which have benefited most from the application.

2. Material and methods

For the literature search, we used Google Scholar citation database. Search terms "lake*" and "high frequency data". In order to focus on recent research only, articles published between 2000 – 2015 were considered. This procedure resulted in total of 1730 records. We selected studies in which measurement intervals of ≤ 60 minutes were used and the deployment time was at least six hours. Papers using measurement intervals longer than one hour or deployment times less than six hours were excluded. The screening yielded in a final list of 154 papers that corresponded to our criteria.

3. Results

According to our meta-analysis, more than 2/3 of the HF studies in lakes were carried out either in North-America or Europe (Fig. 1.) that, on one hand, reflects the global distribution of lakes which latitudinal maximum by area is located in the northern temperate zone between 40°N and 70°N (Lehner and Döll 2004). Two HFM most commonly collected are water temperature and dissolved oxygen (DO). High-frequency recordings of nutrient levels such as nitrate (NO_3^-) and phosphates (PO_4^{3-}) in lakes are scarce, although, nitrate levels are often measured in rivers Sherson et al. (2012, 2015), Feng et al. (2013).

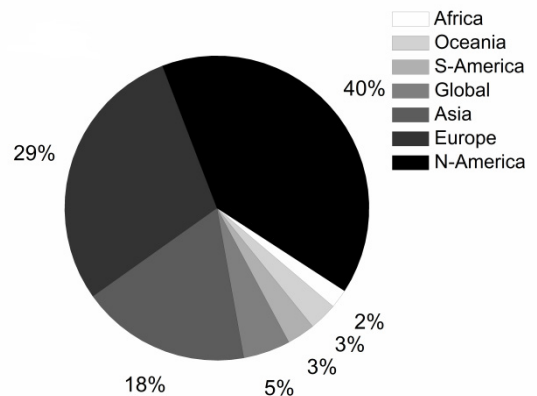


Figure 1. Geographical distribution of high-frequency studies.

The majority of studies using HFM were made in lake ecology (56%) covering fields such as low maintenance monitoring and lake metabolism measurements, followed by physical limnology (28%) dealing with hydrological processes and different water movements and studies in geochemical limnology (16%; measurements of CO_2 , nitrates etc.).

References

- Dur, G., F. G. Schmitt, and S. Souissi (2007) Analysis of high frequency temperature time series in the Seine estuary from the Mareil autonomous monitoring buoy, *Hydrobiol.*, 588., pp. 59-68
- Feng, Z., K.E. Schilling, and K.-S. Chan (2013) Dyanmic regression modeling of daily nitrate-nitrogen concentrations in a large agricultural watershed, *Environ. Monit. Assess.*, 185., pp. 4605-4617
- Lehner, B. and P. Döll (2004) Development and validation of a global database of lakes, reservoirs and wetlands, *J. Hydrol.*, 296., pp. 1-22
- Sherson, L. (2012) Nutrient dynamics in a headwater stream: use of continuous water quality sensors to examine seasonal, event, and diurnal processes in the east fork Jemez river, NM. Ph.D. thesis.Univ. of Oregon.
- Sherson, L. R., D. J. Van Horn, J. D. Comez-Velez, L. J. Crossey, and C. N. Dahm (2015) Nutrient dynamics in an alpine headwater stream: use of continuous water quality sensors to examine responses to wildfire and precipitation events, *Hydrol. Process*, doi: [10.1002/hyp.10426](https://doi.org/10.1002/hyp.10426)
- Vos, R. J., J. H. M. Hakvoort, R. W. J. Jordansand B. W. Ibelings (2003) Multiplatform optical monitoring of eutrophication in temporally and spatially variable lakes, *Sci. Total Environ*, 312., pp. 221–243

Coastal upwelling in the SE Baltic Sea: basic statistics

Toma Mingelaite

Klaipeda University, Lithuania (toma.mingelaite@gmail.com)

1. Introduction

Upwelling in the global ocean has a great importance to coastal productivity and regional climate. Smaller water bodies like the Baltic Sea are not an exception as well.

Baltic Sea is relatively small and shallow sea, which is connected with Atlantic Ocean via Danish narrow straits. Since Baltic Sea is a semi- enclosed basin, the winds from all directions can cause upwelling at some part of the coast (Lehmann and Myrberg, 2008). Although the spatial scale of upwelling is small, its high frequency of occurrence is one of the key physical features in the Baltic Sea.

Wind-induced coastal upwelling is important dynamical feature affecting the circulation and the ecosystem of the region: during intensive upwelling events relatively cool and saline upwelling water affects not only SE Baltic Sea, but during rapid inflows may strongly influence the Curonian lagoon environment.

2. Data and Methods

For analysis of the coastal upwelling impact on SE Baltic Sea waters MODIS Terra/Aqua SST dataset for the SE Baltic Sea and Curonian Lagoon is examined between 2000 and 2014.

MODIS Terra/Aqua Level 2 daytime (MODIS thermal bands 31 (11 μ) and 32 (12 μ) imagery (L2_LAC_SST product) covering the study site with spatial resolution of about 1 km were obtained from the NASA OceanColor website (<http://oceancolor.gsfc.nasa.gov/>).

MODIS sea surface temperature (SST) data for 2000-2014 was utilized for evaluation of upwelling-induced parameters, such as cross-front SST differences and gradients, alongshore and cross-shore length, and the total affected area in the SE Baltic and in the Curonian Lagoon.

Upwelling parameters in the SE Baltic Sea were calculated along eight cross-shore transects also one transect was in the Curonian Lagoon.

3. Results

Upwelling can occur in any time of the year, but during the cold season they are not easy noticeable in satellite pictures. According to many investigations, the signatures of this phenomenon in the Baltic Sea are generally observed when the strongest thermal vertical stratification (with warm surface water and colder water below) occurs: from spring to autumn and the coastal upwelling in the Baltic Sea can be as frequent as 25–30% of the time in some areas (Gidhagen, 1987; Lehmann et al., 2012). In a period of 2000-2014 warm seasons (April-September), 62 upwelling events were recorded in SE Baltic Sea coast.

Satellite images show that the duration of the upwelling in this part of the sea may vary from couple days and under favorable wind conditions it may reach up to several weeks. When a 'chain' of upwelling events is taking place, one

event may play a part in forming the initial stratification for the next one; consequently, SST may drop significantly even with a reduced wind impulse (Myrberg et.al. 2010).

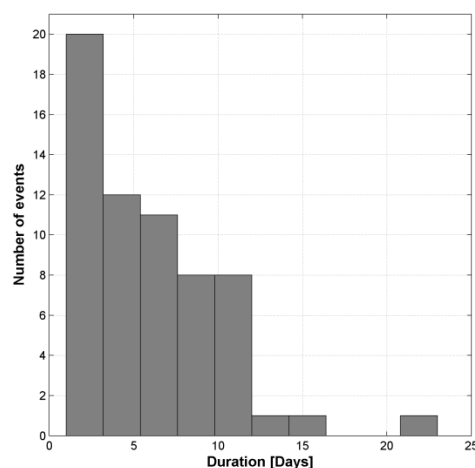


Figure 1. Duration of upwelling events

In this study, the applicability of MODIS sea surface temperature data for documentation and calculation of the SST changes during the coastal upwelling in the SE Baltic Sea and Curonian Lagoon is shown. The maximum observed SST gradients across the front were up to 1.2 °C/km, temperature drop up to 15 °C, with total upwelling-affected area being up to 18000 km². It is also recorded that the horizontal scale of the upwelling can be from 100 to 400 km alongshore, up to 70 km cross-shore.

Furthermore, analysis of available MODIS SST maps revealed that intensive coastal upwelling events strongly influence not only the SE Baltic coastal zone, but also impacts the hydrological regime of the northern part of the Curonian Lagoon when the inflow of relatively cold and saline waters from the SE Baltic takes place. The marine water input and the spatial expansion are strongly influenced by the local wind field here (Kozlov et al. 2014).

References

- Gidhagen L., (1987) Coastal upwelling in the Baltic – satellite and in situ measurements of sea surface temperatures indicating coastal upwelling, *Estuar.Coast. Shelf Sci.*, 24 (4), 449–462
- Kozlov I., Mingelaite T., Dailidienė I., (2014) Space-derived Parameters of Coastal Upwelling in the SE Baltic Sea. *Baltic International Symposium (BALTIC), IEEE/OES.* DOI:10.1109/BALTIC.2014.6887850
- Lehmann A., Myrberg K., (2008) Upwelling in the Baltic Sea – A review, *Journal of Marine Systems* 74, S3–S12.

Lehmann A., Myrberg K., Hoflich K., (2012) A statistical approach to coastal upwelling in the Baltic Sea based on the analysis of satellite data for 1990–2009, *Oceanologia*, 54 (3), 369–393, <http://dx.doi.org/10.5697/oc.54-3.369>.

Myrberg K., Andreev O., Lehman A., (2010) Dynamic features of successive upwelling events in the Baltic Sea – a numerical case study, *Oceanologia*, , 52 (1), pp. 77–99

The basics of Baltic Sea physics covering bathymetry, hydrography, circulation and sea ice

Kai Myrberg

Finnish Environment Institute, Helsinki, Finland (kai.myrberg@ymparisto.fi)

Abstract

The talk will focus on the description of the basic physical properties of the Baltic Sea. It is an elongated sea situating between the maritime temperate and continental sub-Arctic climate zones. In winter it is partly ice-covered; during the most severe winters it is completely frozen over.

The Baltic Sea is a unique basin of the World Ocean, or rather a series of basins, connected to the main Atlantic Ocean (North Sea) only via the shallow and narrow Danish Straits. The sea is very shallow with a mean depth of 54 m only. Due to the limited water exchange with the North Sea, the renewal time of the water masses of the Baltic Sea is rather long, being about 40 years.

The stratification of the Baltic Sea is unique. The interplay between inflowing saline, dense waters from the North Sea in the bottom layer with the excess of light, and fresh riverine waters coming into the system in the upper layer leads to the formation of a permanent two-layer structure of density separated by a sharp jump layer (halocline). Due to the layered structure, the direct atmospheric forcing is restricted to the upper layer with a typical thickness of 40–80 m, while in the bottom layer advection and mixing processes govern the patterns of the hydrographic fields. On the top of the upper layer, a well-mixed surface layer, with a typical thickness of 15–20 m, is formed due to summer-time heating, whereas at the bottom of this layer a rather sharp jump layer of temperature (thermocline) exists. During autumn the vertical temperature gradient vanishes due to thermal convection and turbulent mixing.

The bottom waters of the Baltic main basin are often suffering from oxygen depletion and due to the strong stratification, the deep water masses can be ventilated only

by the so-called Major Baltic Inflows with a large amount of saline, oxygen-rich water which will ventilate the bottom waters.

There are four mechanisms which induce currents in the Baltic Sea: the wind stress at the sea-surface, the surface pressure gradient, the thermohaline horizontal gradient of density and the tidal forces. The currents are steered furthermore by the Coriolis acceleration, topography and friction, forming a general (cyclonic) circulation in this stratified system with positive fresh water budget.



Current and historical patterns of heavy metals pollution in Estonia as reflected in natural media of different ages: ICP Vegetation, ICP Forests and ICP Integrated Monitoring data

Ülle Napa

Institute of Ecology and Earth Sciences, University of Tartu, Estonia (ulle.napa@ut.ee)

1. Introduction

Emissions of heavy metals (HM) have decreased in the European Union during 1990–2012 by: 89% for lead (Pb), 66% for cadmium (Cd), 74% for chromium (Cr), 67% for nickel (Ni), 42% for zinc (Zn) and 1% for copper (Cu) according to European Environment Agency (2014). Since the 1960s Estonia has been the greatest oil shale producer and consumer in the world Raukas (2010). The mineral part of Estonian oil shale is rich in metals especially Cr, Fe, Ni, Pb and Zn Liiv and Kaasik (2004).

In order to find out the historical pattern of metal pollution in Estonia, the comparison of concentrations of HMs (Cd, Cr, Cu, Ni Pb and Zn) in natural media of three different ages was made: moss carpet (ICP Vegetation moss survey data), litter layer (OL), and organic layer (OF) of coniferous forests (in mostly podzolic soils) with main tree species of Norway spruce (*Picea abies*) or Scots pine (*Pinus sylvestris*) (ICP Forest soil survey data). The results presented here are based on the results of a research article by Napa et al. (2015).

2. Material and methods

The current study used data on heavy metals from International Co-operative Programmes (within the framework of the Convention on Long-Range Transboundary Air Pollution of the United Nations Economic Commission for Europe) ICP Forests, ICP Vegetation, and ICP Integrated Monitoring (ICP IM). For estimating HM's bulk deposition, data of Estonian local precipitation network was used. All the datasets were acquired from Estonian National Monitoring Program databases (<http://seire.keskkonnainfo.ee/>). In total 450 samples from 195 plots were analysed (Figure 1).



Figure 1. Plots of sample collection. In order to compare spatial distribution of HMs, Estonia was divided into five different regions: (I) N-W; (II) N-E; (III) S-W; (IV) S-E and (V) Western insular region.

3. Results

The comparison of HM concentrations in moss and soil organics layer samples (OL and OF) revealed three groups of individual retention patterns.

The first group consists of the metals (Cu, Cr, Ni), the concentrations of which increase as follows: Moss layer < OL layer < OF layer. In comparison to moss layer, the concentrations of these metals increased in OF layer as follows: Cr (18 times), Ni (8 times) Cu (2 times).

The second group is formed by Cd and Pb with maximum median and mean concentrations also obtained in the organic layer of soil. A difference from the previous pattern is the almost equal concentration of Pb and Cd in OL and moss layer in comparison to the substantial difference, e.g. as was the case with Ni and Cr for the first group.

The third type of retention pattern is characteristic to Zn and could be described in the increasing order of OF layer < moss layer < OL layer, where the concentrations in moss layer are a half and in OF layer three times lower than Zn concentrations determined in OL layer.

RDA (redundancy analysis) and permutation test (to verify the significance of RDA test) of Canoco programme together with ANOVA test (available in STATISTICA 7.0 programme) were chosen to illustrate and give an overall picture of the distribution of HMs between five different regions and in different media. The results show that the area of higher HM pollution is moved from the N-E industrial area to the capital region in N-W, where the most of the population and traffic are nowadays concentrated.

More precise analyses (by ANOVA test, significant at p value 0.05) of regional differences in OL database showed statistically significant higher concentrations (mg/kg) of Cu ($p = 0.03$), Zn ($p = 0.05$) and Pb ($p = 0.01$) in S-W Estonia and the western insular area (regions 3 and 5). The same analysis of stocks (g/ha) show the highest supplies of Cu ($p = 0.01$) and Zn ($p = 0.02$) only in S-W, but of Pb ($p = 0.01$) and also Cd ($p = 0.05$) in the western insular area. With regards to Ni and Cr, the statistically significant proof of higher concentrations and supplies in S-E Estonia was not found in older and deeper layers of soil organics (in OF), where both average concentrations as well as stocks of Ni and Cr were statistically significantly higher in S-E Estonia in comparison with others regions ($p = 0.01$ – 0.02).

4. Discussion

Over 90% of HM emissions in Estonia are found to originate from stationary sources, particularly from N-E Estonia's oil-shale-related industries Kohv et al. (2009). Currently, (2006–2012), average emissions from Estonia's stationary sources are 44,818 kg/y of Zn, 2236 kg/y of Cu,

32,806 kg/y of Pb, 5635 kg/y of Ni, 8811 kg/y of Cr and 561 kg/y of Cd by Estonian Environment Agency (2013). The estimated annual average input of metals is higher by bulk deposition than by litterfall for Pb, Cu and Zn (10%, 62% and 72%, respectively) indicating that the impact of airborne emissions in Estonia is still higher in comparison to ecosystem's inner cycling.

Despite the continuous retention process in the ecosystem, the decreasing trend of HM concentrations was noticeable especially for mosses. According to the ICP Vegetation programme the concentrations have dropped for all the HMs over the ten years between 1995 and 2005/06 Keskkonnaministeeriumi Info- ja Tehnokeskus (2008). The change in concentrations is less remarkable for Cu and Zn in mosses Kaasik and Liiv (2007), Ukonmaanaho et al. (2008). Nevertheless, bryomonitoring results indicate that the HM concentrations still remain higher in the mosses of the NE region Liiv and Kaasik (2004), Kaasik and Liiv (2007).

The overall level of HM emissions in Estonia is currently low according to European Environment Agency (2013), the effect of previous significantly higher exposure of HM emissions is preserved in OF layer, where the average accumulated stocks of highly accumulative HMs reach the levels of 728.8 g/ha for Cr, 538.5 g/ha for Pb and 372.5 g/ha for Ni. The finding that concentrations of Ni and Cr were significantly higher in OF layer than in moss layer is once again an indication of the influence of previous high HM emissions.

Based on the assumption that the HM content in Estonian forest soils has to be related to emissions originating from the oil shale industry, the chemical composition of oil shale fly ash was observed and compared with HM emissions and HM content in OF layer. As a result the proportions (%) between the HMs in OF layer are very similar to the proportions between the discussed HM's datasets of officially reported emissions by Estonian Environment Agency (2013), as well as between the HM's proportion in the chemical composition of oil shale fly ash presented by Talve and Riipulk (2001)—especially for Ni and Cr. Therefore there is a reason to believe that these HMs are related to air pollution driven by oil shale usage. Ni and Cr clearly stood out in S-E of Estonia, where the highest concentrations (mg/kg) and largest stocks (g/ha) of these HMs were found in OF layer. The accumulated Ni and Cr stocks in S-E therefore originate from the industrial N-E from the period of high activity in the oil shale industry and the higher HM emissions that accompanied it—now accumulated in the organic layer of forest soil in south-eastern part of Estonia.

5. Conclusions

The main conclusions:

(1) Current level of HM deposition in Estonia is modest, but HMs deposited during previous decades have accumulated in the organics of forest soils—especially the HMs that are unnecessary for the functioning of plants (e.g. Pb, Ni and Cr).

(2) The greatest historical stationary emission source of HMs in Estonia—the oil shale industry has left its mark on soil organics of coniferous stands, where the large stocks

have HM ratios that are similar to those characteristic to fly ash emissions of the oil shale industry.

(3) Ni and Cr, originating from the oil shale industry, exhibit the highest stores in S-E Estonia indicating mostly local deposition and a high ability to accumulate in soil organics.

(4) Zn is one of the most reused HMs at the ecosystem level. Despite that Zn has accumulated in soil organics equally in all the studied regions, although the highest and most variable deposition still occurred in the N-E oil shale region.

References

- Estonian Environment Agency, 2013. 2006–2012 õhku heidetud saasteainete heitkogused Eestis kokku ja maakonniti (Database). Estonian Environment Agency, Tallinn, Estonia, [_http://www.keskkonnainfo.ee/_.](http://www.keskkonnainfo.ee/)
- European Environment Agency, 2013. European Union emission inventory report 1990–2011 under the UNECE Convention on Long-range Transboundary Air Pollution (LRTAP). European Environment Agency, Luxembourg (p. 142).
- European Environment Agency, 2014. European Union Emission Inventory Report 1990–2012 under the UNECE Convention on Long-range Transboundary Air Pollution (LRTAP). European Environment Agency, Luxembourg (p. 130).
- Kaasik, M., Liiv, S., 2007. Spatial and temporal variability of trace metals in mosses in Estonia. *Forestry Studies* 46, 35–44.
- Keskkonnaministeeriumi Info- ja Tehnokeskus, 2008. Eesti keskkonnaseire 2004–2006. Keskkonnaministeeriumi Info- ja Tehnokeskus, Tallinn, Estonia (p. 149).
- Kohv, N., Link, A., Mandel, E., N-B, P., 2009a. Õhku eraldunud saasteainete heitkogused paiksetest saasteallikatest aastail 2004–2007. Keskkonnaministeeriumi Info- ja Tehnokeskus, Tallinn, Estonia, pp. 32.
- Liiv, S., Kaasik, M., 2004. Trace metals in mosses in the Estonian oil shale processing region. *J. Atmos. Chem.* 49, 563–578.
- Napa, Ü., Kabral, N., Liiv, S., Asi, E., Timmus, T. and Frey, J. (2015). Current and historical patterns of heavy metals pollution in Estonia as reflected in natural media of different ages: ICP Vegetation, ICP Forests and ICP Integrated Monitoring data. *Ecol. Indic.* 52, 31–39.
- Raukas, A., 2010. Sustainable development and environmental risks in Estonia. *Agron. Res.* 8, 351–356 (Special Issue II).
- Talve, S., Riipulk, V., 2001. Inventory analysis of oil shale energy produced on a small thermal power plant. *J. Cleaner Prod.* 9, 233–242.

Atmospheric column transparency in Europe, 1906-2014

Hanno Ohvri

Institute of Physics, Tartu University, Estonia (hanno.ohvri@ut.ee)

1. Column transparency – what, why, how?

Transparency is one of primary measures indicating the state of the atmosphere. Long-term time series of transparency allow one quantitatively assess the variability of turbidity of air and make climatological conclusions in regard to contamination, radiative exchange and cloud formation, in the atmosphere as well as conditions for remote sensing.

Transparency in turn may be determined in several ways – by visibility of remote objects, by brightness of calibrated lamps or known sources of light etc.

In meteorological practice the Sun – despite of its rotation, sunspot cycles, faculae activities – is considered as a quite stable source of light. The amount of integral (broadband) solar energy at all wavelengths, incident on a unit area at the top of the atmosphere (TOA) may be easily calculated with an error only a few tenths of a percent.

The well-known Bouguer-Lambert law links several parameters of column transparency and turbidity:

$$S_m = S_0 \tau_m = S_0 e^{-m \delta_m} = S_0 p_m^m = S_0 e^{-m \delta_{CDA,m} T_{L,m}} \quad (1)$$

here:

S_m – intensity of direct solar beam, which reaches the Earth's surface after attenuation in the air (direct solar irradiance or simply direct solar radiation);

S_0 – direct solar irradiance at the TOA;

m – number of atmospheric layers or “optical air mass”; $m = 1$ in the direction of the zenith; $m = 2$ for solar elevation $\approx 30^\circ$;

τ_m – transmittance or transmission coefficient;

δ_m – broadband optical depth of the atmosphere;

p_m – the Atmospheric Integral Transparency Coefficient (AITC);

$\delta_{CDA,m}$ – optical depth of a clean and dry atmosphere;

$T_{L,m}$ – the Linke turbidity factor.

The four parameters, τ_m , δ_m , p_m , $T_{L,m}$ represent transparency or turbidity, averaged over the entire solar spectrum. These parameters depend, according to the Forbes effect, on solar elevation, even in the case of a stationary and azimuthally homogeneous atmosphere.

To eliminate the Forbes' effect, it is accepted practice to normalize values of the AITC to a certain solar elevation, usually to $m = 2$ ($\approx 30^\circ$ above the horizon). Problems with this normalization seem to be the main reason for the limited use of the AITC.

In this work, the main parameter is the integral (broadband) transparency coefficient (p_2) transformed from an actual air mass m to a particular one, $m = 2$.

This coefficient, with help of Eq. (1), enables easy calculation of several other broadband parameters of column transparency and turbidity as well as transition to spectral Aerosol Optical thickness, $AOT\lambda$.

2. List of locations and observation periods

Data from six different European locations are used for calculation of multiannual time series of transparency:

- 1) Pavlovsk, 1906–1936 (30 km south from StPetr);
- 2) Voeikovo, 1949–1960 (15 km east from StPetr);
- 3) Karadag, Crimea, 1934–2014;
- 4) Tartu-Tõravere, Estonia, 1932–1940, 1950–2014;
- 5) Moscow, 1955–2014;
- 6) Tiirikoja, Estonia, 1956–2014.



Fig. 1. Time series of observed direct solar beam were used from six locations: Pavlovsk, Voeikovo, Karadag, Tartu-Tõravere, Moscow and Tiirikoja; 1, 2, 3 – thermal electrical power stations.

3. Some numerical values

Column transparency is a quantitative measure of atmospheric clearness. Coefficient of transparency for an *ideal atmosphere* i.e. for a clean and dry atmosphere (CDA), without water vapor and aerosol load, is:

$$p_2(CDA) = 0.905 \quad (2)$$

If the atmosphere were consisted only of water vapor with total column amount of *precipital water*, $W = 2.5$ cm, which is equal to planetary mean value of W , then its coefficient of slant column transparency would be:

$$p_2(W = 2.5\text{cm}) = 0.903 \quad (3)$$

Consider now a clean and wet atmosphere, with $W = 2.5$ cm, but still without aerosol particles, its coefficient of transparency:

$$p_2(CDA+W) = 0.905 \times 0.903 = 0.817 \quad (4)$$

Presence of aerosol particles (smokes, dusts, fogs) lowers column transparency but a level

$$p_2(CDA+W + \text{aerosols}) = 0.8 \quad (5)$$

corresponds to a high annual mean, inherent to clean air at northern latitudes about 60° .

4. Evolution of European column transparency

Figure 2 gives evolution of annual means of column transparency p_2 for different European locations.

The highest annual mean belongs to the northernmost location Pavlovsk where $p_2 = 0.813$ in 1909. But there were also other years with high transparency in Pavlovsk: during the 31-year observational period the high annual mean, $p_2 = 0.8$, was reached in six years.

The lowest annual value, $p_2 = 0.632$ in 1912, belongs again to Pavlovsk and was caused by the eruption of the Katmai/Novarupta (Alaska) volcano in the same year.

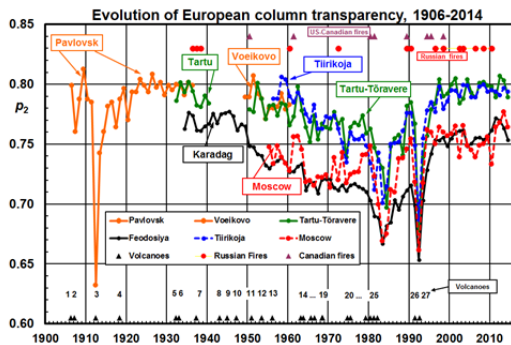


Fig. 2. Annual means of the atmospheric integral transparency coefficient, p_2 , for different locations. Small black triangles in the bottom indicate dates of the largest volcanic eruptions. Triangles and dots above correspond to years with large forest fires in the US/Canada and Russia, respectively.

Because of being in almost the same climatic zone as Pavlovsk, all Estonian stations also reached the level of 'very good transparency', $p_2 = 0.8$. Although the transparency in Moscow and Feodosiya, as representative of more southerly locations, is lower, it is amazing to see the same pattern in variability of annual means as in Estonia. There are several common features in multiannual trends of transparency.

First, impressive is the impact of remote volcanic events. The just mentioned Katmai/Novarupta (1912) eruption apparently caused the most abrupt decrease during the entire 20th century. The Pinatubo (1991) impact was slightly less: in 1992 annual mean column transparency decreased at two Estonian locations to $p_2 = 0.68$ – 0.69 and in the Crimea and Moscow, to $p_2 = 0.65$ – 0.66 . A series of four successive volcanic eruptions during 1979–1982 ending with the El Chichón (Mexico), caused drop in transparency down to the value $p_2 = 0.70$ in Estonia in 1983–1984, and to $p_2 = 0.67$ in the Crimea and Moscow in 1983.

Second, from the beginning of 1960s, there is a long decreasing tendency in column transparency which lasted until 1983/1984. In the Crimea the decrease started already from 1945 and can be related, besides volcanic activity, to a rapid increase of industrial and agricultural activities round the Black Sea, as well as shipping.

It is interesting to note that for the US stations (Madison, Lincoln, Bluehill) even an earlier start of the decrease, from the 1930s, perhaps due to increasing industrial and especially, agricultural pollution, happened.

Focusing on agricultural pollution in the US and Canadian prairies, an aggressive tillage technology and lack of rains turned the unanchored soil to dust, which moved away in huge clouds blackening the sky and travelling cross country to the New York City and Washington. On the

Plains, the visibility was reduced to 1 metre or less. A period of severe American dust storms during the 1930s is called the Dirty Thirties, also known as the Dust Bowl.

Evolution of transparency in Moscow is affected by local urban effects and huge forest and bog fires around the city (1972, 2002, 2010). But a decreasing tendency, at least from the beginning of 1960s, is evident.

Lower column transparency means more aerosol particles participating in cloud formation. In this way lower transparency should lead to more cloudiness and to lower global solar radiation or insolation (global = direct + diffuse). Actually this phenomenon, known as *global dimming* indeed happened in most areas of Europe.

The third common feature in multiannual pattern of column transparency is that the decreasing trends in annual mean values ended in 1983/1984. From 1984/1985 the trends changed their sign from negative to positive and during the next years column transparencies rapidly recovered. The transition from decreasing to increasing transparency was again in line with the increase of global solar radiation, i.e. with *global brightening* from 1985 onward.

5. Reduction of anthropogenic air pollution in Europe

The aerosol load has been different in the western and eastern parts of the continent. In Western Europe, in the 1950s, public opinion was most concerned on high concentration of black carbon (BC) accompanying incomplete combustion in small, low-temperature facilities, such as home fireplaces.

In Britain, for example, the last impetus to a rethinking in air pollution was given by catastrophic days of Big Smoke in London, 5–9 December 1952, which led to regulations, like the Clean Air Acts, restricting the use of dirty burning technologies. As result, by 1970, the emissions of BC had been reduced in London to one tenth of the level what they were in 1956.

In Eastern Europe, decrease in reduction of aerosol emissions was not so rapid but we suggest that the increase in the AITC p_2 in Estonia and Moscow at the end of the 1970s is due to environmentally oriented changes in the region. However, after the collapse of the USSR in August 1991, general economic decline in previous socialist countries favoured a considerable decrease in anthropogenic aerosol emissions from all types of air pollution sources.

6. Before and after the Mt. Pinatubo eruption

From 1983 to 1991 there was volcanically a 8-year calm period interrupted by the Mt. Pinatubo (June 1991) eruption. The second clearing of the atmosphere, after dissipation of emissions of the Mt. Pinatubo eruption, coincided with general economic decline in Eastern European countries after the collapse of the USSR in August 1991. The pre-Pinatubo level in European column transparency was again achieved by 1994. Concerning Estonia, a high level of column transparency, $p_2 = 0.8$, was again reached in 1997, 2001, 2003, 2008, 2012 and 2013.

7. What about the future?

We can not predict how long the present volcanically calm period will last. But, with the rising living standard in the former USSR countries, one can expect a rapid increase in the consumption of fuel by transportation.

Understanding the water and energy exchanges in the coupled atmosphere-land-ocean system

Anders Omstedt

Institute of Marine Sciences, University of Gothenburg, Göteborg, Sweden (anders.omstedt@gvc.gu.se)

1. Global balances

The presentation will discuss the global and the Baltic Basin water and heat cycles. The water and heat cycles are at the heart of climate research and modelling and thus of fundamental importance when trying to understand the coupled atmosphere-land-ocean system. For the global heat balance the sun radiation is the main driving component for the Earth global surface balance. However, other radiation and turbulent fluxes transforms heat in the surface layer. For the global water balance most water exchange is through evaporation at the ocean- atmosphere interface. The connection between the water and heat cycles are through evaporation in ice free waters and through salt rejection during ice growth in ice covered waters.

2. Fresh water storage

The major part of fresh water on Earth (about 96 percent) is stored in the oceans and the oceans supply the major part of the water cycle through evaporation. We will further examine the global hydrology cycle by examine how the net fresh water fluxes change around the globe and illustrate the importance of the atmosphere and oceanic components.

3. Regional balances

The concept of drainage basin is presented and discussed as it plays an important role when closing regional water and heat balances. Estimations on the different water and heat components are then presented based on results from Baltic Basin and integrated properties such as the Baltic Sea mean (vertically and horizontally integrated) temperature and mean salinity are discussed. For more details see the lecture notes (coming) and the references below.

References

- BACC II Author Team (2015). Second Assessment of Climate Change for the Baltic Sea basin. Springer Regional Climate Studies. ISSN 1862-0248 ISSN 1865-505X (electronic). ISBN 978-3-319-16005-4 ISBN 978-3-319-16006-1 (eBook). DOI 10.1007/978-3-319-16006-1. Springer Cham Heidelberg New York Dordrecht London.
- Bengtsson, L., (2010). The global atmospheric water cycle. *Environ. Res. Lett.*, 5.
- IPCC (2013). *Climate Change 2013: The Physical Science Basis. Contribution of Working Group I to the Fifth Assessment Report of the Intergovernmental Panel on Climate Change*. (Stocker, T.F., D. Qin, G.-K. Plattner, M. Tignor, S.K. Allen, J. Boschung, A. Nauels, Y. Xia, V. Bex and P.M. Midgley ,eds.). Cambridge University Press, Cambridge, United Kingdom and New York, NY, USA, 1535 pp.
- Omstedt, A. and C., Nohr (2004). Calculating the water and heat balances of the Baltic Sea using ocean modelling and available meteorological, hydrological and ocean data. *Tellus* 56A, 400-414. DOI 10.1111/j.1600-0870.2004.00070.x
- Omstedt, A. and D., Hansson, (2006). The Baltic Sea ocean climate system memory and response to changes in the water and heat balance components. *Continental Shelf Research* 26, 236-251. DOI 10.1016/j.csr.2005.11.003
- Omstedt, A. and D., Hansson, (2006). Erratum to: 'The Baltic Sea ocean climate system memory and response to changes in the water and heat balance components'. *Continental Shelf Research* 26, 1685-1687. DOI 10.1016/j.csr.2006.05.011
- Omstedt, A., Elken, J., Lehmann, A., Leppäranta, M., Meier, H.E.M., Myrberg, K.,Rutgersson, A., *Progress in physical oceanography of the Baltic Sea during the 2003–2014 period, Progress in Oceanography* (2014), doi: <http://dx.doi.org/10.1016/j.pocean.2014.08.010>
- Wijffels, A. E., et al., (1992).Transport of Freshwater the Oceans. *J. Phys. Oceanogr.*, Febr., pp. 155-162.
- Winsor, P., J. Rodhe, and A. Omstedt (2001). Baltic Sea ocean climate: an analysis of 100 yr of hydrographic data with focus on the freshwater budget, *Clim. Res.*, 18, 5-15, 2001.
- Winsor, P., J. Rodhe, and A. Omstedt (2003). Erratum: Baltic Sea ocean climate: an analysis of 100 yr of hydrographical data with focus on the freshwater budget. *Climate Research*, 18:5-15, 2001. *Climate Research*, 25, 183.

Electric wind in a Differential Mobility Analyzer

Maris Palo

Laboratory of Environmental Physics, Institute of Physics, University of Tartu, Tartu, Estonia (maris.palo@ut.ee)

1. Introduction

Atmospheric aerosols have considerable effect on climate, air quality and human health. Since the effects of the aerosol particles are mostly dependent on their size, atmospheric aerosol is well characterized by the size distribution of the particles. The size distribution is most commonly measured using the electrical separation method developed by Liu and Pui (1974). Differential mobility analyzers (DMA) developed by Knutson and Whitby (1975) use this method and separate particles according to their electrical mobility and determine the mobility spectrum, from which size spectrum is derived.

The measured size spectrum can however be distorted by a number of factors like airflow turbulence, decentralization of electrodes etc. A study by Peil and Tamm (1984) showed that measurements could also be disturbed by electrostatic destabilization of the laminar flow in a DMA. This phenomenon can also be called electric wind. The aim of this work is to investigate the occurrence of the electric wind in a DMA (Differential Mobility Analyzer) and the effect of this phenomenon on the measured size spectra. Electric wind is defined by Robinson (1962) as the movement of gas, induced by ions moving in an electric field. The study by Tamm and Peil (1984) only showed that electric wind could be a distorting factor in size distribution measurements with DMA, but so far this has not been thoroughly investigated.

2. Methods

The onset conditions (total particle concentration, mean particle size and particle layer thickness) for the electric wind in the locally-built VLDMA (Very Long Differential Mobility Analyzer) by Uin and Tamm (2010) were investigated by means of visual detection. The VLDMA is equipped with two windows: one for a laser beam to illuminate the inside of the DMA on the side, near the exit slit and the other for visual observations on the top. Occurrence of the electric wind can be assessed from the changes in the light pattern seen from the observation window: when no electric wind occurs the light pattern is stable (Fig. 1a), when intensive electric wind occurs, the aerosol layer changes and turbulent movements can be seen as waves and eddies (Fig. 1b)

When measuring the particle size spectrum, the voltage applied to the DMA electrodes is gradually increased and at any given voltage, only particles with electrical mobilities in a narrow range, determined by the DMA transfer function corresponding to that voltage, should be separated out. When the electric wind occurs, particles move in turbulent waves and particles that reach the output slit may not represent the expected electrical mobility and the concentration can therefore be either over or under estimated. The effect of the chosen experimental conditions on the formation of the electric wind can

therefore be assessed according to the occurrence and extent of these distortions.

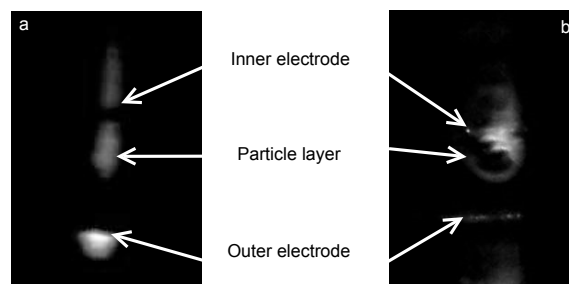


Figure 1. The light pattern seen from the VLDMA observation window when no electric wind occurs (a) and with intensive electric wind (b).

3. Experiments

In the visual detection experiments the effect of the chosen conditions on the formation of electric wind was investigated by changing the voltage applied to the DMA electrodes and determining the conditions close to the onset of the electric wind: increasing the voltage evokes and intensifies waves and decreasing the voltage makes the particle layer more stable. If the formation of the electric wind is promoted under the chosen conditions (total particle concentration, mean particle size and particle layer thickness), then less momentum from the electric field is needed for the electric wind to develop and a lower threshold value is observed.

The electric wind-associated distortions of the size spectra measured by the VLDMA and a TSI Long-DMA were assessed by comparison of spectra measured at different total particle concentrations, mean particle diameters and charge distribution.

4. Results and discussion

According to the analysis using the visual detection method, the electric wind proved to be promoted by the increase of electric field strength, aerosol layer thickness and total particle concentration. Due to the limitations of this method, the effect of particle size on the formation of the electric wind was not determined.

Measured size spectra revealed three types of distortion: widening of the size distribution, shift of the mode of the distribution to smaller diameters and smoothing out the peaks of the multiply charged particles. These distortions were promoted by the increase total particle concentration and particle size. Fig. 2 demonstrates that in case of larger particles increasing the total particle concentration shifts the mode and widens the distribution (Fig. 2a), however these distortions do not appear in case of smaller particles (Fig. 2b).

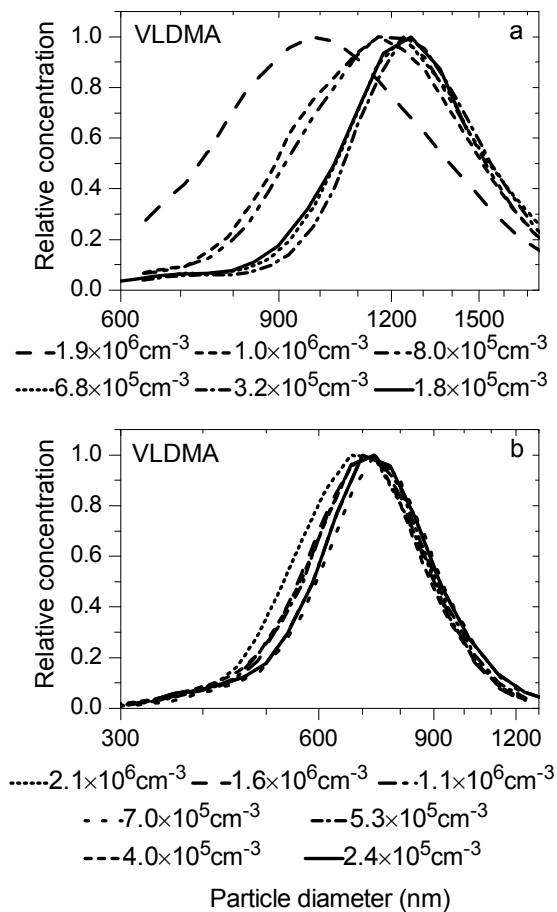


Figure 2 Particle size distributions as measured by the VLDMA at different total particle number concentrations. Particle mean diameter is approximately (a) 1230 nm and (b) 720 nm. Relative concentration is normalized to the highest measured concentration.

The shift of the mode to smaller diameters indicates that the eddies caused by the electric wind pull larger particles to the output slit at voltages corresponding to

smaller particles. The turbulent movements also stretch the aerosol layer wider and therefore seemingly increase the width of the measured distribution. Multiply charged particles are normally seen as additional peaks in the measured size distribution at smaller diameters. In case of electric wind the particles are redistributed by the turbulent movements and the peaks of multiply charged particles are smoothed out.

5. Conclusion

Electric wind proved to be promoted by the increase of electric field strength, aerosol layer thickness, particle concentration and size. Electric wind may therefore be a source of severe distortion of the particle size spectrum when measuring large particles at high concentrations.

References

- Knutson E.O., Whitby K.T. (1975). Accurate measurement of aerosol electric mobility moments. *Journal of Aerosol Science*, 6, pp. 453-460.
- Liu B.Y.H., Pui D.Y.H. (1974). A submicron aerosol standard and the primary, absolute calibration of the condensation nuclei counter. *Journal of Colloid and Interface Science*, 47, pp. 155-171.
- Peil I., Tamm E. (1984). Generation of monodisperse aerosols by the electrostatic separation method. *Acta et Commentationes Universitatis Tartuensis*, 669, pp. 38-52. [In Russian with English summary].
- Robinson M. (1962). A History of the Electric Wind. *American Journal of Physics*, 30, pp. 366.
- Uin J., Tamm E. (2010). Assessment of the Quality of Electrically Produced Standard Aerosols. *Aerosol and Air Quality Research*, 10, pp. 609-615.

On the retrieval of the clumping index from multi-angular SWIR satellite imagery

Kairi Raabe, Jan Pisek

Tartu Observatory, Tõravere, 61202, Estonia (kairi.raabe@gmail.com)

1. Introduction

The spatial distribution of leaves in various canopy structures is often non-random, instead being organized into structures such as branches, three crowns and tree groups (Chen & Leblanc, 1997). As a result, radiation interception and distribution within the canopies is affected, along with evapotranspiration, energy partitioning, carbon uptake etc. (Chen et al., 2012). A clumping index (Nilson, 1971) has been used to describe the deviation of foliage distribution from the random distribution based on a Poisson model (Chen & Black, 1992).

Previously, algorithms for estimating the clumping index from satellite remote sensing have been developed for red and near-infrared bands (Chen et al., 2005), and global coverage maps using different multi-angle sensors have been produced and validated (Pisek et al., 2010; He et al., 2012; Pisek et al., 2015). The aim of the current work was to investigate whether the retrieval of clumping information from the shortwave infrared (SWIR) part of the spectrum might provide even more detailed information or further improve the current retrievals, especially over areas with sparse vegetation cover.

2. Methodology

We used the geometrical-optical model 4-Scale (Chen & Leblanc, 1997) to explore the relationship between the Normalized Difference between Hotspot and Darkspot (NDHD) and clumping index in the SWIR part of the spectrum. The model uses crown shape, tree height, crown diameter, stand density, leaf area index, foliage optical properties, tree group size, and viewing geometry as the main input parameters. The simulations were run with a number of different parameter combinations, describing multiple forest and other vegetation types. The optical properties of foliage and background were varied within a reasonable range for the SWIR band.

After assessing the relationship between NDHD in the SWIR band and clumping, we calculated the clumping index using the Bidirectional Reflectance Distribution Function (BRDF) product from Moderate Resolution Imaging Spectroradiometer (MODIS) (Schaaf et al., 2002) over multiple sites with available in situ measurements (Pisek et al., 2015) according to the regression results from simulations.

3. Conclusions

In this work we assess the suitability of the SWIR portion of the spectrum for deriving clumping information. We present the results from exploring the relationship between clumping and NDHD using the geometrical-optical model 4-Scale. In addition, we provide clumping index

values calculated with this method over multiple sites globally, validated against available in situ measurements. We demonstrate the SWIR part of the spectrum can also include a valuable information about the vegetation clumping, and potentially provide better quality retrievals over particular types of vegetation areas (e.g. sparse vegetation cover).

References

- Chen, J.M., Black, T.A. (1992) Foliage area and architecture of plant canopies from sunfleck size distributions, *Afric. Geost. Meteorol.*, vol. 60, pp. 249-266.
- Chen, J.M., Leblanc, S.G. (1997) A four-scale bidirectional reflectance model based on canopy architecture, *IEEE Trans. Geosci. Remote Sens.*, vol. 35, no. 5, pp. 1316-1337.
- Chen, J.M., Menges C.H., Leblanc, S.G. (2005) Global mapping of foliage clumping index using multi-angular satellite data, *Remote Sens. Environ.*, vol. 97, pp. 447-457.
- Chen, J.M., Mo, G., Pisek, J., Liu, J., Deng, F., Ishizawa, M., Chan, D. (2012) Effects of foliage clumping on the estimation of global terrestrial gross primary productivity, *Global Biogeochem. Cycles*, vol. 26, GB1019.
- He, L., Chen, J.M., Pisek, J., Schaaf, C.B., Strahler, A.H. (2012) Global clumping index map derived from the MODIS BRDF product, *Remote Sens. Environ.*, vol. 119, pp. 118-130.
- Nilson, T. (1971) Theoretical analysis of frequency of gaps in plant stands, *Agric. Meteorol.*, vol. 8, no. 1, pp. 25-38.
- Pisek, J., Chen, J.M., Lacaze, R., Sonnentag, O., Alikas, K. (2010) Expanding global mapping of the foliage clumping index with multi-angular POLDER three measurements: Evaluation and topographic compensation, *ISPRS J. Photogramm. Remote Sens.*, vol. 65, no. 4, pp. 341-346.
- Pisek, J., Govind, A., Arndt, S.K., Hocking, D., Wardlaw, T.J., Fang, H., Matteucci, G., Longdoz, B. (2015) Intercomparison of clumping index estimates from POLDER, MODIS and MISR satellite data over reference sites, *ISPRS J. Photogramm. Remote Sens.*, vol. 101, pp. 47-56.
- Schaaf, C.B., Gao, F., Strahler, A.H., Lucht, W., Li, X.W., Tsang, T., Strugnell, N.C., Zhang, X.Y., Jin, Y.F., Muller, J.P., Lewis, P., Barnsley, M., Hobson, P., Disney, M., Roberts, G., Dunderdale, M., Doll, C., d'Entremont, R.P., Hu, B.X., Liang, S.L., Privette, J.L., Roy, D. (2002) First operational BRDF albedo nadir reflectance products from MODIS, *Remote Sens. Environ.*, vol. 83, no. 1/2, pp. 135-14

Water circulation and nutrient dynamics in the Baltic Sea

Urmas Raudsepp

Marine Systems Institute at Tallinn University of Technology, Tallinn, Estonia (urmas.raudsepp@msi.ttu.ee)

1. Introduction

Eutrophication resulting from direct and indirect input of nutrients is considered one of the major environmental problems in the sub-basins of the Baltic Sea. It has been recognized that cycling of organic matter is a considerable source of nutrients in the Baltic Sea. Nutrient pools in the sediments have increased over the last decades. Major Baltic Inflows (MBI) have great influence for nutrient cycle through oxygenation of the BS deep layers. The stratification of the Baltic Sea sub-basins has significant influence on vertical flux of nutrients to the euphotic layer. The general circulation of the Baltic Sea (BS) has been characterized as cyclonic in all sub-basins based on numerous measurements and model simulations.

Our intention is to present general circulation pattern of the BS and spatial patterns and temporal variation of biogeochemical parameters of the BS using the results of 40 year high-resolution model simulation.

2. Numerical model

Model simulations were performed using a three-dimensional free-surface hydrodynamic model GETM coupled with the ERGOM biogeochemical model. The model domain covers the entire Baltic Sea area and the period modelled is 1966-2006. The model has a 1 nautical mile horizontal resolution, 40 vertical layers and density adaptive bottom following vertical coordinates, which enables to simulate horizontal and vertical density gradients with better precision. The atmospheric forcing from dynamically downscaled ERA40-HIRLAM and parametrized lateral boundary conditions are applied. River runoff and nutrient loads are from Balt-HYPE with 30 main rivers included.

3. Model validation

Model simulation of temperature and salinity show close agreement with measurements conducted in the main monitoring stations of the BS during the simulation period. The timing of the MBIs is well reproduced by the model. In the Gotland Basin, bottom oxygen and nitrate increase during MBIs. Bottom phosphate is well reproduced during inflow events, but underestimated during anoxic conditions. Chlorophyll concentrations are well reproduced. Surface nitrate is underestimated in the model, but follows the seasonal cycle well, while high values of surface phosphate are underestimated two times in the model.

4. Water circulation

The general surface circulation resembles known cyclonic circulations in the central part of the Baltic Proper and the Gulf of Bothnia with persistent currents along the slopes. The reverse circulation scheme from the rest of the

BS is distinguished in the Gulf of Riga and the Gulf of Finland pronounced anticyclonic circulation prevails over cyclonic circulation. Both basins show double gyre circulation at the head of the estuary, consisting of coastal currents and return current in the center of the gulf. The subsurface layer largely resembles surface current system with higher persistency. In the layer between 55 - 100 m, the inflow currents from the Arkona Basin follows the southern slope of the Bornholm Basin, Stolpe Channel and the Gdansk Basin feeding the Eastern Gotland Basin rim current along the eastern slope. Inflowing water along the eastern slope of the Baltic Proper continues its path to the Gulf of Finland along the southern slope.

5. Nutrient cycling

Surface nitrates and phosphates share a similar pattern with highest concentrations in coastal waters (7-10 mmol/m³) and low values in the central parts of the sea (0-2 mmol/m³). Our results indicate high chl-*a* concentrations on the eastern coast of the Baltic Sea with emphasis on the river estuaries. Spatial distribution of biogeochemical parameters is heterogeneous in the bottom layer of the Baltic Sea. The common pattern of the nutrient and primary production cycle in the Baltic Sea is seasonality. The results of primary component analysis indicate that shallow stations display a coupled seasonal pattern of bottom and surface variables. Deep stations have strong seasonal cycle on the surface, which is similar to shallow stations, but low seasonal variability on the bottom, meaning, that there is no coupled seasonality of bottom and surface variables in deep stations. Deep areas act as storage areas for organic matter where halocline acts as a kind of barrier for nutrients to be transported to the upper layer. Deep areas become important source of nutrients during MBIs. Horizontal transport of nutrients from upstream basins of the Baltic Sea is a considerable source of nutrients for downstream basins.

Tree-rings as an indicator of climatic and anthropogenic influences in urban environments – The case study of Stockholm

Eva Rocha

Department of Physical Geography, Stockholm University, Stockholm, Sweden (eva.rocha@natgeo.su.se)

1. Introduction

Tree-ring width is one of the most widely used proxies to represent past climatic variability due to its annual resolution. The Fennoscandia region has a great tradition in dendroclimatology contributing with some of the longest records in the world such as Torneträsk and Finnish Lapland (Grudd et al., 2002; Helama et al., 2008). The use of tree-rings as a paleoclimate archive for temperature or drought reconstruction is well known, however trees can also be very valuable as environmental indicators, since annual rings reflect the ecological conditions present at the time of their formation. In this study we intend to use tree-rings as a monitoring tool for urban environments in Stockholm city.

2. Methods

Urban areas are in constant change and large differences are observed in land use between these areas and the surrounding landscape. To identify the climatic and anthropogenic influences on tree growth a point dendrometer, model DR (Ekomatik, Munich, Germany) will be used. Two sets of dendrometers will be placed in two distinct environments –rural and urban. At each site two trees (*Pinus Sylvestris*) will be monitored at 30 min resolution. The dendrometer measurements will provide information on tree's reaction to short-term changes to various environmental parameters such as temperature or precipitation in these two different environments.

Satellite thermography images will be produced to identify potential areas exposed to the Urban Heat Island in Stockholm and tree cores will be collected from exposed and non-exposed areas with a Swedish increment borer.

3. Expected results

Tree-ring width chronologies will be produced from these sites (urban and rural) and correlated with meteorological data in order to identify the most influencing parameter for tree growth and which one can be effectively reconstructed. By crossdating these chronologies (>400 years) with existent sub-fossil wood from the region the records can be extended up to 1000 years.

Since Stockholm has one of the longest meteorological observations in the world, reaching back to 1756, this direct monitoring approach at a rural and at an urban site will serve as validation for the statistical approach of comparing long term climate data with long tree ring records. Furthermore, by sampling trees and building up chronologies that represent the urban environment the existent uncertainty in the earlier part of the observational record from Stockholm (Moberg 2002) may be corrected.

4. Conclusion

As living organisms trees are sensitive to the surrounding environmental conditions and perform as a

unique historical archive. Monitoring tree growth response in two different environments within the same regional climate will provide a better understanding on their sensitivity and adaptability to seasonal changes over time and bring new insight into the divergence problem. An anomaly characterized by the disagreement between the tree-ring width and the observational data on the late 20th century (D'Arrigo et al. 2008).

References

- D'Arrigo R, Wilson R, Liepert B, Cherubini P (2008). On the 'Divergence Problem' in Northern Forests: A review of the tree-ring evidence and possible causes, *Global and Planetary Change* 60: 289-305
- Grudd, H., Briffa, K.R., Karlen, W., Bartholin, T.S., Jones, P.D. and Kromer, B. (2002). A 7400-year tree-ring chronology in northern Swedish Lapland: natural climatic variability expressed on annual to millennial timescales. *The Holocene* 12: 657-665
- Helama, S., Lindholm, M., Timonen, M., Meriläinen, J., and Eronen, M. (2002). The supra-long Scots pine tree-ring record for Finnish Lapland: Part 2, interannual to centennial variability in summer temperatures for 7500 years. *The Holocene* 12: 681-687.
- Moberg, A., Bergström, H., Krigsman, J. R., and Svanered, O., (2002). Daily air temperature and pressure series for Stockholm (1756–1998). Improved Understanding of Past Climatic Variability from Early Daily European Instrumental Sources s.171-212. Springer Netherlands

About the Quality of Historical Observation Data from Signal Stations along the Southern Baltic Sea Coast

Dörte Röhrbein

Maritime-Climatological Monitoring Centre, German Meteorological Service, Hamburg, Germany
(doerte.roehrbein@dwd.de)

1. Abstract

Historical wind and pressure observations from 1877 to 1999 of overall 160 signal stations along the German Bight and the southern Baltic Sea coast, from Borkum (Germany) to Perlanga (Lithuania) are examined weather they may be used to describe long-term changes and extreme events along the coasts. This study shows an analysis of firstly newly digitized wind and surface air pressure data from 1910 to 1939 of 15 signal stations from Emden (Germany) to Leba (Poland). Also, the storm surge in December 1913 at the coast of the southern Baltic Sea is analyzed by these data. It is shown that the spatial homogeneity of the signal station data is sufficient for the descriptions of historic events, but that temporal homogenization is required for long-term trend analysis.

2. Introduction

The marine weather office of the German Meteorological Service (Deutscher Wetterdienst, DWD) in Hamburg houses a huge archive of historical handwritten journals of weather observations. Among others, a considerable number of original observations sheets of signal stations at the German Bight and the southern Baltic Sea coasts exists which has been until recently almost unnoticed. These stations are called signal stations and are positioned close to the shore to warn sailors near the coasts of severe weather by optical signals.

Figure 1 shows the positions of all 164 Signal stations in the period from 1877 to 1999. To save the handwritten data from physical decomposition and to ensure a scientific analysis the single sheets were and will be scanned and the data digitized. Until now about 25% of the data are digitized.



Figure 1: Positions of the signal stations with weather observations in the time period from 1877 to 1999 of the Naval Observatory Hamburg.

3. Meteorological data of signal stations

All records contain values of wind force and wind direction, but there are specifications of the weather conditions and visibility, and before 1940 also of sea level pressure, precipitation and in some cases of sea state. Most stations reported three to nine times per day, the pressure was usually measured at least once per day and the precipitation twice. In stormy days, observation frequencies

were often increased. The analysis shows the quality of the data for further scientific investigations. Climatological data of 15 signal stations positioned along the coast of the German Bight and the coast of the southern Baltic Sea are evaluated on consistency, quality and plausibility. These 15 stations are Emden, Norderney and Bremerhaven at the German Bight and Flensburg, Kiel, Wismar, Travemünde, Warnemünde, Arkona, Ahlbeck, Ustka, Darłówko, Kołobrzeg and Leba at the Baltic Sea Coast. We choose this 15 station for analysis because of their regular distribution along the coasts, which can be useful for further investigations.

The analyzed variables are SLP in hPa (recalculated from mmHg), wind force (FF) in Beaufort (BFT) and wind direction (DD) in Degree (°). SLP data only exist up to 1939 that is why all following evaluations are made for the time period 1910–1939.

4. Analysis of SLP and wind conditions

First of all, the data are quality controlled on formal, climatological and consistency checks by validat, developed at DWD. The quality check shows for all 15 Stations some formal and climatological uncertainties. Most of these uncertainties arise while digitization and can be delimited. It is shown that the spatial homogeneity of SLP-data from signal station data is sufficient for the descriptions of historic events, but the temporal homogenization is required for long-term trend analysis.

5. Sturm surge in December 1913

The storm surge at the coast at the southern Baltic Sea in December 1913 causes the highest water level in the region Rügen/Usedom after storm surges in 1872 and 1904 (Rosenhagen and Bork, 2008). However, the storm surge occurs at the 31. December 1913 and causes serious damage of landscape and infrastructure in this region. In the following section the storm surge and its evolution of weather conditions will be reconstructed by signal station data of 73 stations along the Baltic Sea coast, by weather information of the daily weather report of the Bundesamt für Seeschifffahrt und Hydrographie (BSH) in Rostock.

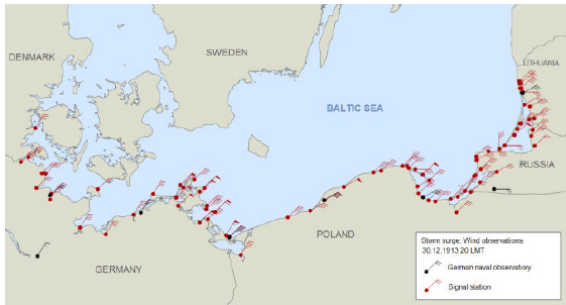


Figure 2: Positions and wind observations of the signal stations which reported on 30th December 1913. The red flags represent the data of signal stations and the black ones represent data of the German Naval Observatory.

6. Conclusion and Outlook

We can conclude that the spatial homogeneity of SLP-data from signal station data is sufficient for the descriptions of historic events, but the temporal homogenization is required for long-term trend analysis. That the data are useful for the description of historic events is also shown by the replication of the storm surge in December 1913 at the Rügen/Usedom region. The signal station data of SLP, wind direction and wind force expands the monitoring network at the Baltic Sea coast, which leads to a higher resolution of observation data along the coast in this region. To deduce long-term trend analysis from this signal stationsdata it is necessary to make a temporal homogenization. The digitization of the signal station data from 1877 until 1939 will be done in 2015.

Natural hazards and extreme events in the Baltic Sea region

Anna Rutgersson

Department of Earth Sciences, Uppsala University, Uppsala, Sweden (anna.rutgersson@met.uu.se)

1. Introduction

Situated in the extratropics of the Northern Hemisphere, the Baltic Sea region is be under the influence of air masses of arctic to subtropical origin. It is therefore a region of very variable weather conditions and far reaching teleconnections (i.e. BACCII; Rutgersson et al., 2014). The region is dominated mainly by two large-scale pressure systems over the northeastern Atlantic, the Icelandic Low and the Azores High, and a thermally driven pressure system over Eurasia (high pressure in winter, low pressure in summer). In general, there are westerly winds over the region, although any other wind direction is observed frequently. The climate of the Baltic Sea shows a strong seasonal cycle, but also large inter-annual to multidecadal variability. Long-term changes and variability of atmospheric parameters have large impacts on hydrological, oceanographic and biogeochemical processes in the region. The shallow and complex bathymetry of the semi-enclosed Baltic Sea makes the ecosystem very sensitive to any atmospheric changes. Precipitation and temperature control the river runoff to the Baltic Sea with a relation between atmospheric circulation patterns and sea-level, sea-ice, salinity and oxygen. The storm frequency clearly influences Baltic Sea mixing as well as marine ecosystems. Many natural hazards - storms, flooding, droughts, blizzards – are of hydrometeorological origin and can potentially be better understood and forecasted. The most devastating natural hazards are, however, often caused by a combination of several factors. Extreme flooding in a coastal city for instance could be caused by a combined effect of storm surge and river flooding, with additional effects on the water storage in the Baltic Sea. Presently, prediction capabilities as well as knowledge of potential future changes in the occurrence of extreme events are very limited.

2. Large-Scale circulation patterns

The atmospheric circulation in the European/Atlantic sector plays an important role for the regional climate of the Baltic Sea basin. It can be described mainly by the North Atlantic Oscillation (NAO), the zonality of the atmospheric flow and the blocking frequency. The first mode of a principal component analysis (PCA) of winter sea-level pressure (SLP) variability is the NAO, which in winter shares a close correlation with atmospheric and marine state variables of the Baltic Sea region (where a positive index indicates mild and wet winters and a negative index indicates cold and dry winters). Fig. 1 shows the winter NAO index for 1823 to 2013. In a long term perspective, the behaviour of the NAO is rather irregular. For all weather types (zonal, meridional, or anticyclonic), an increase in persistence in the order of 2 to 4 d is found from the 1970s to the 1990s (BACCII). This increase in persistence may contribute to an increase in the occurrence of extreme events. Circulation changes in the Baltic Sea region may also be related to climate anomalies in other regions. Many authors discuss the cold temperatures of the winters

2009–2010 and 2010–2011 over large parts of Europe (including the Baltic Sea region). Overland and Wang (2010) point out a possible relationship of circulation changes in the Baltic Sea region to the loss of sea ice in the Arctic.

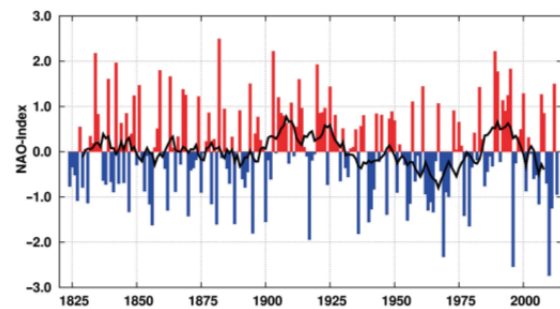


Figure 1. NAO index for boreal winters (DJFM) of 1823–2013. Black line: 11 yr running mean highlights decadal-scale variability. Bars: positive (red) and negative (blue) indices. From Rutgersson et al (2014).

3. Wind climate

Variations in the wind climate are closely linked to the atmospheric circulation and cyclonic activity over the North Atlantic. Since 1958, the number of deep cyclones in winter reached a minimum in the early 1970s and clearly increased in the following decades, reaching their maximum around the last decade of the 20th century (Lehmann et al. 2011). At the same time, a continuous shift of North Atlantic storm tracks towards the northeast regionally increased the impact and number of storms over Northern Europe in winter and spring of recent decades, but decreased in autumn. Following the intensification of deep lows, a significant positive trend exists for storminess since the middle of the last century in reanalysis data over this region (Donat et al. 2011). However an absence of robust long-term trends have been reported confirmed by several studies showing similar high storm levels during the 1880s as observed in the 1990s with a distinct minimum in the 1970s (see BACCII; Schenk and Zorita, 2012; Schmidt and von Storch 1993 for more details).

4. Surface air temperature

A quite significant surface air temperature increase have been observed in the Baltic Sea Region. The warming has partly continued up to the present. The temperature increase is not monotonous but accompanied by large (multi-) decadal variations. Linear trends of the annual mean temperature anomalies during 1871–2013 were $0.10 \text{ K decade}^{-1}$ north of 60° N and $0.08 \text{ K decade}^{-1}$ south of 60° N in the Baltic Sea region. This is larger than the global mean temperature trend, which is about $0.06 \text{ K decade}^{-1}$ for the period 1871–2005.

5. Precipitation

The amount of precipitation in the Baltic Sea area during the past century has varied between regions and seasons, with both increasing and decreasing precipitation and no general trend during the past 200 ys. A tendency of increasing precipitation in winter and spring was detected during the second half of the 20th century. However, as precipitation is highly variable trends depend very much on time frames, seasons and locations. Change in precipitation is also associated with an increase in the frequency and intensity of extreme precipitation events; the number of extreme precipitation days per year and the seasons in which they occur vary for the different catchment areas of the Baltic Sea. Wet periods with daily precipitation exceeding 1 mm have become longer over most of Europe by about 15 to 20% during 1950–2008 (Zolina et al. 2010). The lengthening of wet periods was not caused by an increase of the total number of wet days. Heavy precipitation events during the last two decades have become much more frequently associated with longer wet spells and have intensified in comparison with the 1950s and 1960s (Zolina 2011), Figure 2.

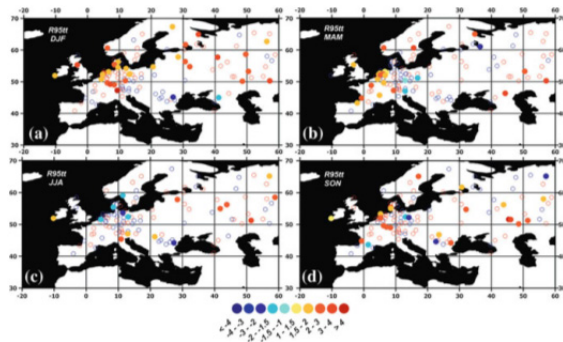


Figure 2. Linear trends (% per decade) in the R95tt index (fraction of total precipitation above 95th percentile of rain-day amounts) for a winter, b spring, c summer and d autumn for the period 1950–2000. Open circles show all trend estimates and closed circles denote locations where the trends are significant at 95 %. Blue indicates negative trends and red indicates positive trends (Zolina et al. 2009 reproduced in BACC II).

6. Extreme events

In terms of Natural disasters and weather related accidents it is the really rare events causing high-impact damages. During the past decades several such events have attained significant attention. In 2013 natural disasters worldwide were responsible for the death of more than 20,000 people and costs of more than \$134 billion. In 1994 the ferry Estonia sank in heavy seas on her route from Tallinn to Stockholm, killing 852 persons. In 2005 a storm surge with record heights of 2.75m associated with storm “Gudrun” hit the Estonian coast, causing damages of approximately 0.7% of the annual Estonian GDP. In July 2011 a cloudburst in Copenhagen produced extreme precipitation of more than 150 mm in 2 hours, resulting in severe damage to critical infrastructure. As reliable in-situ data exists for less than 200 years, statistically significant knowledge on occurrence and trends of the most severe events are very limited. While climate change has received considerable attention in the scientific community for several decades now, the knowledge on changing extremes and their impacts is still fragmented, the confidence level of

the knowledge of relation between climate change and flooding, heat waves and storms ranges from low to medium (IPCC, 2012), in particularly the confidence level reduces when approaching the local scale (IPCC, 2014).

7. Conclusions

Variations and trends of atmospheric parameters in the Baltic Sea region during the last 200–300 years can be summarised as follows. A northward shift in storm tracks and increased cyclonic activity have been observed in recent decades with an increased persistence of weather types. No long-term trend have been observed in annual wind statistics since the nineteenth century, but considerable variations on (multi-)decadal timescales have been observed. An anthropogenic influence cannot be excluded since the middle of the twentieth century. The pattern in wind and wave heights over the Northern Hemisphere with a NE shift of storm tracks appears to be consistent with combined natural and external forcing. Continued warming has been observed, particularly during spring and is stronger over northern regions than southern (polar amplification). No long-term trend was observed for precipitation, but there is some indication of an increased duration of precipitation periods and possibly an increased risk of extreme precipitation events.

References

- BACCII, BACC II Author Team, Second Assessment of Climate Change for the Baltic Sea Basin, Regional Climate Studies, ISSN 1862-0248 ISSN 1865-505X (electronic). ISBN 978-3-319-16005-4 ISBN 978-3-319-16006-1 (eBook). DOI 10.1007/978-3-319-16006-1. Springer Cham Heidelberg New York Dordrecht London.
- Donat M, Renggli D, Wild S, Alexander L, Leckebusch G, Ulbrich U (2011) Reanalysis suggests long-term upward trends in European storminess since 1871. *Geophys Res Lett* 38: L14703, doi: 10.1029/2011GL047995
- IPCC, 2012: Managing the Risks of Extreme Events and Disasters to Advance Climate Change Adaptation. A Special Report of Working Groups I and II of the Intergovernmental Panel on Climate Change. Cambridge University Press, Cambridge, UK, 582 pp.
- IPCC, 2014: Climate Change 2014: Impacts, Adaptation, and Vulnerability. Part A: Global and Sectoral Aspects. Contribution of Working Group II to the Fifth Assessment Report of the Intergovernmental Panel on Climate Change.
- Lehmann A, Getzlaff K, Harlaß J (2011) Detailed assessment of climate variability in the Baltic Sea area for the period 1958 to 2009. *Clim Res* 46: 185–196
- Overland JE, Wang M (2010) Large-scale atmospheric circulation changes are associated with the recent loss of Arctic sea ice. *Tellus A* 62: 1–9
- Rutgersson A, Jaagus J, Schenk F, Stendel M (2014) Observed changes and variability of atmospheric parameters in the Baltic Sea region during the last 200 years, *Clim. Res.*, 60, 177–190
- Schenk F, Zorita E (2012) Reconstruction of high resolution atmospheric fields for Northern Europe using analog upscaling. *Clim Past* 8: 1681–1703
- Schmidt H, von Storch H (1993) German Bight storms analyzed. *Nature* 365: 791
- Zolina O, Simmer C, Belyaev K, Kapala A, Gulev S (2009) Improving estimates of heavy and extreme precipitation using daily records from European rain gauges. *J Hydro - meteorol* 10: 701–716

The effect of climate change and eutrophication on sediment phosphorus fractions: results of a long-term enclosure experiment

Katrin Saar¹, M. Søndergaard², M. Jensen³, C. Jørgensen³, K. Reitzel³, E. Jeppesen², T. Lauridsen², H. S. Jensen³

¹Centre for Limnology, Estonian University of Life Sciences, Tartu, Estonia (katrin.saar@emu.ee)

²Institute of Bioscience, Aarhus University

³Department of Biology, University of Southern Denmark

1. Introduction

In the course of next century climate changes is assumed to affect the functioning of freshwater ecosystems including nutrient cycling and the internal phosphorus loading of lakes (Jeppesen *et al.* 2014). This is expected to have an important consequences for the overall lake water quality and intensify eutrophication (Jeppesen *et al.* 2014, Özen *et al.* 2013). Shallow lakes are assumed to be more influenced by the increasing temperature (Liboriussen *et al.* 2005). In the present study, we focused on potential mobility and accumulation of sediment phosphorus fractions at different temperatures according to Intergovernmental Panel on Climate Change (IPCC) climatic scenarios and two nutrient loading levels.

2. Methods

To evaluate the effect of the climate change an experiment has been conducted over 12 years in 24 outdoor flow-through enclosures with three different temperatures levels (0-5 °C above ambient temperature) and two different nutrient loadings (enclosure experiment described in more detail by Liboriussen *et al.* 2005). Phosphorus fractions, organic phosphorus forms, dry weight, loss of ignition, total phosphorus, iron and aluminium bound to phosphorus in the different fractions were analyzed in sediment cores collected from each enclosure.

3. Results

The analysis showed that high nutrient loading increased mobile phosphorus, loosely bound phosphorus and phosphorus bound to iron, organic compounds, humic substances, calcium and residual pools in sediment. Mobile phosphorus pool and accumulated organic matter showed a trend to decrease with higher temperatures (fig. 1). Temperature had a significant effect on aluminium hydroxides in sediment.

4. Discussion

Higher nutrient loading led to higher sediment accumulation and thereby more nutrient rich sediment. Organic matter in lake sediment was more effectively mineralized at higher temperatures as decomposition rates are more stimulated by temperature than primary production.

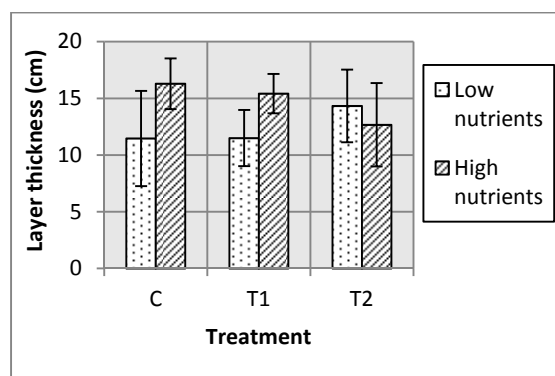


Figure 1. Thickness of the organic layer accumulated in the enclosures. Three temperature treatments used in the experiment: C – reference temperature; T1 – scenario 2070-2100 A2 (2-3°C above ambient); T2 – scenario 2070-2100 A2 + 50 % (4-5 °C above ambient).

5. Conclusions

The study has indicated that the accumulation of phosphorus forms (especially mobile forms) is dependent on nutrient loading as well as the temperature. Insight to the lake ecosystem response to climate change and eutrophication also enables us to decide for proper lake management and restoration measures.

References

- Liboriussen, L., Landkildehus, F., Meerhoff, M., Bramm, M. E., Søndergaard, M., Christoffersen, K., Richardson, K., Søndergaard, M., Lauridsen, T. L., Jeppesen, E. (2005) Global warming: Design of a flow-through shallow lake mesocosm climate experiment, *Limnology and Oceanography: Methods*, 3, pp. 1-9
- Jeppesen E., Meerhoff, M., Davidson, T. A., Trolle, D., Lauridsen, T. L., Beklioglu, M., Brucet, S., Volta, P., Gonzales-Bergonzoni, I., Nielsen, A. (2014) Climate change impacts on lakes: an integrated ecological perspective based on a multi-faceted approach, with special focus on shallow lakes, *Journal of Limnology*, 73, pp. 88-111
- Özen, A., Šorf, M., Trochine, C., Liboriussen, L., Beklioglu, M., Søndergaard, M., Torben, L., Lauridsen, T. L., Johanssonm L. S., Jeppesen, E. (2013) Long-term effects of warming and nutrients on microbes and other plankton in mesocosms, *Freshwater Biology*, 58, pp. 483-493

Potential Ecological Risk of Heavy Metals in Sediments from the Mediterranean Coast, Egypt

Naglaa F. Soliman

Institute of Graduate Studies and Research, Alexandria University, Alexandria, Egypt (naglaa_farag@yahoo.com)

1. Introduction

To date, many methodologies have been developed to assess ecological risks of heavy metals. However, most of them are suitable only for ecological assessment of a single contaminant (e.g. Geoaccumulation index method and Enrichment factor). In reality, many kinds of heavy metals usually accumulate simultaneously and cause combined pollution. To address this, Hakanson (1980) developed the potential ecological risk index, which introduced a toxic-response factor for a given substance and thus can be used to evaluate the combined pollution risk to an ecological system Yang et al. (2009). On the other hand, mean Sediment Quality Guidelines quotient (mSQGQs) has been developed for assessing the potential effects of contaminant mixtures in sediments. Mean SQGQ have been calculated most frequently with SQGs derived with empirical approaches, such as the ERM, PEL values, in which measures of adverse effects were associated with, but not necessarily caused by specific chemicals Long et al. (2000). The aim of the present study was to: (1) provide the concentration and distribution of some heavy metals in the Egyptian Mediterranean Sea sediments. (2) evaluate the potential ecological risk levels of some heavy metals by applying the Potential Risk Index Method. (3) investigate the biological effects of some heavy metals concentrations using available Sediment Quality Guidelines (SQGs); and (4) identify the sources of the heavy metals with multivariate analyses. This study supports metal pollution monitoring and control for the Egyptian Mediterranean Sea. It will be a useful tool to authorities in charge of sustainable marine management.

2. Sample collection and pretreatment

Twenty surficial sediment samples were collected during July 2010 from different selected stations along the Egyptian Mediterranean Sea using Peterson grab sampler. The samples were placed into sealed polyethylene bags, carried to the laboratory in an ice box and stored at -20°C in the dark until analysis.

3. Results and Discussion

The measured heavy metals contents varied greatly as follows: $\text{Cr} > \text{Co} > \text{Fe} > \text{Pb} > \text{Ni} > \text{Mn} > \text{Cu} > \text{Zn} > \text{Cd}$. Among the 9 elements studied, concentrations of Fe and Mn were higher, whereas lower concentrations of Co and Cd were observed in the different sampling locations. The *m-PEL-Q* in surface sediments of the Egyptian Mediterranean coast range from 0.02 to 0.57 (mean value of 0.24), indicating that the combination of Cd, Cr, Cu, Ni, Pb and Zn may have a 25% probability of being toxic. The order of potential ecological risk factor of heavy metal in sediments of the Egyptian Mediterranean coast was $\text{Cd} > \text{Pb} > \text{Ni} > \text{Cr} > \text{Cu} > \text{Mn} > \text{Zn}$. The mean potential ecological risk factors (E_i^i) of Cd, Cr, Cu, Mn, Ni, Pb and Zn were all

lower than 40, which belong to low ecological risk. All the sampling sites were at low risk level where the RI values were much lower than 150. Multivariate analysis (i.e. Principal component analysis; PCA and Cluster analysis; CA) has been proved to be an effective tool for providing suggestive information regarding heavy metal sources and pathways Hu et al. (2013). The results of the principal component analysis; PCA on the data matrix obtained from total metal analysis of surface sediments along the study area are shown in Table 1. Two main components with Eigenvalues greater than 1 were determined, explaining 80.14% of the total variance. The first component (PC1), with a variance of 55.059%, was highly correlated with Ni, Fe, Co, Mn and Cr; correlation coefficients among this group of elements exceed 0.7 (0.945, 0.953, 0.924, 0.911 and 0.833, respectively). On the other hand, cadmium and lead showed strong negative loading (-0.648 and -0.542). Co, Ni and Cr belong to the siderophile elements, and are main rocks forming elements. It is easy for them to enter into iron magnesium silicate minerals, because of their similar ionic radius. This element association is considered to represent the lithology of the study area, and a natural input, i.e., they are derived from terrigenous detritus material transported by surface runoff. The second component (PC2) explained 25.11% of the total variance with significant loadings on Zn and Cu (0.966 and 0.876 respectively), which suggests similar sources. However, Pb also showed moderate positive loading (0.669), suggesting that the sources of Pb could be both natural and anthropogenic. Cadmium displays none of strong correlations between the other metals, suggesting that Cd has another different sources or pathways Hu et al. (2013). PC1 and PC2 together explained 80.14% of the total variance, indicating that the lithogenic factor dominates the distribution of most part of the considered metals in the study.

Table 1. Factor loadings on elements in surficial sediments samples along the Egyptian Mediterranean coastal area (n=20)

Element	PC1	PC2
Zn	0.037	0.966
Ni	0.945	-0.052
Pb	-0.542	0.669
Cd	-0.648	0.209
Fe	0.953	0.190
Cu	0.229	0.876
Mn	0.911	0.110
Co	0.929	0.129
Cr	0.833	-0.032
Eigenvalue	4.955	2.260
% variance explained	55.059	25.115
Cumulative % variance	55.059	80.174

Extraction method: Principal component analysis
 Rotation method: Varimax with Kaiser Normalization

Cluster analysis is often coupled with PCA to confirm results and provide grouping of variables (Hu et al., 2013). In this study, CA was performed on the same data as PCA to understand the similarities among them. Figure 1 depicts a dendrogram with single linkage Euclidean and correlation coefficient distance. The cluster analysis results indicate two clusters: (1) Pb-Zn-Cu; (2) Ni-Mn-Fe-Co-Cr in terms of similarities. This indicates that Ni, Mn, Fe, Co, and Cr appear to have originated mainly from natural sources. In addition, Pb, Zn and Cu seem to drive partly from sources other than Ni, Mn, Fe, Co and Cr. This is consistent with our PCA results.

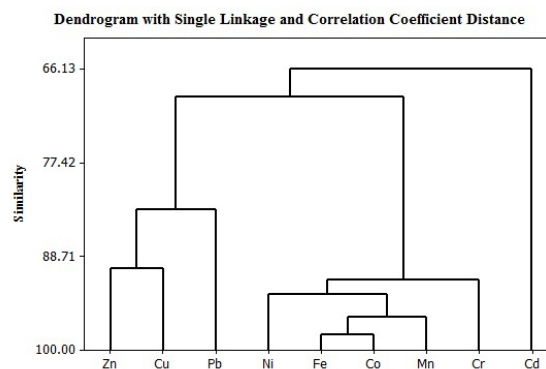


Figure 1. Dendrogram showing cluster of variables on the basis of similarity

4. Conclusion

Mediterranean Sea, Egypt is an economically important marine environment. During the last decades there has been extensive increase in the levels of urbanization and industrialization along its coastal area. The results of this study provide valuable information about metal contamination in sediments along the Mediterranean Sea from El-Salloum to Rafah for over than 1200km.

References

- Hakanson, L. (1980). An ecological risk index for aquatic pollution control: a sedimentological Approach, *Water Research*, 14, 975-1001.
- Yang, Z., Wang, Y., Shen, Z., Niu, J., Tang, Z. (2009). Distribution and speciation of heavy metals from the mainstream, tributaries, and lakes of the Yangtz River catchment of Wuhan, China, *Journal of Hazardous Materials*, 166, 1186-1194.
- Long, E.R., MacDonald, D.D, Seven, C.G, & Hong, C.B. (2000). Classifying the probabilities of acute toxicity in marine sediments with empirically derived sediment quality guidelines, *Environmental Toxicology and Chemistry*, 19, 2598-2601.
- Hu, D., He, J., Lu, C., Ren, L., Fan, Q., Wang, J., Xie, Z. (2013). Distribution characteristics and potential ecological risk assessment of heavy metals (Cu, Pb, Zn, Cd) in water and sediments from Lake Dalinouer, China, *Ecotoxicology and Environmental Safety*, 93, 135-144.

Influence of the direct radiative effect of aerosols on atmospheric dynamics over Europe

Velle Toll, Emily Gleeson

Institute of Physics, University of Tartu, Tartu, Estonia (velle.toll@ut.ee), Met Éireann, Dublin, Ireland (emily.gleeson@met.ie)

1. Introduction

In this study the influence of the direct radiative effect of aerosols on atmospheric dynamics over Europe is simulated using the Hirlam Aladin Research for Mesoscale Operational Numerical Weather Prediction in Euromed (HARMONIE) numerical weather prediction (NWP) model. In recent years the direct radiative effect of aerosols has become more accepted as a physical mechanism that should be included in NWP models in order to improve the accuracy of weather forecasts. For example Mulcahy et al. (2014) show that considering the influence of aerosols in NWP results in an improved radiation budget.

The main goal of this study is to quantify the influence of the direct radiative effect of aerosols on atmospheric dynamics over short time scales. NWP models often use climatological aerosol data to consider the direct radiative effect of aerosols. In this study, the influence of considering direct radiative effect of climatological and real time aerosol distributions on the simulated atmospheric state is compared. Moreover, the direct radiative effect of aerosols during Russian wildfires in summer 2010 is studied to evaluate the magnitude of the aerosol influence during this heavily polluted situation.

2. Models and methods

The HARMONIE NWP model (Seity et al., 2011) is used for simulating the direct radiative effect of aerosols. Within HARMONIE, the ALARO physical parameterizations package is used at a horizontal resolution of 15 km. The IFS cy25 radiation scheme from the ECMWF global model is used. The treatment of shortwave radiation follows Fouquart and Bonnel (1980) and longwave follows Mlawer et al. (1997).

By default monthly averages of the aerosol optical depths (AOD) of dust, sulphates, sea salt, black carbon and organic matter at 550 nm from the Tegen et al. (1997) climatology are used in the HARMONIE model to calculate the direct radiative effect of aerosols. The aerosols are distributed vertically, following climatological vertical profiles. In addition to the Tegen et al. (1997) climatology, aerosol data from the more up-to-date Max-Planck-Institute Aerosol Climatology version 1 (MACv1) (Kinne et al., 2013) and time-varying aerosol data from the Monitoring Atmospheric Composition and Climate (MACC) reanalysis (Inness et al., 2013) are used. The influence of aerosols over Europe during the 15 day period in the second half of April 2011 (16th-30th) is simulated using the HARMONIE model. Aerosol data from the MACC reanalysis is also used to study summer 2010 wildfire event in Russia (intense fire period 06.08.2010 to 11.08.2010 is studied). The maximum observed aerosol optical depth was more than 4 at 550 nm during this event.

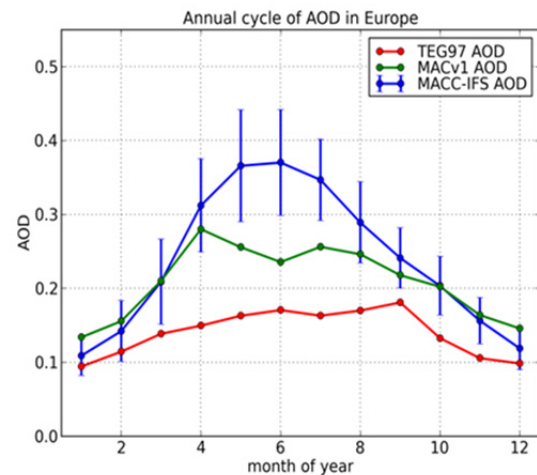


Figure 1. Monthly averages of areal average AOD in Europe for different datasets and standard deviation of AOD time series (shown as blue bars) from the MACC reanalysis.

3. Results

Monthly averages of areal average AOD in Europe (Figure 1) have different values in different datasets. There is a clear annual cycle in AOD in all datasets, lowest in winter months. The Tegen et al. (1997) climatology underestimates AOD compared to the MACv1 climatology, and the MACC climatology overestimates AOD compared to MACv1.

A small improvement in the radiation budget is simulated when the direct radiative effect of real time aerosol distribution is considered for cases where the aerosol amounts are close to average. However, there is a considerable improvement in the simulation of temperatures in the lower troposphere. Also the near surface humidity is better forecast when the direct radiative effect of aerosols is considered because the representation of the surface energy budget is improved.

The influence of aerosols during heavily polluted Russian wildfire case is much more pronounced. The diurnal average shortwave radiation flux at the surface was more than 100 W/m² lower and 2m temperatures were up to 4°C (Figure 2) lower during the intense wildfire period in summer 2010. Simulated near-surface temperatures and vertical temperature profiles agree better with observations when the direct radiative effect of aerosols is considered in the meteorological forecast.

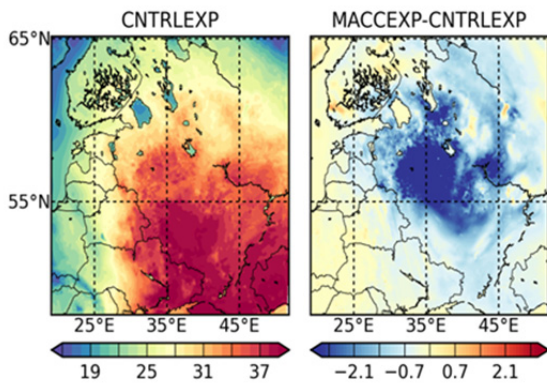


Figure 2. 2m temperature (°C) at 12 UTC on August 8, 2010. Temperature is over 3°C lower when the radiative influence of the realistic aerosol distribution from the MACC reanalysis is included.

4. Conclusions

Considering the direct radiative effect of aerosols is shown to improve the accuracy of simulated radiative fluxes and temperatures in the lower troposphere for cases where the aerosol distribution is close to normal in Europe (i.e. not heavily polluted). During heavy pollution there is a considerable influence of aerosols on atmospheric dynamics over Europe and the accuracy of meteorological forecast is significantly improved when the direct radiative effect of aerosols is included. The capability of NWP models to consider the direct radiative effect of aerosols should be further developed.

Acknowledgments

This work is supported by the research grant No 9140 of the Estonian Science Foundation and the institutional research grant IUT20-11 of the Estonian Research Council.

References

- Fouquart, Y., & Bonnel, B. (1980). Computations of solar heating of the earth's atmosphere- A new parameterization. *Beitraege zur Physik der Atmosphaere*, 53, 35-62.
- Inness, A., Baier, F., Benedetti, A., Bouarar, I., Chabrillat, S., Clark, H., & Zerefos, C. (2013). The MACC reanalysis: an 8 yr data set of atmospheric composition. *Atmospheric chemistry and physics*, 13, 4073-4109.
- Kinne, S., O'Donnel, D., Stier, P., Kloster, S., Zhang, K., Schmidt, H., & Stevens, B. (2013). MAC-v1: A new global aerosol climatology for climate studies. *Journal of Advances in Modeling Earth Systems*, 5(4), 704-740.
- Mlawer, E. J., Taubman, S. J., Brown, P. D., Iacono, M. J., & Clough, S. A. (1997). Radiative transfer for inhomogeneous atmospheres: RRTM, a validated correlated-k model for the longwave. *Journal of Geophysical Research: Atmospheres* (1984–2012), 102(D14), 16663-16682.
- Mulcahy, J. P., Walters, D. N., Bellouin, N., & Milton, S. F. (2014). Impacts of increasing the aerosol complexity in the Met Office global numerical weather prediction model. *Atmospheric Chemistry and Physics*, 14(9), 4749-4778.

Seity, Y., Brousseau, P., Malardel, S., Hello, G., Bénard, P., Bouttier, F., & Masson, V. (2011). The AROME-France convective-scale operational model. *Monthly Weather Review*, 139(3), 976-991.

Tegen, I., Hollrig, P., Chin, M., Fung, I., Jacob, D., & Penner, J. (1997). Contribution of different aerosol species to the global aerosol extinction optical thickness: Estimates from model results. *Journal of Geophysical Research: Atmospheres* (1984–2012), 102(D20), 23895-23915.

Observations and analysis of coastal changes in West Estonian Archipelago to study the impacts of climatic and sea-level fluctuations and wave parameters on shore processes.

Hannes Tõnisson

Institute of Ecology, Tallinn University, Tallinn, Estonia (Hannes.Tonisson@tlu.ee)

1. Introduction

Large-scale atmospheric circulation is one of the main factors influencing climate in every region. During the second half of the 20th century, significant changes have occurred in circulation. An increase in mean sea-level pressure gradient in the Northern Hemisphere mid-latitudes and associated intensification of westerly circulation in winter has been the most important change (IPCC, 2007). Such change has shifted the North Atlantic storm track about 180 km northward (Wang *et al.*, 2006).

Estonia is a small country (approximately 45,000 km²) on the eastern coast of the Baltic Sea with a wide variety of different coast and shore types. This is due to a relatively long coastline (3,800 km) and its location in a transitional area between major geological structures. In addition, Estonia lies in a transitional zone between regions with a maritime climate (in the west) and a continental climate (in the east).

Therefore, Estonia is very sensitive to climate change manifestations such as an increase in cyclonic activity, westerly circulation and a northward shift of the Atlantic storm track over the last decades. Changes in meteorological conditions have changed wave climate and sea-level conditions as well the rate at which shore processes occur. Shore processes have accelerated over the last 50 years at many locations in Estonia (Orviku *et al.*, 2009).

The current study analyzed how the consequences of changes in large-scale atmospheric circulation have influenced the coastal sea and the shore processes in various locations in Estonia with different exposure to the sea.

2. Study area

Several sites with different exposure to the open sea were studied along the coast of Estonia. All the sites described full erosion-accumulation systems. It enabled us to find the changes in the erosion/accumulation balance and changes in the rate of which shore processes occur.

North Estonian study sites were exposed to the Gulf of Finland and mostly to the northerly winds while western sites were mainly exposed to westerlies – the Baltic Proper and Gulf of Livonia.

3. Data and Methods

Topographic and geomorphic assessments of coastal changes were based on a combination of field and GIS-based studies carried out in 10 study sites. The information describing coastal changes is not continuous and the further we go back in time, the less data we have. Since 2000, the shoreline positions and shore profiles have been measured in situ (Suursaar *et al.*, 2013). The shoreline

positions and geomorphic data also originate from old orthophotos, aerial photos, topographic maps, and a few precise levelling studies.

The quality of the historical topographic maps was controlled using several certain points. Low-quality maps, which were distorted by the Soviet military forces, were eliminated from the study. Nevertheless, the maps produced in different years varied somewhat between the study sites. However, it was possible to distinguish similar sub-periods for each study site that enabled to compare the total changes during the sub-periods and calculate the average annual changes.

The rates of coastal change were calculated as a ratio of the sum of volume to the duration of the measured period for both erosion and accumulation (as an average per meter of shoreline). The method made it possible to compare the rates of shore processes in space and time (Tõnisson *et al.*, 2011). Finally, the recent yearly measured shore profiles (since 2000 with Garmin handheld GPS devices and since 2011 with Trimble and Leica RTK-GPS devices) helped us to detect some abrupt changes (shifts) in the character of shore processes.

4. Results and discussion

Two main patterns in the character of shore processes were identified – one for the shores exposed to the north in north Estonia and the other for the shores exposed to the west in W Estonia.

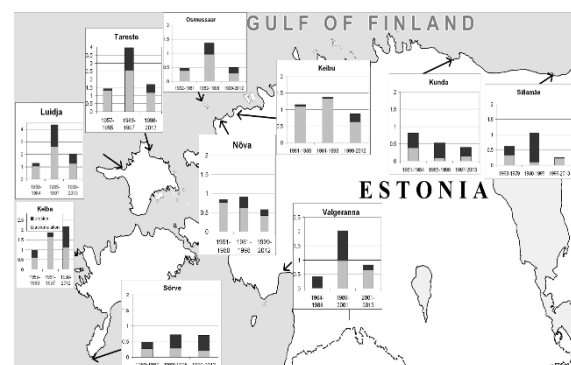


Figure 1. Changes in the speed of shore processes ((erosion+accumulation)/period length (x-axis), per one meter of shoreline (y-axis).

The velocities of erosion, sediment transport and accumulation are the highest on the western coast being in good accordance with the roughest wave climate off the western coast. Sõrve study site provides an exception in W Estonia due to more erosion-resistant character of shore sediments. The shores exposed to the north are rather stable ones, like in Sillamäe and Kunda (Figure 1).

An increase in the velocity of shore processes was registered from the beginning of the 1980s until the middle of the 1990s (second sub-period) in almost every study site where the rates of coastal changes increased up to 4 times (Figure 1). Major changes come from a rapid increase in the erosion areas and re-deposition of the eroded sediments. Notable decrease in erosion and in total velocity of changes can be observed since the middle of the 1990s (last sub-period) in most of the north-exposed study sites.

Different trends can be observed in west-facing study sites. The rates of changes have been slightly faster, whereas the changes in widely-exposed Sõrve site have remained on the level of the second sub-period but with an increasing share of erosion in both sites. Finally, west-exposed Luidja and Osmussaar sites in NW Estonia have experienced a decreasing trend in the total rate of changes, but the share of erosion has remained rather high. Such a phenomenon confirms the revealed trend in wave climate development, in general.

5. Conclusions

Such a phenomenon that shore processes are still accelerating in west-exposed sites in west Estonia and the rate of coastal changes is decreasing in north-exposed northern Estonia confirms the trends in wave climate development in general.

It is highly likely that a new equilibrium state has been quickly restored in N and NW Estonia, and most of the shores exposed to the north have been almost stable since the middle of the 1990s. Good evidence is the volume of the coastal profiles measured at Sillamäe study site during the last decade (Tõnisson *et al.*, 2014). Despite 1/3 of the most significant (3 from 9 events) storm events during the last 50 years in Sillamäe region has been registered in the last decade (Suursaar *et al.*, 2014), no major changes have been observed on the shores.

It is likely that the change in the forcing conditions in W Estonia is still going on and the shores have not reached a new equilibrium state yet. For instance, Kelba and Sõrve study sites in W Estonia have not reached a new equilibrium state and the rates of changes are still increasing (Figure 1), which is well correlated with the intensifying forcing conditions (Tõnisson *et al.*, 2011). It is likely that the

changes in the forcing conditions in W Estonia are still taking place and the shores have not reached a new equilibrium state yet.

References

- IPCC. (2007). Climate change 2007: The physical science basis, Contribution of Working Group I to the Fourth Assessment report of the Intergovernmental Panel on Climate Change, S. Solomon, D. Qin, M. Manning, Z. Chen, M. Marquis, K.B. Averyt, M. Tignor, H.L. Miller (eds.), Cambridge Univ. Press, New York. 996p.
- Orviku, K.; Suursaar, Ü.; Tõnisson, H.; Kullas, T.; Rivas, R., and Kont, A., 2009. Coastal changes in Saaremaa Island, Estonia, caused by winter storms in 1999, 2001, 2005 and 2007. *Journal of Coastal Research*, SI 56, pp. 1651-1655.
- Suursaar, Ü.; Alari, V.; Tõnisson, H. (2014). Multi-scale analysis of wave conditions and coastal changes in the north-eastern Baltic Sea. *Journal of Coastal Research*, SI 70, 223 - 228.
- Suursaar, Ü.; Tõnisson, H.; Kont, A.; Orviku, K. (2013). Analysis of relationships between near-shore hydrodynamics and sediment movement on Osmussaar Island, western Estonia. *Bulletin of the Geological Society of Finland*, 85, 35 - 52.
- Tõnisson H., Suursaar Ü., Orviku K., Jaagus J., Kont A., Willis D.A. and Rivas, R. (2011). Changes in coastal processes in relation to changes in large-scale atmospheric circulation, wave parameters and sea levels in Estonia. *Journal of Coastal Research*, SI64-1, 701 - 705.
- Tõnisson, H.; Aps, R.; Orviku, K.; Suursaar, Ü.; Sasi, S.; Kont, A. (2014). The impact of a port to the surrounding shores based on the 10 years monitoring results: Port of Sillamäe case study (Gulf of Finland, Baltic Sea). In: *IEEE Xplore: Baltic International Symposium (BALTIC), 2014 IEEE/OES*. IEEE, 2014, 1 - 6.
- Wang, X.L., Swail, V.R. and Zwiers, F.W., 2006. Climatology and changes of extratropical cyclone activity: comparison of ERA-40 with NCEP-NCAR reanalysis for 1958-2001. *Journal of Climate*, 19, 3145-3166.

Analysis of convective storms in Estonia based on the data from polarimetric weather radars and lightning detectors

Tanel Voormansik ⁽¹⁾ and Piia Post ⁽²⁾

⁽¹⁾ Institute of Physics, University of Tartu, Tartu, Estonia (tanel.voormansik@ut.ee)

⁽²⁾ Institute of Physics, University of Tartu, Tartu, Estonia (piia.post@ut.ee)

1. Introduction

Convective storms represent considerable hazard as they may cause large damage to the areas they cross. These storms generally do not have large spatial dimensions and can have relatively short lifetime. That makes them difficult to analyze based on regular meteorological data and that is where remote sensing data can be used for benefit. Weather radars have previously been used only in the analysis of single storms in Estonia and as part of modelling experiments (Toll *et al.* 2013). Severe convective storms have previously been analyzed based on weather radar and lightning sensor data by e.g. Rossi *et al.* (2014) and Mäkelä *et al.* (2010). The objective of this study is to investigate the local characteristics of convective storms over longer period and to provide basis for storm severity classification in Estonia.

2. Data used

Data from two dual polarization C-band weather radars located in Estonia, lightning detector data from The Nordic Lightning Information System (NORDLIS) network and rain gauge data of Estonian Weather Service were used to study the properties of the convective storms in Estonia. The investigated period ranges from 2011 – 2014 and includes the months with most convective activity in the area, from May to September.

3. Storm severity classification

Statistical analysis of radar and lightning data of Estonian convective storms is chosen as a starting point of severity classification. The statistical approach is based on the gridded datasets of ground flash density and radar rainfall intensity distributions. To construct them, the area of Estonia was divided into grids of 10 km x 10 km. The grid of this size was chosen because the usual convective storm cells are generally not larger than that. It is followed by the statistical storm severity classification based on the fractiles of observed severity parameter distributions. To classify the storm severities, percentile values were chosen similarly to

Rossi *et al.* (2014): 50, 90, 99 and 99.9% correspond respectively to the lower boundaries of the classes 'weak', 'moderate', 'intense' and 'severe' storms.

Clustering-based tracking algorithm is used to detect individual storm areas. It is followed by the analysis of radar data and lightning activities in the pre-classified storm areas. The storm severity attributes used in the analysis are storm maximum radar reflectivity value, maximum echo top height 20 dBZ, maximum echo top height 45 dBZ and storm maximum lightning activity.

4. Rainfall rate in convective storms

Heavy precipitation that often accompanies thunderstorms is studied as a comparison of radar rainfall accumulation and rain gauge measurements. Radar rainfall estimation algorithm used in the study is based on horizontal reflectivity (Z_h) and also specific differential phase (KDP) data for strong reflectivity areas (dBZ > 40). It could have great operational benefit as this demonstrates that KDP could be used in the routine calculations of rainfall intensity in the cores of convective storms, as Z_h overestimates the intensity in these cases.

References

- Mäkelä A, Rossi P, Schultz D. M. (2010), The Daily Cloud-to-Ground Lightning Flash Density in the Contiguous United States and Finland, American Meteorological Society, 139, 1323-1337
- Rossi P. J., Hasu V, Koistinen J, Moisseev D, Mäkelä A, Saltikoff E (2014), Analysis of a statistically initialized fuzzy logic scheme for classifying the severity of convective storms in Finland, Meteorological Applications, 21, 656-674
- Toll V, Männik A, Luhamaa A (2013), Modelling derecho dynamics with NWP model HARMONIE, 7th European Conference on Severe Storms (ECSS2013)

Investigation of the climate impact on the snow and ice thickness in Lake Vanajavesi, Finland

Yu Yang¹, Matti Leppäranta², Bin Cheng³

¹ Department of Basic Sciences, Shenyang Institute of Engineering, Shenyang 110136, China (yangyang-0606@hotmail.com)

² Department of Physics, University of Helsinki, FI-00014 Helsinki, Finland

³ Finnish Meteorological Institute, FI-00101 Helsinki, Finland

1. Application of HIGHTSI model

a one-dimensional high-resolution thermodynamic snow and ice model (HIGHTSI, Launiainen and Cheng, 1998; Cheng et al., 2003, 2008) was applied for Lake Vanajavesi (61.13°N, 24.27°E), located in southern Finland (Fig. 1). This model contains congelation ice, snow-ice and snow layers with full heat conduction equation. Atmospheric forcing was derived from weather observations and climatology, which also drove the snow cover evolution. The simulation results were compared with measured ice and snow thickness. A case study was performed for the ice season 2008-2009, forced by daily weather observations. Ice climatology was examined for the 30-year period 1971-2000; also the correlation between the observed monthly total precipitation and snow accumulation was investigated in order to understand the uncertainties of precipitation as model forcing for climatological simulation.

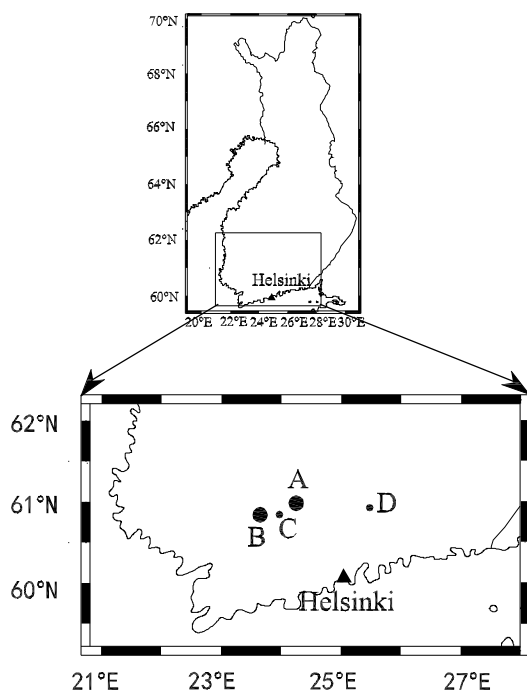


Figure 1. Geographical location of Lake Vanajavesi (A); surrounding observation sites Jokioinen meteorological observatory (B), Lake Kuivajärvi (C) and Lake Pääjärvi (D).

A number of climate sensitivity simulations were carried out for the ice season. The objectives of the present work were to assess the applicability of the HIGHTSI model for lake snow and ice thermodynamics, to find out the most important factors affecting lake ice growth and melting,

and to evaluate the influence of climate variations on the lake ice season.

2. Data

Synoptic-scale weather conditions and regional climate over this area are represented by Jokioinen meteorological observatory (60.8°N, 23.5°E; WMO station 02863), located some 50 km southwest of Lake Vanajavesi (Fig. 1). The weather forcing data for the lake ice model consist of wind speed (V_a), air temperature (T_a), relative humidity (Rh), cloudiness (CN) and precipitation (Prec), collected at three-hour time intervals. The winter 2008-2009 was mild (Fig. 2).

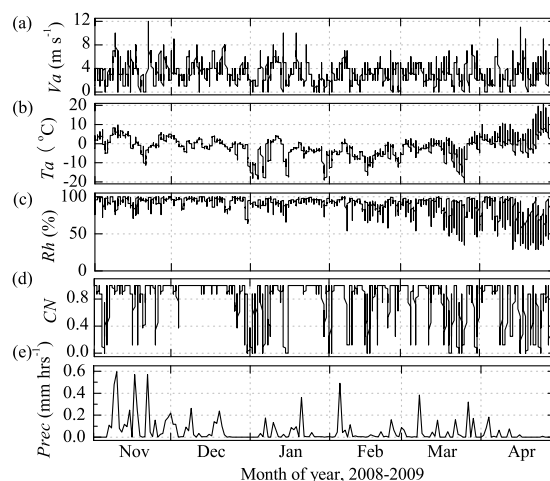


Figure 2. Time series of wind speed (a), air temperature (b), relative humidity (c), cloudiness (d), and precipitation (e). The data were initially observed at three-hour time interval.

3. Results and discussion

The ice season 2008-2009 lasted four months. Model simulations were started up in the beginning of January from the initial snow and ice thicknesses of 0.5 cm and 2 cm, respectively. The simulated snow thickness agreed well with the observations (Fig. 3).

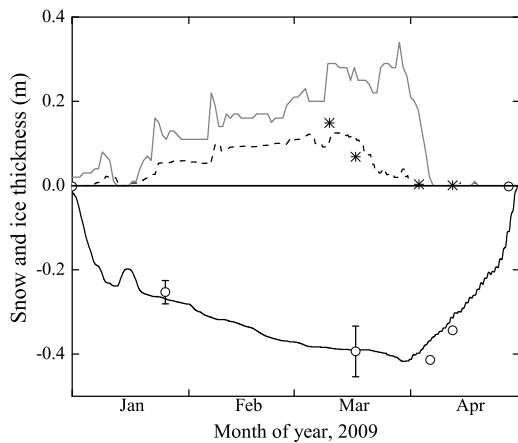


Figure 3. Time series of observed and modelled snow and ice thickness. The dark gray line and the asterisk are the observed snow thickness in Jokioinen and on Lake Vanajavesi, respectively. The black dashed and solid lines are modelled snow and ice thickness (reference experiment), respectively. The circles are the observed average ice thickness and the spatial standard deviation is indicated by the vertical bar (Lei et al., 2011).

Overall, lake-ice processes are closely associated with weather conditions from autumn through spring. The freezing of lake surface largely depends on the lake heat storage and the cooling rate of the air temperature during the autumn. Ice breakup can be explained mainly by the net solar radiation (e.g. Leppäranta, 2009). Fig. 4 shows a comparison of the results of the HIGHTSI simulations using climatological forcing (Table 1), with the air temperature artificially shifted by $\pm 1^\circ\text{C}$ or $\pm 5^\circ\text{C}$. Compared to the reference run, shifting by $\pm 1^\circ\text{C}$ may lead to about 5 days change of freezing date and 8 days change of breakup date. These values are close to 5 days for both dates, obtained by linear regression on lake phenology time series for lakes in southern Finland (Palecki and Barry, 1986). The breakup date seems to be more sensitive to the air temperature in the model.

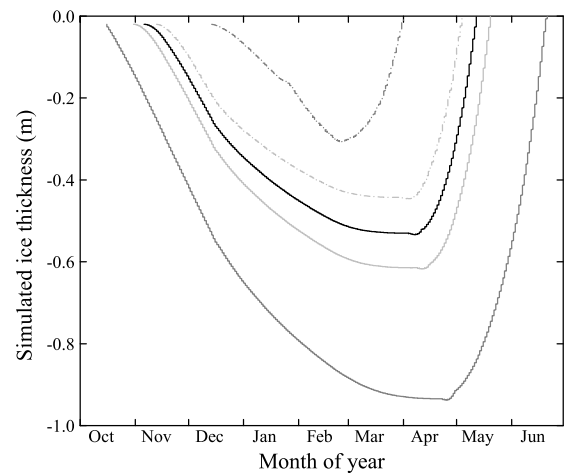


Fig. 4. Model sensitivity to the air temperature level. The black solid line is the reference (present climate). The gray solid (dashed) line and the light gray solid (dashed) line are modelled ice thickness based on the air temperature decreasing (increasing) 5°C and 1°C , respectively.

References

- Cheng, B., Vihma, T. and Launiainen, J. 2003. Modelling of the superimposed ice formation and sub-surface melting in the Baltic Sea. *Geophysica* 39, 31-50.
- Cheng, B., Zhang, Z., Vihma, T., Johansson, M., Bian, L., Li, Z. and Wu, H. 2008. Model experiments on snow and ice thermodynamics in the Arctic Ocean with CHINAREN 2003 data. *J. Geophys. Res.* 113, C09020, doi: 10.1029/2007JC004654.
- Launiainen, J. and Cheng, B. 1998. Modelling of ice thermodynamics in nature water bodies. *Cold Reg. Sci. Technol.* 27, 153-178.
- Lei, R., Leppäranta, M., Erm, A., Jaatinen, E. and Pärn, O. 2011. Field investigations of apparent optical properties of ice cover in Finnish and Estonian lakes in winter 2009. *Est. J. Earth Sci.* 60, 50-64.
- Leppäranta, M. 2009. Modelling the formation and decay of lake ice. In: *Climate change impact on European lakes* (ed. George, G.), *Aquatic Ecology Series* 4, 63-83.
- Palecki, M. A. and Barry, R. G. 1986. Freeze-up and breakup of lakes as an index of temperature changes during the transition seasons: A case study for Finland. *J. Appl. Meteorol. Climatol.* 25, 893-902.

Smooth temperature decreasing FOR nitrogen removal in cold (9-15° C) ANAMMOX biofilm reactor tests

Ivar Zekker^a, (PhD), Ergo Rikmann^a, Anni Mandel^a, Markus Raudkivi^a, Kristel Kroon^a, Liis Loorits^b, Jana Mihkelson^a, Andrus Seiman^b, Laura Daija^a, Toomas Tenno^a and Taavo Tenno^a

^a Institute of Chemistry, University of Tartu, 14a Ravila St., 50411 Tartu, Estonia. E-mail. (Ivar.Zekker@ut.ee)

^b Tallinn University of Technology, 5 Ehitajate Rd., 19086 Tallinn. E-mail. (Liis.Loorits@ttu.ee)

For N-rich wastewater treatment the anaerobic ammonium oxidation (anammox) and nitritation-anammox (deammonification) processes are widely used. In a deammonification moving bed biofilm reactor (MBBR) a maximum total nitrogen removal rate (TNRR) of 1.5 g N m⁻² d⁻¹ (0.6 kg N m⁻³ d⁻¹) was achieved. During biofilm cultivation, temperature was gradually lowered by 0.5° C per week, and a similar TNRR was sustained at 15° C. qPCR analysis showed an increase in *Candidatus Brocadia* quantities from 5×10³ to 1×10⁷ anammox gene copies g⁻¹ TSS despite temperature lowered to 15° C. Fluctuations in TNRR were rather related to changes in influent NH₄⁺ concentration. To study the short-term effect of temperature on the TNRR, a series of batch-scale experiments were performed which showed sufficient TNRRs even at 9-15° C (4.3-5.4 mg N L⁻¹ h⁻¹, respectively) with anammox temperature constants ranging 1.3-1.6. After biomass was adapted to 15° C, the decrease in TNRR in batch tests at 9° C was lower (15-20%) than for biomass adapted to 17-18° C. Our experiments show that a biofilm of a deammonification reactor adapted to 15° C successfully tolerates short-term cold shocks down to 9° C retaining a high TNRR.

1. Introduction:

The anaerobic ammonium oxidation (anammox) is a efficient method for the treatment of NH₄⁺-rich and low organic content reject water coming from anaerobic treatment occurring with the participation of anammox bacteria according to the following equation: NH₄⁺ + 1.32NO₂⁻ + 0.066HCO₃⁻ + 0.13H⁺ → 1.02 N₂ + 0.256NO₃⁻ + 2.03H₂O + 0.066CH₂O_{0.5}N_{0.15} ΔG₀ = - 360 kJ mol⁻¹ Anammox process can be used in moving bed biofilm reactors (MBBRs) as anammox bacteria are able to form a stable biofilm. Anammox process-based MBRRs have achieved a high total nitrogen removal rate (TNRR) (>5 kg N m⁻³ d⁻¹ (~1-2 g N m⁻² d⁻¹)) at temperatures above 20° C. Also, an anammox MBBR can have up to 5 times higher TN removal efficacy than deammonifying systems.

We define temperatures below 20° C as moderate temperatures for nitrogen removal similarly to other authors. The optimal temperature for most mesophilic anammox organisms was 40 ± 3° C. Also, there was showed that at temperatures below 15° C the anammox process was stopped.

2. Materials and Methods

Continuous reactor. A 20 L plexiglass MBBR filled ~50% with polyethylene carriers (specific surface 800 m⁻² m⁻³) (Aquamyc, Germany) was continuously fed with diluted reject water coming from the methane digester of the

Tallinn municipal wastewater treatment plant (Estonia). Intermittent aeration cycles with 45 min. aeration 45 min. non-aeration were applied. Within aerobic cycle oxygen concentration fluctuated between 0-1.5 mg L⁻¹. HRT of 0.5-2 d was applied.

3. Batch tests

60 batch tests were performed in 0.8-L volume three-necked glass bottles, which were filled with 200 biofilm carriers and placed on a magnetic stirrer located in a thermostated room. NO₂⁻-N/NH₄⁺-N ratio of 1.32/1 was maintained as a suitable anammox process stoichiometrical ratio.

4. Results

In a temperature range of 9-30° C, a decrease in the TNRR was linear without an abrupt rate drop - a fact that is in disagreement with the results reported by others who have observed decrease in the TNRR almost to zero below 15° C. We can conclude that a slow, gradual lowering of temperature down to 17° C is beneficial from the point of view of practical applications since anammox biomass adapted to lower-temperature has an ability to perform autotrophic nitrogen removal in a short term at a temperature as low as 9° C.

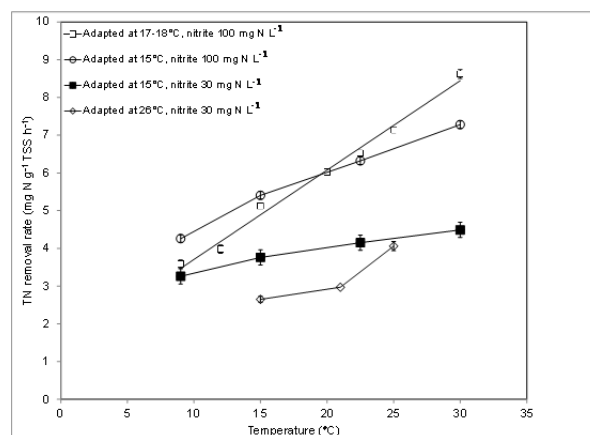


Figure 1: TN removal rates of biofilm carriers with different applied temperatures at NO₂⁻ concentrations of 100 mg NO₂⁻-N L⁻¹ and 30 mg NO₂⁻-N L⁻¹ with different applied temperatures in the reactor. Error bars represent standard deviation of 3 parallels of independent tests.

5. Conclusions

The effects of low temperature on the deammonification the maximum total nitrogen removal

rate (TNRR) of the deammonification reactor of $1.5 \text{ g N m}^{-2} \text{ d}^{-1}$ ($0.60 \text{ kg N m}^{-3} \text{ d}^{-1}$) at a low temperature ($15 \text{ }^\circ\text{C}$) was shown.

TNRR at $9 \text{ }^\circ\text{C}$ with the biomass cultivated at $17\text{-}18 \text{ }^\circ\text{C}$ was only 40% as compared with that of for highest temperature of $30 \text{ }^\circ\text{C}$ applied. The adaptability of biomass to lower temperatures by gradually lowering the reactor's temperature from $18 \text{ }^\circ\text{C}$ to $15 \text{ }^\circ\text{C}$ was studied in batch tests.

Regarding to practical applications, biofilm deammonification system could be set up at colder regions for treatment of mainstream wastewater when developing biomass with gradual temperature adaption methods.

Participants

Alari, Victor	Helmholtz-Zentrum Geesthacht, Germany victor.alari@hzg.de
Alber, Regina	University of Tartu, Estonia regina.alber@ut.ee
Aun, Margit	University of Tartu, Estonia margit.aun@ut.ee
Baiduk, Volha	Russian State Hydrometeorological University olya4ok@list.ru
Gallego-Urrea, Juliàn	University of Gothenburg, Sweden julian_gallego@hotmail.com
Gulev, Sergei	P.P. Shirshow Institute of Oceanology, Moscow, Russia gul@sail.msk.ru
Jaagus, Jaak	University of Tartu, Estonia jaak.jaagus@ut.ee
Jakobson, Liisi	University of Tartu, Estonia Liisi.Jakobson@ut.ee
Kabral, Naima	University of Tartu, Estonia naima.kabral@ut.ee
Kamenik, Jüri	University of Tartu, Estonia kamenikmeister@gmail.com
Kangro, Evelin	Tartu Observatory, Estonia evelin.kangro@to.ee
Komsaare, Kaupo	University of Tartu, Estonia kaupo.komsaare@ut.ee
Kõuts, Mariliis	Marine Systems Institute at Tallinn University of Technology, Estonia mariliis.kouts@msi.ttu.ee
Kriiska, Kaie	University of Tartu, Estonia kaie.kriiska@ut.ee
Lapo, Palina	Center of Hydrometeorology And Control of Radioactive Contamination And Environmental Monitoring of the Republic of Belarus, Minsk, The Republic of Belarus, Polly_LO@tut.by
Lavrinovičs, Aigars	Latvian Institute of Aquatic Ecology, Riga, Latvia aigars.lavrinovics@lhei.lv)

Lehmann, Andreas	GEOMAR Helmholtz-Zentrum für Ozeanforschung Kiel, Germany alehmann@geomar.de
Maljutenko, Ilja	Marine Systems Institute at Tallinn University of Technology, Estonia ilja.maljutenko@msi.ttu.ee
Meinson, Pille	Center for Limnology, Institute of Agricultural and Environmental Sciences, Estonian University of Life Sciences, Estonia pille.meinson@student.emu.ee
Mingelaite, Toma	Klaipeda University, Lithuania toma.mingelaite@gmail.com
Myrberg, Kai	Finnish Environment Institute SYKE kai.myrberg@ymparisto.fi
Napa, Ülle	University of Tartu, Estonia ulle.napa@ut.ee
Ohvril, Hanno	University of Tartu, Estonia hanno.ohvril@ut.ee
Omstedt, Anders	Göteborg University, Sweden anom@gvc.gu.se
Palo, Maris	University of Tartu, Estonia maris.palo@ut.ee
Post, Piia	University of Tartu, Estonia piia.post@ut.ee
Raabe, Kairi	Tartu Observatory, Estonia kairi.raabe@gmail.com
Raudsepp, Urmas	Marine Systems Institute at Tallinn University of Technology, Estonia raudsepp@phys.sea.ee
Reckermann, Marcus	Helmholtz-Zentrum Geesthacht, Germany marcus.reckermann@hzg.de
Rocha, Eva	Stockholm University, Sweden eva.rocha@natgeo.su.se
Röhrbein, Dörte	German Meteorological Service, Hamburg, Germany doerte.roehrbein@dwd.de
Rutgersson, Anna	Uppsala University, Sweden anna.rutgersson@met.uu.se
Saar, Katrin	Estonian University of Life Sciences, Tartu, Estonia katrin.saar@emu.ee

Soliman, Naglaa F.	Alexandria University, Alexandria, Egypt naglaa_farag@yahoo.com
Tammiksaar, Erki	Meteorological Observatory of Tartu University, Estonia erki.tammiksaar@emu.ee
Tõnisson, Hannes	Tallinn University, Estonia hannes.tonisson@tlu.ee
Toll, Velle	University of Tartu, Estonia velle.toll@ut.ee
Voormansik, Tanel	University of Tartu, Estonia tanel.voormansik@ut.ee
Yang, Yu	Shenyang Institute of Engineering, Shenyang, China yangyang-0606@hotmail.com
Zekker, Ivar	University of Tartu, Estonia Ivar.Zekker@ut.ee

International Baltic Earth Secretariat Publications

ISSN 2198-4247

- No. 1 Programme, Abstracts, Participants. Baltic Earth Workshop on "Natural hazards and extreme events in the Baltic Sea region". Finnish Meteorological Institute, Dynamicum, Helsinki, 30-31 January 2014. International Baltic Earth Secretariat Publication No. 1, 33 pp, January 2014.
- No. 2 Conference Proceedings of the 2nd International Conference on Climate Change - The environmental and socio-economic response in the Southern Baltic region. Szczecin, Poland, 12-15 May 2014. International Baltic Earth Secretariat Publication No. 2, 110 pp, May 2014.
- No. 3 Workshop Proceedings of the 3rd International Lund Regional-Scale Climate Modelling Workshop "21st Century Challenges in Regional Climate Modelling". Lund, Sweden, 16-19 June 2014. International Baltic Earth Secretariat Publication No. 3, 391 pp, June 2014.
- No. 4 Programme, Abstracts, Participants. Baltic Earth - Gulf of Finland Year 2014 Modelling Workshop "Modelling as a tool to ensure sustainable development of the Gulf of Finland-Baltic Sea ecosystem". Finnish Environment Institute SYKE, Helsinki, 24-25 November 2014. International Baltic Earth Secretariat Publication No. 4, 27 pp, November 2014.
- No. 5 Programme, Abstracts, Participants. A Doctoral Students Conference Challenges for Earth system science in the Baltic Sea region: From measurements to models. University of Tartu and Vilsandi Island, Estonia, 10 - 14 August 2015. International Baltic Earth Secretariat Publication No. 5, 66 pp, August 2015.

For a list of International BALTEX Secretariat Publications (ISSN 1681-6471), see
www.baltex-research.eu/publications

International Baltic Earth Secretariat Publications
ISSN 2198-4247